

UNIVERSITY OF OKLAHOMA  
GRADUATE COLLEGE

LABORATORY CHARACTERIZATION OF FOAMED WMA CONTAINING RAP

A THESIS  
SUBMITTED TO THE GRADUATE FACULTY  
in partial fulfillment of the requirements for the  
Degree of  
MASTER OF SCIENCE

By  
MOHAMMAD ASHIQUR RAHMAN  
Norman, Oklahoma  
2019

LABORATORY CHARACTERIZATION OF FOAMED WMA CONTAINING RAP

A THESIS APPROVED FOR THE  
SCHOOL OF CIVIL ENGINEERING AND ENVIRONMENTAL SCIENCE

BY

Dr. Musharraf Zaman, Chair

Dr. Gerald A. Miller

Dr. Rouzbeh Ghabchi

© Copyright by MOHAMMAD ASHIQUR RAHMAN 2019  
All Rights Reserved.

## **Dedication**

*“To my Parents and Family Members”*

## **Acknowledgements**

At the beginning, I would like to express my deepest gratitude to Almighty Allah (SWT) for being generous to give me the strength and the ability to accomplish this work.

I would like to express my sincere gratitude and heartiest thanks to my mentor and the chair of my thesis committee, Dr. Musharraf Zaman. I was truly inspired by Dr. Zaman's energy, passion, and commitments to add something new to the research community. It was his hardworking attitude and positive energy that encouraged me to work harder. His expert guidance, affection, encouragement and critical suggestions provided me with the necessary insight and paved the way for a meaningful ending of this thesis work. Without his constant supervision, valuable advice and suggestions, and encouragement to improve my writing skill, I would not have been able to complete my thesis work. It has been a great honor and privilege for me to work under his tutelage. He was a great mentor for my academic, social and professional endeavors. May the Almighty give him even greater rewards throughout his life.

I would like to express my deepest gratitude to Dr. Rouzbeh Ghabchi for serving on my thesis committee. His guidance and mentorship helped me to complete my thesis work. Whenever I faced any problems related to my thesis work, Dr. Ghabchi was always there to guide me. His vast depth of knowledge in the pavement arena helped me think deeply about my research work. His valuable comments also helped me improve my technical writing.

I would also like to acknowledge and thank Dr. Gerald A. Miller for serving on my thesis committee. My first graduate class at the University of Oklahoma (OU) was Dr. Miller's "In-Situ Soil Testing." I also took "Unsaturated Soil Mechanics" offered by

Dr. Miller. These classes truly helped me to enhance my knowledge in the applied science fields. I was truly inspired by Dr. Miller's practical experience and in-depth theoretical knowledge during my course work. I am truly grateful to him for sharing his valuable inputs in completing my thesis. I would also like to thank Dr. K.K. Muraleetharan, Dr. Amy B. Cerato, and Dr. Kianoosh Hatami for helping me with their diverse knowledge throughout my coursework at OU.

I also want to express my deepest appreciation to every member of the Pavement Materials and Systems Group at OU for their valuable contributions. I specially want to thank Mr. Syed Ashik Ali for helping me in different aspects of this study. His suggestions on different laboratory test methods and discussions on various research issues were a great help in completing my thesis. More than a colleague, I found him as a great friend and a brother in my life. His precious comments also helped me in improving my technical writing. I also want to thank Dr. Shivani Rani, Mr. Kenneth Hobson, Dr. Amir Arshadi, and Dr. Manik Barman for sharing their field and laboratory experiences with me. Special thanks to Mr. Sagar Ghos, and Mr. Sai Srikanth Kola for helping me in conducting some laboratory tests related to my thesis. I am truly grateful to Mr. Micheal Schmitz (Mike) for his technical support in the laboratory throughout the course of this study.

I would like to offer my sincere appreciations to the Oklahoma Department of Transportation (ODOT) and the Southern Plains Transportation Center (SPTC) for providing financial support for this study. Also, I want to acknowledge the laboratory support from Mr. Matt Romero, Mr. Kevin Sutor, and Mr. Scott Garland, all from ODOT, in conducting some tests for this study. I want to thank Silver Star Construction

Co. for providing required aggregates and binders for this study. Without their generous support, it would be very tough to complete this study.

Lastly, I want to express my respectful gratitude to my mother, Mrs. Afroja Rahman and father, Mr. Md. Aaur Rahman for their encouragement, sacrifice and support. Special thanks to my wife Mrs. Zerine Binte Alam for her endless patience, inspiration and sacrifice throughout my study.

# Table of Contents

ACKNOWLEDGEMENTS .....	IV
TABLE OF CONTENTS .....	VIII
LIST OF TABLES .....	XII
LIST OF FIGURES .....	XIV
ABSTRACT .....	XVII
CHAPTER 1: INTRODUCTION.....	1
1.1 BACKGROUND .....	1
1.2 SIGNIFICANCE OF THIS STUDY .....	7
1.3 OBJECTIVES .....	8
1.4 RESEARCH APPROACH.....	9
1.5 THESIS ORGANIZATION .....	10
CHAPTER 2: LITERATURE REVIEW.....	12
2.1 WARM MIX ASPHALT (WMA) TECHNOLOGIES .....	12
2.2 TYPES OF WMA TECHNOLOGIES .....	12
2.2.1 Organic Additive-Based WMA .....	13
2.2.2 Chemical Additive-Based WMA.....	14
2.2.3 Foamed WMA .....	14
2.2.3.1 Water-containing technologies .....	15
2.2.3.2 Water-based technologies.....	15
2.3 RECLAIMED ASPHALT PAVEMENT (RAP) .....	16
2.4 LABORATORY AND FIELD PERFORMANCE OF WMA CONTAINING RAP .....	17
2.5 CURRENT PRACTICE FOR DESIGN OF WMA CONTAINING RAP.....	20
2.6 PERFORMANCE TESTS .....	24
2.6.1 Dynamic Modulus Tests .....	25
2.6.2 Fatigue Cracking Performance Tests.....	26
2.6.3 Rutting Performance Tests .....	31
2.6.4 Moisture-Induced Damage Tests.....	34



2.7 SUMMARY .....	40
CHAPTER 3 MATERIALS AND METHODS .....	44
3.1 INTRODUCTION .....	44
3.2 AGGREGATES AND RAP .....	45
3.3 ASPHALT BINDER .....	47
3.4 ASPHALT MIXES .....	48
3.5 MIX DESIGN VOLUMETRICS.....	51
3.5.1 Volumetric Properties.....	51
3.5.2 Statistical Analysis .....	53
3.6 LABORATORY PERFORMANCE TESTS OF ASPHALT MIXES.....	54
3.6.1 Sample Preparation.....	54
3.6.2 Laboratory Testing .....	55
3.6.2.1 Dynamic Modulus (DM) Test .....	55
3.6.2.2 Louisiana Semi-Circular Bend (SCB) Test .....	57
3.6.2.3 Illinois Flexibility Index (I-FIT) Test.....	59
3.6.2.4 Abrasion Loss Test (Cantabro Test).....	61
3.6.2.5 Hamburg Wheel Tracking (HWT) Test .....	62
3.6.2.6 Flow Number (FN) Test .....	65
3.6.2.7 Indirect Tensile Strength Ratio (TSR) Test.....	67
3.6.3 Moisture Conditioning.....	68
3.6.3.1 AASHTO T 283 Method .....	68
3.6.3.2 Moisture Induced Sensitivity Test (MIST) Conditioning .....	68
3.7 HIGH-TEMPERATURE GRADING OF RECOVERED RAP BINDER .....	69
CHAPTER 4: VOLUMETRIC PROPERTIES OF FOAMED WMA CONTAINING RAP.....	73
4.1 INTRODUCTION .....	73
4.2 CURRENT FOAMED WMA MIX DESIGN PRACTICE .....	73
4.3 REDUCTION IN MIXING AND COMPACTION TEMPERATURES .....	80
4.4 SUMMARY .....	84

CHAPTER 5: LABORATORY PERFORMANCE OF WMA CONTAINING RAP.....	86
5.1 INTRODUCTION .....	86
5.2 DYNAMIC MODULUS TEST .....	86
5.3 FATIGUE CRACKING RESISTANCE.....	90
5.3.1 Louisiana SCB Test.....	91
5.3.2 I-FIT or Illinois SCB Test .....	96
5.3.3 Abrasion Loss Test .....	100
5.3.4 Ranking of Asphalt Mixes Based on Fatigue Cracking Resistance.....	102
5.4 RUTTING PERFORMANCE.....	103
5.4.1 Hamburg Wheel Tracking (HWT) Test.....	104
5.4.2 Flow Number (FN) Test .....	108
5.4.3 Ranking of Asphalt Mixes Based on Rutting Performance.....	110
5.5 MOISTURE-INDUCED DAMAGE .....	112
5.5.1 Stripping Infection Point (SIP) .....	112
5.5.2 AASHTO T 283 Method .....	114
5.5.3 MIST Conditioning.....	116
5.5.4 Visual Rating of Fractured Faces .....	118
5.5.5 Ranking of Asphalt mixes based on Moisture-Induced Damage Potential.....	122
5.6 SUMMARY .....	123
CHAPTER 6: CONCLUSION AND RECOMMENDATIONS.....	125
6.1 CONCLUSIONS.....	125
6.1.1 Volumetric Properties.....	126
6.1.2 Laboratory Performance .....	127
6.1.2.1 Dynamic Modulus Test .....	127
6.1.2.2 Cracking Properties .....	127
6.1.2.3 Rutting Properties.....	128
6.1.2.4 Moisture-Induced Damage Potential .....	129

6.2 RECOMMENDATIONS.....	130
REFERENCES.....	131
APPENDIX A: ABBREVIATION .....	151

## List of Tables

Table 2.1 List of Laboratory Tests Conducted in this Study.....	41
Table 3.1 Aggregate Components for S3 Mixes .....	46
Table 3.2 Aggregate Components for S4 Mixes .....	46
Table 3.3 Properties of the Asphalt Mixes .....	50
Table 3.4 Test Matrix for Asphalt Mixes .....	51
Table 3.5 A Summary of Volumetric Properties for Mix-1 .....	52
Table 3.6 A Summary of Volumetric Properties for Mix-5 .....	53
Table 3.7 Model Evaluation Criteria (Witczak, 2005).....	57
Table 3.8 Minimum Average FN Requirements (AASHTO, 2017) .....	66
Table 4.1 Percent Air Voids for Mix-1 and Mix-2.....	76
Table 4.2 t-Test Results at 95% Confidence Level .....	76
Table 4.3 High-Temperature PG of Recovered RAP Binder .....	77
Table 4.4 Percent Air Voids for Mix-5 and Mix-6.....	79
Table 4.5 t-Test Results at 95% Confidence Level .....	79
Table 4.6 A Summary of Statistical Results for S3 Mixes.....	82
Table 4.7 A Summary of Statistical Results for S4 Mixes.....	84
Table 5.1 Dynamic Modulus Master Curve Model Parameters.....	87
Table 5.2 Dynamic Modulus Master Curve Shift Factor Model Parameters .....	87
Table 5.3 Coefficient of Variance (%) at Different Notch Depths for S3 Mixes.....	91
Table 5.4 Coefficient of Variance (%) at Different Notch Depths for S4 Mixes.....	94

Table 5.5 Ranking of Asphalt Mixes based on Fatigue Cracking performance .....	103
Table 5.6 Rut Depths (mm) for Foamed WMA and HMA at Different Numbers of Wheel Passes .....	106
Table 5.7 Performance Parameters Obtained from HWT Tests.....	106
Table 5.8 Ranking of Asphalt Mixes Based on Rutting Resistance.....	111
Table 5.9 Fractured Faces of Asphalt Mixes, and Visual Ratings of TSR Test for Mix-1 and Mix-2.....	120
Table 5.10 Fractured Faces of Asphalt Mixes, and Visual Ratings of TSR Test for Mix-5 and Mix-6.....	121
Table 5.11 Ranking of Asphalt Mixes Based on Moisture-Induced Damage Resistance .....	122

## List of Figures

Figure 2.1 Crack Initiation at the Corner of Prefabricated Notch .....	28
Figure 2.2 Schematic Diagram Illustrating the Demonstration of Fracture Energy and Dissipated Creep Strain Energy (After Shu et al., 2012).....	38
Figure 3.1 Work Flow Diagram of the Study.....	44
Figure 3.2 Collection of Materials (a) Collection of Aggregates for Laboratory Produced Asphalt Mixes (b) Storage of Collected Aggregates .....	46
Figure 3.3 Combined Aggregate Gradation Curves (S3 Mixes and S4 Mixes) .....	47
Figure 3.4 AccuFoamer Schematic Diagram (After InstroTek <sup>®</sup> Inc., 2015).....	48
Figure 3.5 Test Setup for Semi-Circular Bend (SCB) Testing.....	59
Figure 3.6 Computation of $J_c$ Using SCB Test Results (After Kim et al., 2012a).....	59
Figure 3.7 A Typical Outcome of the Illinois-SCB Test (After Al-Qadi et al., 2015) .....	61
Figure 3.8 Abrasion Loss Test Sample (a) Before Testing (b) After Testing .....	62
Figure 3.9 HWT Saw-Cut Molded Sample After Testing.....	63
Figure 3.10 Results Showing Rut Depth vs Number of Wheel Passes .....	65
Figure 3.11 Typical Test Results for FN Tests (After Copeland et al., 2010) .....	66
Figure 3.12 Moisture Induced Sensitivity Tester (a) Photographic Image (b) Conditioning Mechanism (After Tarefder et al., 2014) .....	69
Figure 3.13 RAP Binder Extraction (a) Bowl (b) Centrifuge Extractor.....	70
Figure 3.14 RAP Binder Recovery Using Rotary Evaporator .....	71
Figure 4.1 Percent Air voids for Mix-1 and Mix-2.....	76
Figure 4.2 Percent Air voids for Mix-5 and Mix-6 .....	79

Figure 4.3 Uncoated Volumetric Samples at Lower Mixing and Compaction	
Temperatures (a) After Mixing and (b) After Compaction .....	81
Figure 4.4 Percent Air Voids for S3 Mixes .....	82
Figure 4.5 Percent Air Voids for S4 Mixes .....	84
Figure 5.1 Master Curve for Mix-1 and Mix-2 at a Reference Temperature	
of 21.1°C.....	88
Figure 5.2 Master Curve for Mix-5 and Mix-6 at a Reference Temperature	
of 21.1°C.....	88
Figure 5.3 Average Strain Energy at Failure for Mix-1 and Mix-2 .....	92
Figure 5.4 $J_c$ Values for Mix-1 and Mix-2 .....	93
Figure 5.5 Average Strain Energy at Failure for Mix-5 and Mix-6 .....	94
Figure 5.6 $J_c$ Values for Mix-5 and Mix-6 .....	95
Figure 5.7 Cracking Mechanism for (a) S3 Mixes (b) S4 Mixes .....	96
Figure 5.8 SCB Tested Specimens (a) Louisiana SCB (b) I-FIT .....	96
Figure 5.9 Load-Displacement Diagram for Louisiana SCB and I-FIT Tested	
Specimens (a) Mix-1 (b) Mix-2 (c) Mix-5 (d) Mix-6.....	98
Figure 5.10 Flexibility Index for Mix-1 and Mix-2 .....	99
Figure 5.11 Flexibility Index for Mix-5 and Mix-6 .....	99
Figure 5.12 Percent Abrasion Loss for Mix-1 and Mix-2.....	101
Figure 5.13 Percent Abrasion Loss for Mix-5 and Mix-6.....	101
Figure 5.14 Comparison of HWT graphs for Mix-1 and Mix-2.....	105
Figure 5.15 Comparison of HWT graphs for Mix-5 and Mix-6.....	105
Figure 5.16 Comparison of FN for Mix-1 and Mix-2 .....	109

Figure 5.17 Comparison of FN for Mix-5 and Mix-6 .....	110
Figure 5.18 Indirect Tensile Strength ( $ITS_{dry}$ and $ITS_{wet}$ ) and TSR ( $TSR_{F-T}$ ) Values for S3 mixes (AASHTO T 283 method) .....	115
Figure 5.19 Indirect Tensile Strength ( $ITS_{dry}$ and $ITS_{wet}$ ) and TSR ( $TSR_{F-T}$ ) Values for Mix-5 and Mix-6 (AASHTO T 283 method) .....	116
Figure 5.20 Indirect Tensile Strength ( $ITS_{dry}$ and $ITS_{MIST}$ ) and $TSR_{MIST}$ Values for Mix-1 and Mix-2 (MIST Conditioning) .....	117
Figure 5.21 Indirect Tensile Strength ( $ITS_{dry}$ and $ITS_{MIST}$ ) and $TSR_{MIST}$ Values for Mix-5 and Mix-6 (MIST Conditioning) .....	117



## ABSTRACT

For more than two decades, the asphalt paving industry has been using Reclaimed Asphalt Pavement (RAP) and various types of Warm Mix Asphalt (WMA) technologies in the production of asphalt mixes to reduce impact on the environment and promote sustainable construction. Despite their significant economic and environmental benefits, the validity of using volumetric mix design method for WMA mixes containing RAP and their performance remain a matter of concern. Among the current WMA technologies, the plant foaming technique (called “*foamed WMA*” in this study) has gained the most attention because it eliminates the need for using any chemical additives in this process. In this study, the mix design volumetrics and laboratory performances, namely rutting, cracking and moisture-induced damage potential of foamed WMA containing RAP were evaluated and compared with their Hot Mix Asphalt (HMA) counterparts. One coarse (S3) mix having a Nominal Maximum Aggregate Size (NMAS) of 19 mm and one fine (S4) mix (NMAS = 12.5 mm), containing 25% and 5% RAP, respectively, were used for evaluation.

It was found that the foaming process increased the coating ability of the binder which in turn lowered mixing and compaction temperatures for foamed WMA. Therefore, both HMA and foamed WMA exhibited similar mix design volumetrics up to certain lower mixing and compaction temperatures. However, further reduction in the mixing and compaction temperatures for foamed WMA was found to exhibit improper mixing between aggregates and binder. Also, to ensure presence of sufficient active binder from the RAP, it was found that the compaction temperature for foamed WMA

should be greater than the high-temperature Performance Grade (PG) of the extracted RAP binder.

In spite of foamed WMA exhibiting similar volumetric properties as compared to those of HMA, their laboratory performance was found to be significantly different. The foamed WMA was found to exhibit a lower stiffness compared to HMA in the dynamic modulus test. The reduced aging at lower mixing and compaction temperatures is believed to be responsible for lowering the stiffness of foamed WMA compared to HMA. Also, an increase in RAP content was found to increase the stiffness of asphalt mixes due to incorporation of aged binder from RAP. A stiffer asphalt mix is expected to exhibit lower cracking resistance and higher rutting resistance. Therefore, foamed WMA was found to exhibit higher cracking resistance compared to HMA in Louisiana Semi-Circular Bend (SCB) and Illinois Flexibility Index Test (I-FIT) tests. A similar trend in the cracking resistance was observed for coarser mixes in the Abrasion Loss Test (commonly known as Cantabro test). However, the Cantabro test could not screen finer mixes for their cracking resistance as it lacks a mechanistic basis. The coarser mixes were found to exhibit lower cracking resistance compared to finer mixes due to higher RAP content and differences in crack propagation mechanisms. The rutting performance of foamed WMA was found to be of concern as they exhibited lower resistance compared to their HMA counterparts. Coarser mixes exhibited higher rutting resistance compared to finer mixes due to higher RAP content. The foamed WMA exhibited higher moisture-induced damage potential compared to HMA. The presence of moisture from partially dried aggregates at lower WMA mixing and compaction temperatures and use of water in the foaming process were reasons for the reduction in

moisture-induced damage resistance for foamed WMA. The Moisture Induced Sensitivity Test (MIST) conditioning was found to be a better method for simulating moisture-induced damage potential of asphalt mixes than the AASHTO T 283 method. Application of adhesion cycles followed by loading cycles instead of a freeze-thaw cycle (AASHTO T 283) in the moisture conditioning process in MIST is believed to better represent field conditions. Also, increase in RAP content was found to lower moisture-induced damage potential due to strong bonding between RAP aggregate and binder. Therefore, the foamed WMA was found to increase cracking resistance, rutting potential and moisture-induced damage potential of asphalt mixes. On the contrary, addition of RAP was expected to reduce cracking resistance, rutting potential and moisture-induced damage potential. Therefore, foamed WMA containing RAP can exhibit mixed performance particularly when the RAP content is higher than certain level.

# CHAPTER

# *1*

## INTRODUCTION

### 1.1 Background

Construction of sustainable and environment-friendly transportation infrastructure results in saving natural resources, conserving the environment and reducing energy consumption (Bonaquist, 2011; Kheradmand et al., 2014; Abuawad et al., 2015; Al-Qadi et al., 2015; Zaman et al., 2019). For more than two decades, asphalt paving companies have been using Reclaimed Asphalt Pavement (RAP) and various Warm Mix Asphalt (WMA) technologies in the production of asphalt mixes and construction of flexible pavements as a part of efforts toward establishing sustainable and eco-friendly construction practices (Kim and Lee, 2006; Kim et al., 2007; Kasozi et al., 2012; Zhao et al., 2013; Guo et al., 2014; Dong et al., 2017).

The WMA technologies improve the workability of asphalt mixes using chemical additives, organic additives, and water-based or water-containing foaming processes (Bonaquist, 2011; Alhasan et al., 2014; Kheradmand et al., 2014). Both mixing and compaction temperatures of traditional Hot Mix Asphalt (HMA) can be reduced by about 20° to 40°C using these WMA technologies (Jones, 2004; Prowell et al., 2007; Rubio et al., 2012). Approximately 25 to 70% savings in energy consumption can be attained by lowering the mixing and compaction temperatures compared to HMA (Kristjansdottir, 2014). Other benefits associated with using WMA technologies

include the following: an extended paving season; reduced turnover time to traffic; improved working conditions due to lower odor, fume, and emission levels; enhanced compactability; reduced oxidative hardening of binders; and reduced cracking in pavements (Hurley et al., 2006; Gandhi et al., 2009; Rubio et al., 2012). However, WMA technologies produce relatively softer mixes than HMA due to reduced aging at lower mixing and compaction temperatures, which can cause higher pavement deformation under traffic loading (Hurley and Prowell, 2006; Hill, 2011; Bonaquist, 2011; Alhasan et al., 2014). Also, a lower mixing temperature of WMA than HMA can be responsible for partially dried aggregates and resulting a weaker bond between the asphalt binder and aggregates (Hurley and Prowell, 2005; Hurley and Prowell, 2006; Prowell et al., 2007; Wasiuddin et al., 2007; Ali et al., 2013).

Among existing WMA technologies, plant foaming (called “*foamed WMA*” in this study) is being successfully used by many contractors in Oklahoma and other states. Water is added to preheated asphalt binder as a foaming agent in the production of foamed WMA, which makes the foamed WMA more cost-effective because no chemical WMA additives are needed (Jenkins, 2000; Van et al., 2007). The water produces steam, which increases the volume of the binder and decreases its viscosity (Van et al., 2007; Zaumanis, 2010). Although production cost of foamed WMA is relatively low compared to chemical-based or organic-based WMA, concerns over the moisture susceptibility of foamed WMA due to incorporation of water and reduction in mixing and compaction temperatures have been reported by several researchers (Hurley and Prowell, 2005; Hurley and Prowell, 2006; Prowell et al., 2007).

Additionally, the utilization of RAP in asphalt mixes has increased rapidly due to its economic and environmental benefits. The availability of binder in RAP reduces the amount of virgin binder needed in producing asphalt mixes. Also, the aggregates in the RAP are reused to lower initial construction costs and preserve environmental resources (FHWA, 1997; Jones, 2008; Ghabchi, 2014; Al-Qadi et al., 2015). Due to financial and environmental benefits, most WMA and HMA used by the Oklahoma Department of Transportation (ODOT) contains RAP, when specifications allow. Also, many other state Departments of Transportation (DOTs) are in process of updating their specifications or test protocols for asphalt mixes containing RAP (Ghabchi, 2014). A study conducted by Williams et al. (2018) found that RAP usage reached 76.2 million tons in 2017, which is 36% higher than the usage in 2009. The special provision used by ODOT allows a maximum 30% binder replacement for the base course and 12% binder replacement for the surface course from RAP materials (ODOT, 2013a). However, incorporation of RAP in specifications has many challenges, such as change in binder Performance Grade (PG) due to the addition of stiffer binder, uncertainty in blending between virgin and aged binder, high amount of filler materials, quality of RAP, and lack of performance data (McDaniel and Shah, 2003; Lee et al., 2009; Al-Qadi et al., 2015; Ali, 2016). Also, while using RAP in WMA, the blending of aged binder from RAP and new binder may be hindered due to the lower mixing and compaction temperatures of WMA (Bonaquist, 2011). The amount of total blended binder (commonly known as active binder) mainly controls the mix design of asphalt mixes (Brown et al., 2009). Therefore, evaluation of mix design volumetrics of foamed WMA with different RAP contents is necessary to avoid potential problems.

Currently, no distinct mix design procedure is available for foamed WMA containing RAP. Several factors, such as aggregate gradation, binder content, number of gyrations, mixing and compaction temperatures, RAP binder grade and proper mixing of aged binder from RAP with virgin binder influence the design of WMA (Brown et al., 2009). The current state of practice for WMA mix design is to prepare a HMA mix in the laboratory according to the AASHTO R 35 method (AASHTO, 2013). This method targets the volumetric properties of four percent air voids at required number of gyrations. The number of gyrations is determined based on the anticipated traffic level (AASHTO, 2013). The same method is then used to produce foamed WMA in an asphalt plant without making modifications to the mix design (NCHRP, 2012). Also, most asphalt mix design laboratories do not own a laboratory foamer to produce foamed binder. As a result, mix designs of foamed WMA, including those containing RAP, are generally performed using the corresponding mix designs for HMA containing RAP without using a foamer. However, a combination of RAP and low mixing and compaction temperatures for WMA may lead to mixes that are more temperature sensitive compared to HMA (NCHRP, 2012).

According to Bonaquist (2011), the volumetric properties of foamed WMA may be similar to those of their HMA counterparts, when other parameters (e.g., aggregate gradation, binder content, number of gyrations and RAP content) remain constant. However, the compactability, stripping resistance, rutting resistance and cracking resistance of WMA can be significantly different from HMA (Bonaquist, 2011). Also, these characteristics become more complex with the addition of a higher percentage of RAP in asphalt mixes (Kasozi et al., 2012; Guo et al., 2014; Dong et al., 2017). A study

conducted by Zhao et al. (2013) reported that the rutting resistance was found to increase with the addition of RAP for both WMA and HMA. It was observed by Guo et al. (2014) that fatigue life of WMA decreased with the addition of RAP due to incorporation of stiffer and aged binder. Also, a decrease in moisture-induced damage potential with the increase in RAP content was reported by several other researchers due to stronger bonding between RAP aggregate and binder (Zhao et al., 2012; Shu et al., 2012; Hill et al., 2012a). On the contrary, an increase in moisture-induced damage potential was observed by Moghadas et al. (2014) and Guo et al. (2014) with the increase in RAP content. It was reported that the increase in the viscosity of asphalt binder due to the addition of RAP can increase the moisture-induced damage potential of asphalt mixes (Moghadas et al., 2014; Guo et al., 2014). Therefore, foamed WMA containing RAP might show significantly different rutting, fatigue, and moisture-induced damage performance under traffic loading and environmental conditions compared to HMA in roadway pavements.

For evaluating the rutting potential of asphalt mixes, many transportation agencies are currently using Hamburg Wheel Tracking (HWT) and Flow Number (FN) tests (Witczak et al., 2002; Lu and Harvey, 2006; Copeland et al., 2010; Grebenschikov and Prozzi, 2011; Zhao et al., 2013; Roy et al., 2015; Chaturabong, 2016). In fact, HWT test is the most common test procedure used for evaluating the rutting resistance (Lu and Harvey, 2006). Flow number (FN), another test for determining rutting resistance, is defined as the number of loading cycles related to tertiary deformation in a repeated loading test of asphalt specimen (Copeland et al., 2010). Currently, there is no general agreement on a single test method for evaluating the fatigue resistance of asphalt mixes



(Barman et al., 2018). Both Louisiana Semi-Circular Bend (SCB) and Illinois SCB, commonly known as Illinois Flexibility Index Test (I-FIT), are used by several DOTs for evaluating the fracture performance of asphalt mixes (Kim et al., 2012a; Ozer et al., 2016). Also, some transportation agencies are using Abrasion Loss Test (commonly known as Cantabro test) to check the cracking potential of asphalt mixes (NAPA, 2015; NCAT, 2017). Stiffness of asphalt mixes is generally evaluated using the dynamic modulus tests. A stiffer mix is expected to exhibit higher resistance to rutting, but more prone to cracking (Flintsch et al., 2007; Tashman and Elangovan, 2008; Singh et al., 2011; Ghabchi, 2014). Several test methods have been used by different researchers to quantify moisture-induced damage potential of asphalt mixes (Solaimanian et al., 2003; Hurley et al., 2010; Goh and You, 2011a; Weldegioris and Tarefder, 2011; Kim et al., 2012b). Among test methods, the Stripping Inflection Point (SIP) obtained from a HWT test and Tensile Strength Ratio (TSR) obtained from an Indirect Tensile Strength (ITS) test are the most commonly used parameters to evaluate the moisture-induced damage potential of asphalt mixes (Kim et al., 2012b; Abuawad et al., 2015).

Designing an asphalt mix resistant to fatigue and moisture-induced damage with an acceptable rutting performance is essential for having a sustainable pavement with long service life. The current literature lacks information about the performance of foamed WMA containing RAP. Therefore, the present study was undertaken to examine the factors affecting mix design volumetrics of foamed WMA containing RAP and to evaluate laboratory performance of such mixes pertaining to rutting, fatigue and moisture-induced damage.

## 1.2 Significance of this Study

As mentioned earlier, there are several benefits of using foamed WMA with RAP in the construction of flexible pavements. Several DOTs are currently using the same mix design methods for WMA containing RAP, which were originally developed for HMA (Bonaquist, 2011; WSDOT, 2012; Xiao et al., 2012; Malladi, 2015). Because of differences in mixing and compaction temperatures, binder properties, presence of water in foamed WMA and differences in aggregate coating quality and binder film thickness, using HMA mix design for a foamed WMA may not be appropriate. As noted earlier, the compactability, stripping potential, rutting resistance and fatigue resistance of WMA can be different from those of their HMA counterparts (Prowell et al., 2007; Wasiuddin et al., 2007; Hill, 2011; Bonaquist, 2011; Ali et al., 2013; Zhao et al., 2013). Lower mixing temperature for foamed WMA can cause inadequate utilization of RAP binder in effective binder and limit its mixing with the virgin binder (Bonaquist, 2011). It was suggested by Bonaquist (2011) that compaction temperature of WMA should be greater than the high-temperature PG of the binder recovered from RAP. Also, according to Bowering and Martin (1976), the maximum temperature difference between foamed WMA binder and aggregates should lie between 13°C to 23°C to ensure proper mixing. However, no recommendations were made for temperature differences of more than 23°C.

It is expected that reduced aging of WMA due to lower mixing temperature will produce softer mixes compared to HMA (Hurley and Prowell, 2006; Alhasan et al., 2014; Malladi, 2015). Aged binder from RAP, on the other hand, makes asphalt mixes stiffer (Shu et al., 2008; Hong et al., 2010; Zhao et al., 2013; Guo et al., 2014; Dong et

al., 2017). The level of stiffness depends on the amount of RAP used in the mix as well as other factors such as level of oxidation, type of binder used in the original mix and type of rejuvenators. A stiffer mix is expected to exhibit low resistance to fatigue cracking and strong resistance to pavement deformation or rutting (Prowell et al., 2007; Zhao et al., 2013; Guo et al., 2014). It is believed that a softer WMA mix would counteract the stiff and aged binder from RAP and balance the cracking and rutting resistance of WMA (Malladi, 2015). Also, lower mixing and compaction temperatures of foamed WMA can result in partially dried aggregates. Therefore, foamed WMA can exhibit more moisture-induced damage potential compared to HMA. On the contrary, a stronger bond between RAP binder and aggregate can increase the moisture-induced damage potential of foamed WMA. The laboratory and field performance data for WMA containing RAP, particularly for a high amount of RAP, are lacking. The present study is expected to fill this gap by generating laboratory performance data for WMA and HMA containing a high amount of RAP. The HMA mixes are regarded as control mixes in this study.

### **1.3 Objectives**

The specific objectives of the current study are listed below:

- (i) Evaluate and compare the mix design volumetrics of foamed WMA and HMA containing the same amount of RAP;
- (ii) Evaluate and compare the rutting, fatigue cracking, and moisture-induced damage potential of foamed WMA and HMA containing the same amount of RAP.

## 1.4 Research Approach

The present study was pursued to characterize the foamed WMA containing RAP using laboratory testing. Specifically, the mix design volumetric properties of WMA were compared with those of the HMA containing the same amount of RAP. A two-tail t-test was conducted to identify the difference in percent air voids statistically. Modifications to the current mix design for WMA with RAP were proposed for mixes having a statistically significant difference in percent air voids compared to control HMA. The experimental design for this study was based on the consideration that mixing and compaction temperatures control the volumetric parameters of WMA (Jones, 2004; Prowell et al., 2007; Rubio et al., 2012). In the present study, foamed WMA binder was mixed with aggregates at a temperature of as low as 95°C to observe the change in percent air voids compared to traditional HMA. Also, a temperature difference (between heated aggregates and foamed WMA binder) of up to 40°C was used to observe the mixing quality. The higher-temperature grade of the recovered RAP binder was determined to evaluate the effect of lowering WMA mixing and compaction temperatures on blending quality of aged and virgin binders.

In addition, the rutting, cracking and moisture-induced damage potential of foamed WMA containing RAP were compared with those of the HMA containing RAP. Hamburg Wheel Tracking (HWT) test and Flow Number (FN) tests were conducted to evaluate the rutting resistance of these relatively softer mixes. The fatigue cracking potential was assessed using Louisiana SCB test, I-FIT Test and Abrasion Loss or Cantabro test. The effect of loading rate and notch depth on the SCB tested samples were examined through comparison of SCB results obtained from the Louisiana and

Illinois methods. The SIP from HWT test and TSR values from two different conditioning methods were used for screening of moisture-induced damage potential of asphalt mixes. Moreover, the dynamic modulus master curves were developed for both HMA and foamed WMA containing RAP, which could be used in the mechanistic design of asphalt pavements using AASHTOWare. Experimental results showing the effect of using a high amount of RAP on the performance of asphalt mixes are expected to benefit the design of WMA containing RAP.

## **1.5 Thesis Organization**

The materials of this thesis are organized in the following order:

**Chapter 1: Introduction** – This chapter identifies the weaknesses in the existing knowledge of mix design and performance of WMA containing RAP, focusing on particularly high amounts of RAP. The background is followed by the significance of the present study, research objectives, research approach and thesis organization.

**Chapter 2: Literature Review** – Types of WMA technologies, benefits of foamed WMA and usages of RAP in conventional mixes are discussed in the first part of this chapter. Previous studies on mix design aspects, dynamic modulus, and fatigue cracking of asphalt mixes containing RAP are summarized in the second part of this chapter. The literature review is focused on rutting and moisture-induced damage potential of asphalt mixes.

**Chapter 3: Materials and Methods** – This chapter discusses the selection and collection of materials for preparing HMA and foamed WMA. The mix design approach for foamed WMA is also presented in this chapter. Descriptions of various test methods, namely Dynamic Modulus tests, Louisiana SCB test, I-FIT test, Abrasion

Loss test, HWT test, FN Test and TSR test are presented in this chapter. Determination of high-temperature PG of extracted RAP binder is also discussed.

**Chapter 4: Volumetric Properties of Foamed WMA Containing RAP –**

Analyses of Superpave<sup>®</sup> volumetric test results for both WMA and HMA containing RAP are discussed in this chapter. Effect of lowering mixing and compaction temperatures on percent air voids for foamed WMA is presented.

**Chapter 5: Laboratory Performance of WMA Containing RAP –** Dynamic

modulus values of HMA and foamed WMA are presented in Chapter 5. Fatigue cracking resistance of WMA containing RAP is discussed in this chapter. Analyses of the HWT, FN and TSR test results conducted on asphalt mixes are also presented. Additionally, the rutting, cracking and moisture-induced damage potential of foamed WMA containing RAP are compared with HMA.

**Chapter 6: Conclusions and Recommendations–** A summary of the important

findings of this study and the recommendations based on these findings are presented in this chapter. Recommendations for future studies are also included in this chapter.

The details of the abbreviations used in this thesis are included in Appendix A: List of Abbreviations.

## **CHAPTER**

# **2**

## **LITERATURE REVIEW**

### **2.1 Warm Mix Asphalt (WMA) Technologies**

Warm Mix Asphalt (WMA) technologies were first introduced in Europe about two decades ago for producing asphalt mixes at a much lower temperature than the temperature used in producing Hot Mix Asphalt (HMA) (Malladi, 2015). The initial reports of these technologies were published during 1999-2000 (Brown, 2008). In 2002, WMA technologies were introduced in the U.S. (Malladi, 2015). These technologies allow a reduction in both mixing and compaction temperatures (about 30°C) of asphalt mixes compared to traditional HMA by reducing the viscosity of asphalt binder. Reduced mixing and compaction temperatures lead to major savings in fuel cost, reduced emission of greenhouse gases, and better workability of mixes at a lower temperature (NCHRP, 2012; AASHTO, 2013; NCHRP, 2013; ODOT, 2013b). However, WMA technologies are expected to produce relatively softer mixes due to a lower degree of aging at lower mixing and compaction temperatures. WMA can cause higher rutting under traffic loading than HMA (Hurley and Prowell, 2006; Hill, 2011; Bonaquist, 2011; Alhasan et al., 2014).

### **2.2 Types of WMA Technologies**

Based on the production process or the type of additive, WMA is commonly classified into the following types: (i) organic additive-based process; (ii) foaming

process; and (iii) chemical additive-based process (Rubio et al., 2012). The commonly used WMA organic additives are Fischer-Tropsch synthesis wax, fatty acid amides, and Montan wax (Kheradmand et al., 2014). Based on the water addition process, the foaming process can be sub-divided into the following categories: (a) Water-containing technologies; (b) Water-based technologies. The emulsification agents or polymers are generally used for chemical-based WMA technologies (Rubio et al., 2012; Kheradmand et al., 2014).

### **2.2.1 Organic Additive-Based WMA**

In this technology, waxes are augmented by organic additives in the mix. When temperature exceeds the melting point of a wax, a reduction in the viscosity of the binder is observed (Zaumanis, 2010; Kheradmand et al., 2014). As the mix cools down, these additives transform into microscopically small and uniformly dispersed solid particles, which work in the same manner as fiber-reinforced materials by increasing the stiffness of the binder. It was suggested by Silva et al. (2010) that the type of wax should be selected cautiously to avoid possible temperature-related issues. Specifically, difficulties may arise if the wax has a higher melting point than the mixing temperature. Waxes used in this technology consist of high molecular hydrocarbon chains with a melting point of 80°C to 120°C and can modify the workability of the binder (Rubio et al., 2012). The temperature at which the wax melts is basically controlled by the length of the carbon chain (Bueche, 2009). In practice, two to four percent wax is added to a mix based on the total mass of the binder. This WMA technology was developed around late 1980s (Rubio et al., 2012).



### **2.2.2 Chemical Additive-Based WMA**

A chemical additive-based WMA involves the use of chemicals in the asphalt binder to reduce mixing and compaction temperatures. These additives are mixed with the asphalt binder before mixing asphalt binder with aggregates. Based on the given circumstances, different types of chemical additives can be used. They generally include a combination of surfactants, polymers, emulsifying agents, and adhesion promoting additives (i.e., antistripping agents) to improve workability, coating, and compaction (Rubio et al., 2012). For example, by using the chemical additive Rediset™, a reduction in both mixing and compaction temperatures of up to 30°C can be achieved. Another commonly used additive, Evotherm, can reduce the mixing and compaction temperatures up to 85°C (Rubio et al., 2012; Kheradmand et al., 2014). The surface-active chemical polymer, Revix, can reduce both mixing and compaction temperatures up to 25°C (Rubio et al., 2012).

### **2.2.3 Foamed WMA**

Foamed WMA involves adding a small amount of water at a high temperature by either injecting it into the binder or directly adding to the mixes (Larsen, 2001). A large volume of foam is generated by the addition of water, which temporarily increases the volume of the binder and reduces its viscosity. The existence period of the foam can vary depending upon the technology used in producing the foamed binder. The workability and coating ability of the asphalt binder is generally improved by this foaming process (Rubio et al., 2012). Water is usually injected at a rate of approximately one to two percent by the weight of binder (Butz et al., 2001). The optimum water content is determined based on two major factors: maximum expansion

ratio of foamed binder; and half-life of the maximum expansion (Maccarrone et al., 1994; Muthen, 1998; Yongjoo and Lee, 2006). The expansion ratio is defined as the ratio between the maximum volume attained in the foamed state and the final volume of the binder once the foam has dissipated (Muthen, 1998). The term “*half-life*” is defined as the time in seconds it takes for the foam to become half of the maximum volume of the foamed asphalt (Maccarrone et al., 1994; Muthen, 1998; Yongjoo and Lee, 2006). Generally, at a temperature above 150°C a good foaming of asphalt binder can be achieved. An increase in the expansion ratio and reduction in the half-life are expected with increasing foaming temperature and water, which is not desirable for the foamed asphalt. At a temperature of 170°C, an air pressure of 400 kPa, and a water pressure of 500 kPa, an optimum amount of water for foaming is found as 1.3% (Kim and Lee, 2006). Based on the water addition process, foamed WMA is further classified into following groups:

#### *2.2.3.1 Water-containing technologies*

In this process, synthetic zeolite is used to produce foamed WMA. It is basically the aluminosilicates of alkali metals and contains approximately 20% water by weight. With increasing temperature, water is released from the crystalline zeolite structure, creating a micro-foaming effect on the mixes (Rubio et al., 2012). This foaming process can last up to seven hours (Chowdhury and Button, 2008; D’Angelo et al., 2008).

#### *2.2.3.2 Water-based technologies*

In this foaming method, water is used directly. Normally water is injected in the heated binder using special nozzles. In this process, a large amount of foamed binder is generated, while water vaporizes (Zaumanis, 2010). Generally, a mechanical foamer

with temperature and pressure controlling system is used to produce water-based foamed WMA.

### **2.3 Reclaimed Asphalt Pavement (RAP)**

RAP is generated when asphalt pavements are milled for reconstruction or resurfacing (FHWA, 1997; ICT, 2007). Among various recycled materials, RAP is the most widely used recycled material by the asphalt industry (Sengoz and Oylumluoglu, 2013). Utilization of RAP in asphalt mixes is beneficial because it reduces cost, reduces the need for virgin asphalt binder and reduces the use of virgin aggregates in asphalt mixes. Also, it preserves natural resources and the environment.

A survey conducted by Williams et al. (2018) indicated a dramatic change in RAP use from 2009 to 2017. The yearly RAP consumption in the asphalt industry increased from 56 million tons to 76.2 million tons within 2009 to 2017 (Williams et al., 2018). A survey conducted by Ghabchi et al. (2016) found that the use of RAP was permitted by the state DOTs in constructing about 95% interstate highway, 90% state highway and 90% city roads. The usage of RAP by the paving industry continues to increase in recent time. Based on the literature, 3.4 million tons of RAP was used as aggregate and 102.1 million tons of RAP was stockpiled for future use in 2017 (Williams et al., 2018). However, there are some technical issues that need to be addressed in order to incorporate RAP in asphalt mixes.

Technical issues are equally important in using RAP in new mixes. For example, the binder type, production location, and construction temperature should be considered in the selection of recycling techniques (Dinis-Almeida et al., 2012). A national survey conducted by Jones (2008) listed storage management, binder class and mix property as

major issues in deciding the amount of RAP that can be safely used in new mixes. Storage management issues consist of unknown material properties, inconsistent gradation of aggregates and processing requirement. Binder issues include compaction problem, unknown grade of blended binder and bumping of binder grade due to blending with the RAP binder. The RAP binder was found to be six to eight times more viscous than the virgin binder (Hossain et al., 2013). Lastly, mix issues involve uncertainty in fatigue cracking and rutting performance, variability in RAP source and early failure concerns (Jones, 2008). Therefore, laboratory and field performance evaluation of asphalt mixes containing RAP is important in the design of WMA containing a high amount of RAP. The current study aims to address these issues.

## **2.4 Laboratory and Field Performance of WMA Containing RAP**

Although the volumetric properties of foamed WMA can be similar to those of their HMA counterparts, the compactability, stripping, rutting, and fatigue cracking resistance of WMA can be different from those of HMA (Bonaquist, 2011). Also, adding RAP to new asphalt mixes make the characteristics of such mixes more complex.

Laboratory performance of WMA containing high amounts or percentages of RAP was evaluated by Zhao et al. (2013). The WMA was found to exhibit lower rutting resistance compared to HMA regardless of the WMA technology, RAP content, and structural layer. The rutting resistance of both WMA and HMA was found to increase with the increase in RAP content. The use of RAP, however, had a greater favorable effect on the rutting resistance of HMA than the corresponding WMA. The results of

TSR tests indicated that the moisture-induced damage potential in base layer remained a concern for foamed WMA containing RAP (Zhao et al., 2013).

The rutting and cracking resistance of WMA containing RAP was evaluated in the laboratory by Guo et al. (2014). Addition of RAP was found to increase the rutting resistance of WMA. This was mainly attributed to an increase in stiffness of the blended binder due to increase in RAP content. This stiffer binder was found to increase the dynamic modulus of asphalt mixes. A slightly better rutting resistance was observed for WMA containing S-I additives (developed in China, as a chemical surfactant additive) compared to WMA containing Evotherm-DAT additives, regardless of the RAP amount. In their study, Bending Beam tests were conducted to evaluate the low temperature (-10°C) cracking resistance of WMA. In that test, asphalt beam shaped samples were monotonically loaded along mid-span at a constant rate of 50 mm/min. It was reported that the cracking resistance decreased with the addition of RAP. Also, TSR and fatigue life of the WMA were found to decrease with the increase in RAP content. The fatigue life was defined as the number of load applications required to propagate a dominant flaw in the mix. Therefore, increase in RAP content was expected to make WMA more prone to fatigue cracking.

Effects of temperature reduction, foaming water content, and aggregate moisture content on the performance of WMA were studied by Ali et al. (2013). It was observed that with the reduction in mixing and compaction temperatures, the foamed WMA became more susceptible to rutting and moisture-induced damage. Therefore, a maximum reduction of 16.7°C temperature from the HMA mixing and compaction temperatures was recommended for the foamed WMA. However, increasing foaming

water to 2.6% of the weight of asphalt binder did not have any negative effect on the foamed WMA with respect to rutting and moisture-induced damage performance.

Low-temperature cracking performance of foamed WMA was characterized by Alhasan et al. (2014). The production process of WMA and asphalt binder type were found to control the low-temperature cracking performance of WMA. In their study, Bending Beam Rheometer (BBR) tests were conducted to evaluate the low-temperature performance of two asphalt binders (PG 70-22 and PG 64-28), and the low-temperature cracking behavior of the asphalt mixes was evaluated with the thermal stress restrained specimen test (TSRST) on Pressure Aging Vessel (PAV) conditioned specimens. The TSRST tests were conducted on cylindrical specimens to determine the fracture temperature and tensile strength of asphalt mixes, while cooling at a constant rate according to AASHTO TP 10 (AASHTO, 1993). A PAV was used to simulate long-term aging of binder in the field. The BBR test results were found to be less conservative than the TSRST results. The fracture temperatures for short-term aged specimens were found to be approximately 2.5°C to 6.5°C lower than the long-term aged specimens in the TSRST tests. Therefore, the low temperature cracking resistance of asphalt mixes was found to decrease gradually with aging. Overall, PG 64-28 binder showed relatively higher low-temperature cracking performance compared to PG 70-22 in the TSRST test. Also, for short-term aging the HMA exhibited a slightly better low-temperature cracking performance compared to WMA. However, similar cracking resistance was observed for both mixes at long-term aging condition.

The microstructure and rutting resistance of foamed WMA and HMA prepared with various amounts of RAP binder contents (0, 20, 40, 60, and 80% by weight of

binder) were studied by Dong et al. (2017). It was found that with an increase in the RAP binder content, both the foamed WMA and HMA became stiffer. However, the extent of increase in stiffness was more pronounced for HMA than that of foamed WMA. Therefore, a more prominent increase in rutting resistance and reduction in workability were expected for HMA compared to foamed WMA with the addition of RAP binder.

A field study conducted by Wielinski et al. (2009) suggested that both HMA and WMA performed equally in the arid Southern California climate and subjected to heavy traffic loads. After two weeks of service, WMA pavements seemed to be darker in appearance compared to their HMA counterparts (Wielinski et al., 2009). Sargand et al. (2011) and Prowell et al. (2007) also reported similar field performance for both WMA and HMA. An excellent rutting resistance in the field was observed for two WMA and one HMA pavement sections after the application of 515,333 Equivalent Single-Axle Loads (ESAL) over a 43-day period (Prowell et al., 2007). The aforementioned reviews indicate a need for additional laboratory and field investigations to evaluate the performance of WMA containing RAP.

## **2.5 Current Practice for Design of WMA Containing RAP**

No distinct mix design procedure is available for foamed WMA containing RAP until now. Several factors, such as aggregate gradation, binder content, number of gyration, mixing and compaction temperatures, RAP binder grade and proper mixing of aged binder from RAP with virgin binder influence the mix design of asphalt mixes (Brown et al., 2009). The current state of practice for WMA mix design is to prepare a HMA in the laboratory according to the AASHTO R 35 method (AASHTO, 2013).

The AASHTO R 35 method is used to determine if the prepared HMA sample has a proper amount of air voids and binder to ensure performance (AASHTO, 2013). A higher air voids can cause an adverse effect on the durability of asphalt pavements. Adequate stiffness is needed to prevent vertical deformation or rutting under traffic loading. Also, asphalt mixes should contain an optimum amount of asphalt binder to ensure durability and control excess rutting (Brown et al., 2009). The AASHTO R 35 mix design method is based on the volumetric properties of the asphalt mixes in terms of the Air Voids (AV), Voids in the Mineral Aggregate (VMA), and Voids Filled with Asphalt (VFA). The air voids can be defined as the total volume of small pockets of air in compacted asphalt mixes. The total available voids in the compacted aggregate batch is defined as VMA, and VFA represents the percent of VMA filled with asphalt binder. The gradation of aggregates is selected in such a manner to keep the VMA and VFA values within certain limits. The optimum asphalt content of compacted asphalt mixes is determined based on the volumetric properties of four percent air voids at required number of gyration. The number of gyration is determined based on the anticipated traffic level of the pavement (AASHTO, 2013).

A similar method is then used for the production of foamed WMA in an asphalt plant without making modifications or changes to the mix design (NCHRP, 2012). Most asphalt mix design laboratories do not own a foamer to produce foamed binder. As a result, mix designs of foamed WMA, including those containing RAP, are generally performed using the corresponding mix designs for HMA containing RAP without using a foamer. However, a combination of RAP and low mixing and compaction temperatures for WMA may lead to mixes that are more temperature sensitive than



HMA (NCHRP, 2012). Therefore, verifications of mix design volumetrics are necessary for WMA containing RAP.

Similar volumetric properties of both foamed WMA and HMA were reported by several researchers (Hurley and Prowell, 2006; Wielinsk et al., 2009; Jones et al., 2010; Bonaquist, 2011; Malladi, 2015). It was observed by Bonaquist (2011) that the mix design parameters of asphalt mixes were governed by the aggregate structure, if the absorbed binder content is less than 1%. The term absorbed binder is defined as the percent of total binder absorbed by permeable pores of aggregates in asphalt mixes (Brown et al., 2009). Also, two hours of aging time at compaction temperature was suggested for WMA containing RAP after mixing. Furthermore, a compaction temperature higher than the high-temperature PG of the recovered RAP binder was proposed to ensure proper mixing between the aged and virgin binders in WMA. However, in that study no separate mix design procedure was suggested for WMA containing RAP by Bonaquist (2011), although asphalt mixes with up to 40% RAP content was considered. Therefore, it is possible that the RAP binder may not be fully engaged in the new mix containing high RAP (greater than a certain amount, e.g., 40%).

Several other studies were conducted to determine suitable mixing and compaction temperatures for foamed WMA (Bowering and Martin, 1976; Jenkins et al., 1999; Hurley and Prowell, 2006; Abbas and Ali, 2011; Bonaquist, 2011). It was suggested by Bowering and Martin (1976) that the temperature difference between foamed WMA and aggregates should lie between 13°C and 23°C to ensure proper mixing. At a higher temperature gradient, the collapse of foam in contact with aggregates becomes more rapid due to quick heat transfer (Jenkins et al., 1999).

Additionally, preheating of aggregates was found to improve the distribution of foamed binder in asphalt mixes. However, the compaction quality of asphalt mixes was found to be controlled by compaction temperature and binder viscosity, whereas aggregate temperature was found to have an insignificant effect (Jenkins et al.,1999).

Furthermore, the workability of foamed WMA was found to be higher than the control HMA even at 17°C lower mixing and compaction temperatures (Abbas and Ali, 2011).

The optimum water and asphalt content for foamed WMA were studied by Kim and Lee (2006). It was found that a good foaming of asphalt could be achieved at a temperature of 150°C or above. More specifically at 170°C temperature under an air pressure of 400 kPa and water pressure of 500 kPa, a water content of 1.3% by weight of binder was found to produce optimum foaming. Hence, it was called “*optimum foaming water content.*”

The mix design aspects of foamed WMA containing RAP were investigated by Kuna et al. (2017). It was suggested that the extracted aggregates from RAP exhibited more uniform gradation than RAP’s aggregates before asphalt recovery. The results from ITS tests were considered as mechanical properties of asphalt mixes in that study. The optimum mechanical properties were found at 4% and 3% foaming water contents for virgin aggregate mix and 75% RAP mix, respectively. A clear optimum foaming water content was not found for mixes with 50% RAP with respect to mechanical properties.

The Superpave<sup>®</sup> mix design aspects of WMA containing various amounts of RAP were studied by Xiao et al. (2016). In their study, both Evotherm and foamed WMA were considered in evaluating the volumetric properties. An increase in the

viscosity of asphalt binder was observed with the addition of RAP. Also, the VMA value increased with an increase in RAP content. Furthermore, dust to asphalt ratio decreased with the reduction in RAP amount. No significant effect was found on the binder viscosity due to incorporation of Evotherm. The air voids in the optimum asphalt binder analysis were observed to vary depending on the WMA technology and binder source. Also, similar optimum binder content was found for both foamed WMA and control HMA. However, WMA mix with Evotherm was found to exhibit slightly higher values of optimum binder content. (Xiao et al., 2016).

Because of factors noted above including differences in mixing and compaction temperatures, binder properties, presence of water in foamed WMA and differences in aggregate coating quality and binder film thickness, use of HMA mix design method for a foamed WMA is expected to produce mixes with noticeably different performance. Therefore, it is important to consider both mix design volumetrics and laboratory performance for assessment of foamed WMA containing RAP, which was the primary goal of this study.

## **2.6 Performance Tests**

As noted earlier, WMA technologies are expected to produce softer asphalt mixes due to a lower degree of aging (Hurley and Prowell, 2006; Alhasan et al., 2014; Malladi, 2015). Addition of RAP, however, is expected to increase the stiffness of asphalt mixes (Shu et al., 2008; Hong et al., 2010; Zhao et al., 2013; Guo et al., 2014; Dong et al., 2017). Therefore, the overall properties and performance of foamed WMA is expected to be dictated by these competing influences. Several test methods have been followed by different researchers to evaluate performance of asphalt mixes in the

laboratory. Some of the common performance tests to quantify fatigue, rutting and moisture-induced damage potential of asphalt mixes are discussed next.

### **2.6.1 Dynamic Modulus Tests**

Dynamic modulus is an important contributor to laboratory and field performance of asphalt mixes (Flintsch et al., 2007; Tashman and Elangovan, 2008; Singh et al., 2011; Ghabchi, 2014). Stiffness of asphalt mixes is often evaluated by dynamic modulus. A stiffer mix is expected to exhibit higher resistance to rutting, but more prone to cracking (Flintsch et al., 2007; Tashman and Elangovan, 2008; Singh et al., 2011; Ghabchi, 2014).

Also, dynamic modulus is considered a key material input parameter in the Mechanistic-Empirical Pavement Design Guide (M-EPDG) software or AASHTOWare (Li et al., 2008; AASHTO, 2004). The M-EPDG software is used frequently by pavement engineers for designing asphalt pavements (Huang, 2004; Coree et al., 2005; Li et al., 2011). The M-EPDG is based on the principles of engineering mechanics and considers traffic, climate, pavement structure and material properties as input parameters (Huang, 2004; Li et al., 2011). In this software, pavement responses, such as stress and strain, are evaluated as the output parameters (Huang, 2004). Implementation of this design requires mechanistic input parameters of asphalt mixes and other materials. Lack of specific input parameters is one of the major issues faced by many state DOTs in implementing mechanistic empirical design method (Ghabchi, 2014). For all levels of input (Level 1, Level 2 and Level 3), dynamic modulus is used to characterize the stiffness of asphalt mixes.

The rutting resistance of WMA containing RAP was evaluated using dynamic modulus and Flow Number (FN) tests by Copeland et al. (2010). The WMA was found to show relatively low stiffness in the dynamic modulus test compared to control HMA containing the same amount of RAP. As a result, relatively lower FN values were observed for WMA compared to their HMA counterparts. Also, WMA is expected to be more prone to rutting than HMA.

### **2.6.2 Fatigue Cracking Performance Tests**

Fatigue cracking is one of the common distresses in asphalt pavements caused by thermal gradients and traffic loading (Colombier, 1997; Baek J., 2010; Moreno and Rubio, 2013). The mastic type (composed of asphalt binder, filler and fine aggregate fraction) plays an important role in reducing fatigue cracking of asphalt mixes. The cracking process in asphalt mixes usually starts in the mastic and propagates through the mix (Jenq and Perng, 1991; Kim and Little, 2005; Dave et al., 2007).

A survey conducted by Barman et al. (2018) revealed that many DOTs do not perform fatigue tests for screening of asphalt mixes during the design phase due to lack of trained personnel, unavailability of proper equipment and lack of consensus on the most suitable test method. It was found that ITS is the most commonly used fatigue test method for many DOTs. Barman et al. (2018) proposed a new parameter called fatigue index ( $f_i$ ), based on the ITS test data, for screening of mixes. The test results indicated that  $f_i$  can differentiate the fatigue resistance of different asphalt mixes in an effective way. Finer mixes with modified binders were found to show better cracking resistance compared to coarser mixes with unmodified binders.

Effect of RAP content on the fatigue resistance of HMA was evaluated by Shu et al. (2008). In their study, ITS and BBR tests were conducted to evaluate the fatigue resistance of HMA containing 0%, 10%, 20%, and 30% RAP. From ITS test results, incorporation of RAP was found to increase the stiffness of HMA. It was reported that the fatigue life of a mix may be compromised due to the addition of RAP. Also, increasing the RAP amount from 0% to 30% was found to reduce the fatigue life. This was mainly attributed to an increase in the brittleness of the HMA due to increased RAP content.

It was reported by several researchers that the Semi-Circular Bend (SCB) test method can be used successfully for evaluation of fatigue cracking of asphalt mixes (Abuawad et al., 2015, Pirmohammad and Ayatollahi, 2014; Kim et al., 2012a; Biligiri et al., 2012; Ozer et al., 2016; Wu et al., 2005). It is evident from the literature that SCB test was originally developed for the characterization of rock (Mull et al., 2002). Subsequently, this test was adopted for evaluating asphalt mixes for fracture resistance (Mull et al., 2002). In this test, a load is applied monotonically on a semi-circular asphalt sample till failure. This test could be used to test both field cores and laboratory compacted samples. It was reported that the remaining life of asphalt pavements can be predicted by using the fracture mechanics of SCB tests (Biligiri et al., 2012).

A fatigue test based on the measurement of the critical strain energy release rate ( $J_c$ ) in SCB samples with different notch depths was suggested by Kim et al. (2012a). Three different notch depths, namely 25.4, 31.8, and 38.0 mm, were used to develop a linear regression correlation between strain energies and notch depths for each mix. Three semi-circular specimens were prepared for each notch depth. The specimens were

loaded monotonically at a rate of 0.5 mm/min and tested until failure. A good correlation was observed between fatigue performance of asphalt pavements in the field and  $J_c$  values. Asphalt mixes with polymer-modified asphalt binders were found to exhibit greater fracture resistance than those containing non-modified asphalt binders. Moreover, the results from that study indicated that a reduction in mixing and compaction temperatures of WMA did not adversely affect the fracture resistance.

Finite element method (FEM) was used to model notched SCB tests by Huang et al. (2013) and used to evaluate the fracture resistance of asphalt mixes. In FEM model, the fracture mechanics approach was used to characterize the fatigue damage. It was observed that, due to stress concentrations, the crack in the notched specimen does not initiate at the center of the cut but close to one of the corners of the notch (Figure 2.1).

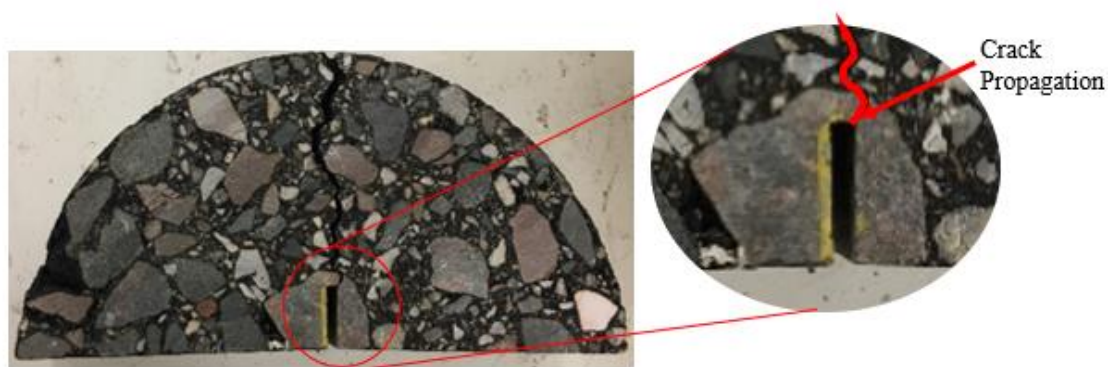


Figure 2.1 Crack Initiation at the Corner of Prefabricated Notch

Therefore, an asymmetric mesh was considered because the sample was not symmetric, once the crack is initiated at either of corner of the notch. The results also indicated that the asphalt binder plays an important role in the fracture performance of a mix. Significant improvements in the fracture resistance of the asphalt mixes were observed with the addition of suitable additives in the asphalt binder.

To evaluate fracture potential of asphalt mixes I-FIT (commonly known as Illinois SCB) test was proposed by Ozer et al. (2016). It was suggested that the I-FIT test be performed at a temperature of 25°C and a loading rate of 50 mm/min due to reasonable repeatability of results under these conditions. An increase in fracture strength with increased displacement rate was found up to a certain limit. After that, an adverse effect on fracture energy was observed with the increase in loading rate. Also, dissipation of the crack towards the outer side of the specimen was observed as the specimen turns into softer material with the increase in testing temperature. It was reported by Khan (2016) that asphalt mixes become too soft to contribute to fracture energy after 25°C. Therefore, 25°C testing temperature and faster displacement rate (50 mm/min) were suggested to evaluate the cracking resistance of asphalt mixes (Ozer et al., 2016). In their study, a good correlation between the I-FIT test and Texas overlay test results was observed.

An index, called Flexibility Index (FI) was proposed by Ozer et al. (2016) to characterize fatigue cracking of asphalt mixes. According to that study, the FI depends on the total fracture energy and post-peak slope of the load-deformation curve, discussed in Chapter 3. The FI values of laboratory-produced mixes varied between 2 to 10. A higher FI value indicates a ductile material and vice versa. According to Ozer et al. (2016), asphalt mixes with FI values greater than 6.7 can be classified as “best performing,” while mixes with FI values less than 2 can be considered “poor performing.” Mixes with values between 2 and 6.7 are expected to exhibit “intermediate performance,” relative to fatigue cracking.



Many researchers have considered Abrasion Loss Test (commonly known as Cantabro test) as a potential candidate for evaluating cracking resistance of asphalt mixes (Mallick, 2000; Mo et al., 2009; Shaowen and Shanshan, 2011; NAPA, 2015; NCAT, 2017). A study conducted by Doyle and Howard (2011) suggested that Mass Losses (ML) in the Cantabro test decreased linearly with an increase in asphalt content and reduction in percent of air voids. The Cantabro test is commonly used to check the durability of open graded asphalt mixes. In their study, this test was used to check the durability of dense graded asphalt mixes. The mean ML of specimens was found to be no greater than 15% for seven tested un-aged surface mixes. Moreover, repeatability of test results was observed for all seven asphalt mixes.

Shaowen and Shanshan (2011) used Cantabro tests to measure cracking resistance of long-term aged and unaged asphalt mixes. The test results indicated a good correlation between the Cantabro ML and the 5°C ductility for the asphalt binder. The ML for the freeze-thaw conditioned aged specimens was found to be much higher (about 70% to 80%) than the standard conditioned aged specimens (about 15% to 25%) for all types of asphalt mixes.

From the above reviews it is evident that no unique test method is available yet for characterization of asphalt mixes for fatigue cracking. Different agencies are currently using different test methods to characterize cracking resistance of asphalt mixes. In the present study, both Louisiana SCB and I-FIT tests were used to evaluate the fracture performance of asphalt mixes (WMA and HMA). Also, Cantabro test was used for characterization of fracture performance, in view of its simplicity and cost-effectiveness.

### **2.6.3 Rutting Performance Tests**

To evaluate the rutting potential of asphalt mixes, many transportation agencies have been using Loaded Wheel Tester (LWT). Repeated wheel loading is applied in LWT for simulating field traffic condition. Different types of LWTs are currently being used for accelerated evaluation of rutting potential of asphalt mixes, which include Georgia Loaded Wheel Tester, Hamburg wheel tracking (HWT) device, Asphalt Pavement Analyzer (APA) and Purdue University Laboratory Wheel Tracking Device (PURWheel) (Miller et al., 1995; Choubane et al., 2000; Cooley et al., 2000; Corte, 2001; Kandhal and Cooley, 2002).

The effectiveness of HWT tests to determine the moisture sensitivity of asphalt mixes and to predict field rutting performance was evaluated by Lu and Harvey (2006). From that study, it was found that the correlation between HWT test results and actual field performance was influenced by the binder type of asphalt mixes. Better predictions of field performance were found for mixes containing polymer-modified binders than mixes containing non-modified binders. The field rutting performance was overestimated for binders with no polymers.

The rut depths obtained from the HWT tests were compared with the rut depths from the M-EPDG by Grebenshikov and Prozzi (2011). The results of two types of asphalt mixes from a previous project in Texas were used for this purpose. Each mix was prepared using five different binder contents and three different aggregate gradations, namely fine, target and coarse. It was found that both the M-EPDG and the HWT tests ranked the mixes in a similar manner.

Effect of test temperature on HWT rut depths was evaluated by Sel et al. (2014). Statistical analyses of collected data showed that the binder grade is an influential factor on HWT-based rut performance. Asphalt mixes containing binders with a higher PG grade were found to exhibit higher resistance to rutting than those containing binders with a lower PG grade. Significant differences in performance were observed when the samples were tested at 40° and 50°C, indicating a high sensitivity of rutting to test temperature.

To attain consistent results in the HWT test some important provisions were suggested by Tsai et al. (2016). From the 2-D Micro Mechanical Finite Element (MMFE) model, it was suggested that the specimens should be glued together during HWT testing to ensure full bonding of cylindrical specimens. Otherwise, localized failures may occur around the joint. From the MMFE analyses, it was found that segments less than 120 mm wide can result in lower rut depths due to shape effect. It was also observed that rutting in slab specimens occurred at a faster rate than that in glued cylindrical specimens. Therefore, an agency may not allow cylindrical and slab specimens simultaneously in a given project. Lastly, it was suggested that the Weibull three stage curve fitting could be used to fit HWT rutting evolution curve. The Stripping Inflection point (SIP) can be determined more effectively using this method than the traditional SIP suggested in AASHTO T 324 (AASHTO, 2014c). The SIP indicates the starting point of tertiary deformation of asphalt specimens.

An image processing software, Image Processing and Analysis System 2 (IPAS<sup>2</sup>), was used by Chaturabong, and Bahia (2017) to identify the mechanism(s) responsible for permanent deformations or rutting in asphalt mixes in dry HWT tests.

An increase in contact/proximity zones between aggregates was observed during the initial creep stage due to load application. In the secondary creep stage, the aggregate structure was found to begin dilating due to deformation along the loading directions and shifting to the sides. At this stage, the aggregate structure was still in a stable condition and no significant reduction in proximity zone was observed. In the tertiary stage, however, the aggregate structure was observed to dilate completely. The failure in the mix in the dry HWT test was mainly attributed to localized deformation in the mix skeleton showing failure criteria similar to that observed in the confined and unconfined FN test (AASHTO, 2017).

Also, the FN test was considered by several researchers to characterize the rutting resistance of asphalt mixes (Witczak et al., 2002; Copeland et al., 2010; Zhao et al., 2013; Roy et al., 2015; Chaturabong, 2016). The FN can be defined as the number of load cycles related to the minimum rate of change in permanent axial strain in a repeated loading test of asphalt specimen (Copeland et al., 2010). Specifically, FN is the number of repeated load cycles an asphalt specimen can resist before it starts to flow (Brown et al., 2009). This test is also commonly known as Repeated Load Permanent Deformation (RLPD) test when conducted without confinement and known as Triaxial Repeated Load Permanent Deformation (TRLPD) when performed with minor principal stresses (Brown et al., 2009). The Francken's (1977) model is most commonly used to differentiate the permanent strain versus load cycles curve and to identify the minimum value on the fitted curve (Biligiri et al., 2007).

In a study conducted by Kaloush et al. (2003), it was reported that both confined and unconfined FN values correlate well with the field rutting performance. In that

study, optimum binder content of asphalt mixes was suggested based on the maximum FN values. Also, an increase in FN value was observed with the reduction in percent air voids. This trend was found to be consistent even for mixes with air voids less than the “critical threshold” values of 2-3% (Kaloush et al., 2003).

Walubita et al. (2012) evaluated three laboratory tests, namely Dynamic Modulus, RLPD, and HWT, for characterizing permanent deformations or rutting of HMA relative to the field performance. Repeated compressive haversine loading was applied in RLPD tests to determine the viscoelastic properties of asphalt mixes. Repeated sinusoidal dynamic compressive loading at different temperatures and frequencies was applied on unconfined specimens during dynamic modulus testing. All three test methods were found to show consistent results in terms of rutting. Also, the Superpave<sup>®</sup> mixes were found to exhibit higher moduli values with greater resistance to rutting than the conventional mixes. Overall, the HWT test was found to exhibit the best repeatability and the lowest variability in results compared to the dynamic modulus and RLPD tests. It was suggested that the HWT test can be used for routine stripping assessment and rutting performance prediction of HMA (Walubita et al., 2012).

#### **2.6.4 Moisture-Induced Damage Tests**

Due to reduction in mixing temperatures many researchers have concern over the moisture-induced damage potential of WMA (Hurley and Prowell, 2005; Hurley and Prowell, 2006; Prowell et al., 2007; Wasiuddin et al., 2007; Ali et al., 2013). Reducing mixing temperatures may produce partially dried aggregates, resulting in weaker bond between asphalt binder and aggregates. Ali et al. (2013) suggested a longer drying period for aggregates in case of WMA so that the entrapped water can escape. It was

observed that moist aggregates increased the potential for moisture-induced damage for WMA, leading to inadequate aggregate coating in presence of water (Ali et al., 2013). Moreover, for water-based WMA technologies water is injected directly in the asphalt binder to produce foamed WMA binder. As a result, water-based foaming can increase the moisture-induced damage potential of asphalt mixes (Xu et al., 2017). Several researchers have reported that at testing temperatures below 100°C, foamed WMA have lower dry and moist ITS values compared to control HMA, although both foamed WMA and control HMA may show similar TSR values (Kavussi and Hashemian, 2012; Ali et al., 2013; Sebaaly et al., 2015). Some other researchers, however, did not find any major differences between moisture-induced damage potential of foamed WMA and HMA (Punith et al., 2012; Xiao et al., 2012; Hailesilassie et al., 2015). It is believed that moisture susceptibility of WMA primarily depends on the technology used in producing these mixes (Ghabchi, 2014; Xu et al., 2017). Overall, additive content and mixing temperature are considered crucial factors for WMA, relative to moisture susceptibility (Xu et al., 2017).

Effect of RAP content on the moisture-induced damage potential of WMA was studied by several researchers (Zhao et al., 2012; Shu et al., 2012; Hill et al., 2012a; Moghadas et al., 2014; Guo et al., 2014). The results from these studies were sometime contradictory. Some researchers found a decrease in moisture-induced damage potential with the increase in RAP content due to stronger adhesive bonding between RAP aggregate and binder (Zhao et al., 2012; Shu et al., 2012; Hill et al., 2012a). On the contrary, an increase in moisture susceptibility with increasing RAP content was reported by Moghadas et al. (2014) and Guo et al. (2014). It was noted that improper

blending between virgin binder and aged RAP binder can result in uncoated aggregates in asphalt mixes, which can increase the moisture-induced damage potential (Moghadas et al., 2014; Guo et al., 2014).

Evaluation of moisture-induced damage potential is a complex problem for pavement engineers (Abuawad et al., 2015). Several researchers have followed different test methods to quantify the moisture-induced damage potential of asphalt mixes (Solaimanian et al., 2003; Hurley et al., 2010; Goh and You, 2011b; Weldegioris and Tarefder, 2011; Kim et al., 2012b). In 1930, the boil water test was introduced to evaluate the moisture-induced damage potential of asphalt mixes (Abuawad et al., 2015). This was mainly a qualitative test performed on loose asphalt mixes (Solaimanian et al., 2003). In this test method, loose asphalt mixes were added in boiled water and uncoated aggregate surfaces were assessed qualitatively. A higher area represents a more moisture susceptible mix. Currently, several other moisture-induced damage potential tests are available for asphalt mixes including moisture vapor sensitivity test, immersion compression test, Marshall Immersion test, freeze-thaw pedestal test, Lottman indirect tensile test, HWT test, energy ratio test and multiple freeze-thaw test (Solaimanian et al., 2003; Hurley et al., 2010; Goh and You, 2011b; Weldegioris and Tarefder, 2011; Kim et al., 2012b). Among existing test methods, the SIP from HWT tests and TSR from ITS tests are most commonly used parameters for evaluating moisture-induced damage potential of asphalt mixes (Kim et al., 2012b; Abuawad et al., 2015).

Moisture-induced damage potential of foamed WMA containing a high percentage of RAP was evaluated by Shu et al. (2012). It was found that using water as

the foaming agent and a lower mixing and compaction temperature increases the possibility of existence of moisture in the mix, which may increase moisture susceptibility of foamed WMA. The test results indicated that ITS and resilient modulus of asphalt mixes increased with the addition of RAP. However, a reduction in Dissipated Strain Energy ( $DCSE_f$ ) was observed with an increase in RAP content. The  $DCSE_f$  can be defined as the difference between Fracture Energy (FE) and Elastic Energy (EE) in the ITS stress-strain curves, as shown in Figure 2.2. The increase in ITS and resilient modulus values was primarily attributed to a stiffer and more brittle asphalt mix due to incorporation of RAP. This increase in brittleness reduced the  $DCSE_f$  value. Also, addition of RAP was found to lower the moisture-induced damage potential of asphalt mixes. It was also reported that the Moisture Induced Sensitivity Test (MIST) conditioning resulted in a larger reduction in resilient modulus and  $DCSE_f$ , whereas freeze-thaw caused a larger reduction in ITS (ASTM, 2016). A plant-produced WMA was found to show similar moisture-induced damage potential compared to its HMA counterpart. The test results indicated that the moisture resistance of asphalt mixes can be characterized based on resilient modulus and ITS.



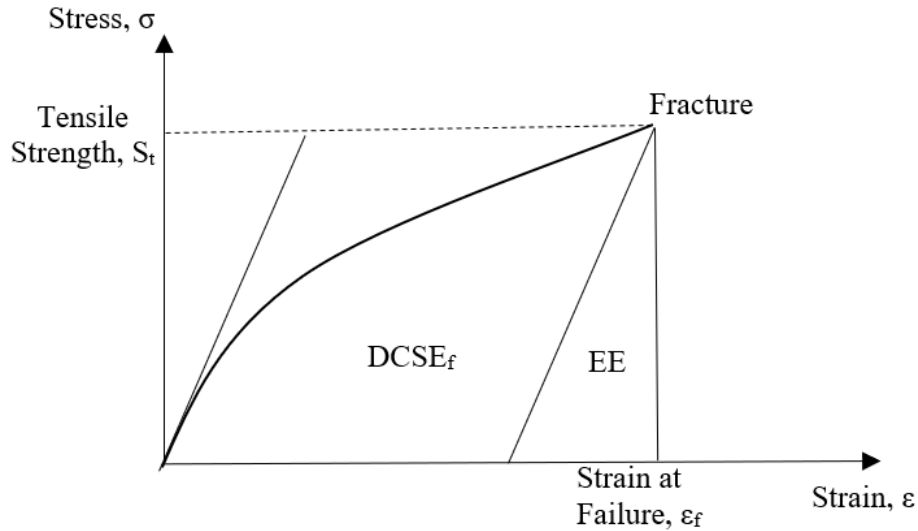


Figure 2.2 Schematic Diagram Illustrating the Demonstration of Fracture Energy and Dissipated Creep Strain Energy (After Shu et al., 2012)

A mechanistic approach in understanding moisture-induced damage of asphalt mixes was proposed by Weldegiorgis and Tarefder (2015). In that study, effect of moisture conditioning using MIST on dynamic modulus values was evaluated (ASTM, 2016). Generation and dissipation of pore water pressure in saturated pavement due to vehicular movement was simulated by the moisture conditioning using MIST. Stripping of asphalt mixes was mainly caused by pore water pressure (Tarrer and Wagh, 1991; Parker, 1989; Karlson, 2005; Kutay and Aydilek, 2007; Jiang et al., 2013). Also, adhesion failure due to rupture in binder film between aggregate and binder of asphalt mixes was specified as one of the mechanisms for moisture-induced damage. The degree of moisture-induced damage was directly related to number of cycles, pressures and temperatures of MIST conditioning. For MIST conditioning, 3,500 cycles, 276 kPa pressures and 60°C temperatures were suggested in ASTM D 7870 (ASTM, 2016). According to that study, number of cycles and pressures can be increased for heavy traffic roads in simulating the actual field condition. Lastly, correlations between

moisture susceptibility with number of cycles in MIST and pressures were developed using two four-degree polynomial equations for all dynamic modulus testing temperatures and frequencies.

Laboratory and field moisture-induced damage potential of WMA was characterized by Kim et al. (2012b). In their study, APA test under water, AASHTO T 283 test and nonlinear elastic fracture mechanics-based SCB tests were used to simulate the laboratory moisture-induced damage of asphalt mixes. To identify field performance, pavement sections with both WMA and control HMA were constructed in Antelope County, Nebraska. Both WMA and HMA were found to satisfy the 12 mm failure criteria for APA laboratory test. Also, for all mixes similar rut depth values were observed after 8,000 cycles. Therefore, the APA test in water could not identify the moisture-induced damage potential of asphalt mixes. However, AASHTO T 283 test and SCB test results showed an identical trend after moisture conditioning. For both cases, WMA showed higher moisture-induced damage potential compared to their HMA counterparts and this trend was confirmed by strength ratio and fracture energy ratio obtained from AASHTO T 283 test and SCB tests, respectively. It was noted that in the SCB test the crack sensitivity of specimen tip may cause a lower fracture energy after conditioning. Both WMA and HMA were found to show similar moisture susceptibility in the field for the first three years after construction. It was concluded that resistance to moisture-induced damage potential for WMA can be severely affected after rutting and cracking occur in the field.

## 2.7 Summary

As a part of efforts toward establishing a sustainable and eco-friendly asphalt pavement, foamed WMA containing RAP can be a viable solution. However, in asphalt plants foamed WMA containing RAP is generally produced following a mix design procedure initially developed for HMA without any modifications. A compaction temperature greater than the high-temperature PG of RAP binder is suggested for foamed WMA containing RAP (Bonaquist, 2011). Actually, high-temperature PG of RAP binder is an important parameter for engaging the required binder from RAP. Also, it is important to recognize that the compactability, fatigue performance, and rutting resistance of foamed WMA can differ significantly when designed as HMA (Bonaquist, 2011). Such differences are influenced by different factors including RAP content, RAP source, binder type, and rejuvenators. Among the available test procedures, the HWT and FN tests have been found to be effective tools for assessing the rutting performance of asphalt mixes. For evaluating the fatigue resistance, different agencies are currently using different test methods. Both Louisiana SCB and I-FIT tests have been found capable of evaluating fracture performance of asphalt mixes. Some agencies are also using Cantabro test to evaluate fatigue cracking resistance of asphalt mixes. TSR and SIP are commonly used to evaluate the moisture-induced damage potential of asphalt mixes. A summary of the test methods used in this study, including their purpose, is presented in Table 2.1. More detailed descriptions of these test methods are given in Chapter 3.

Table 2.1 List of Laboratory Tests Conducted in this Study

Test Name	Standards	Purpose	Test Outcomes	Specifications/ Recommendations
Superpave <sup>®</sup> Volumetric Mix Design	AASHTO R 35 (2013)	Estimate Volumetric Parameters	<ul style="list-style-type: none"> <li>Theoretical Maximum Specific Gravity (<math>G_{mm}</math>)</li> <li>Bulk Specific Gravity (<math>G_{mb}</math>)</li> <li>Percent Air Voids (<math>V_a</math>)</li> </ul>	<u>Target Percent Air Voids (<math>V_a</math>)</u> Four
Hamburg wheel tracking (HWT) Test	AASHTO T 324 (2014c)	Evaluate Rutting Resistance and Moisture- Induced Damage Potential	<ul style="list-style-type: none"> <li>Rut Depths at Various Wheel Passes</li> <li>Post- Compaction, Inverse Creep Slope, Stripping Inflection Point (SIP), Stripping Slope</li> </ul>	<u>Rutting Potential</u> Rut Depth < 12.5 mm at 10,000 Wheel Passes for PG 64-22  <u>Moisture-Induced Damage Potential</u> SIP > 20,000 passes
Flow Number (FN) Test	AASHTO T 378 (2017)	Estimate Rutting Resistance	<ul style="list-style-type: none"> <li>Starting Point of Tertiary Deformation/ Flow Number (FN)</li> </ul>	<u>Equivalent Single Axle Load (ESAL)s</u> < 3 millions No Specification  <u>ESALs 3 to 10 millions</u> FN > 50 for HMA FN > 300 for WMA  <u>ESALs 10 to 30 millions</u> FN > 190 for HMA FN > 105 for WMA  <u>ESALs &gt; 30 millions</u> FN > 740 for HMA FN > 415 for WMA

Dynamic Modulus (DM) Test	AASHTO T 378 (2017)	Evaluate the Stiffness of Asphalt Mixes	<ul style="list-style-type: none"> <li>Dynamic Modulus Master Curves</li> </ul>	
Louisiana Semi-Circular Bend (SCB) Test	ASTM D 8044 (2013)	Evaluate Cracking Resistance	<ul style="list-style-type: none"> <li>J- Integral (<math>J_c</math> Value)</li> </ul>	<u><math>J_c</math> Value</u> Typically Greater than 0.5 to 0.60 kJ/m <sup>2</sup>
Illinois Semi-Circular Bend (SCB)/ Illinois Flexibility Index Test (I-FIT)	AASHTO TP 124 (2016)	Evaluate Cracking Resistance	<ul style="list-style-type: none"> <li>Flexibility Index (FI)</li> </ul>	
Abrasion Loss Test (Cantabro Test)	AASHTO TP 108 (2016)	Estimate Cracking Resistance	<ul style="list-style-type: none"> <li>Percent Abrasion Loss</li> </ul>	
Moisture Induced Sensitivity Test (MIST) Method	ASTM D 7870 (2016)	Estimate Moisture-Induced Damage Potential	<ul style="list-style-type: none"> <li>Dry and MIST-Conditioned ITS of Asphalt Mixes</li> <li>TSR Value after MIST Conditioning</li> </ul>	
AASHTO T 283 Method	AASHTO T 283 (2014b)	Estimate Moisture-Induced Damage Potential	<ul style="list-style-type: none"> <li>Dry and MIST-Conditioned ITS of Asphalt Mixes</li> <li>TSR Value after Freeze-Thaw Conditioning</li> </ul>	<u>Moisture-Induced Damage Potential</u> TSR $\geq$ 0.80
Asphalt Binder Extraction	AASHTO T 164 (2014a)	Extract Binder with Solvent from RAP	<ul style="list-style-type: none"> <li>Extracted RAP Binder Solution</li> </ul>	
Asphalt Binder Recovery	ASTM D 5404 (2017)	Recover Asphalt from	<ul style="list-style-type: none"> <li>Recovered RAP binder</li> </ul>	

		Solution Using Rotary Evaporator		
Dynamic Shear Rheometer (DSR)	AASHTO T 315 (2015)	Evaluate High- Temperature PG of RAP Binder	<ul style="list-style-type: none"> <li>• Rutting Factor (<math>G^*/\sin \delta</math>) at Different Temperatures</li> </ul>	$G^*/\sin \delta \geq 1.0 \text{ kPa}$ (Unaged Condition)  $G^*/\sin \delta \geq 2.2 \text{ kPa}$ (RTFO Condition)

# CHAPTER

# 3

## MATERIALS AND METHODS

### 3.1 Introduction

This chapter provides information about material selection and collection processes, mix design volumetrics, performance tests for asphalt mixes and high-temperature Performance Grade (PG) of recovered RAP binder. The technique used for producing foamed binder is also discussed. Different laboratory test methods for evaluating rutting, cracking and moisture-induced damage potential are briefly discussed in this chapter. Figure 3.1 presents the workflow of this study.

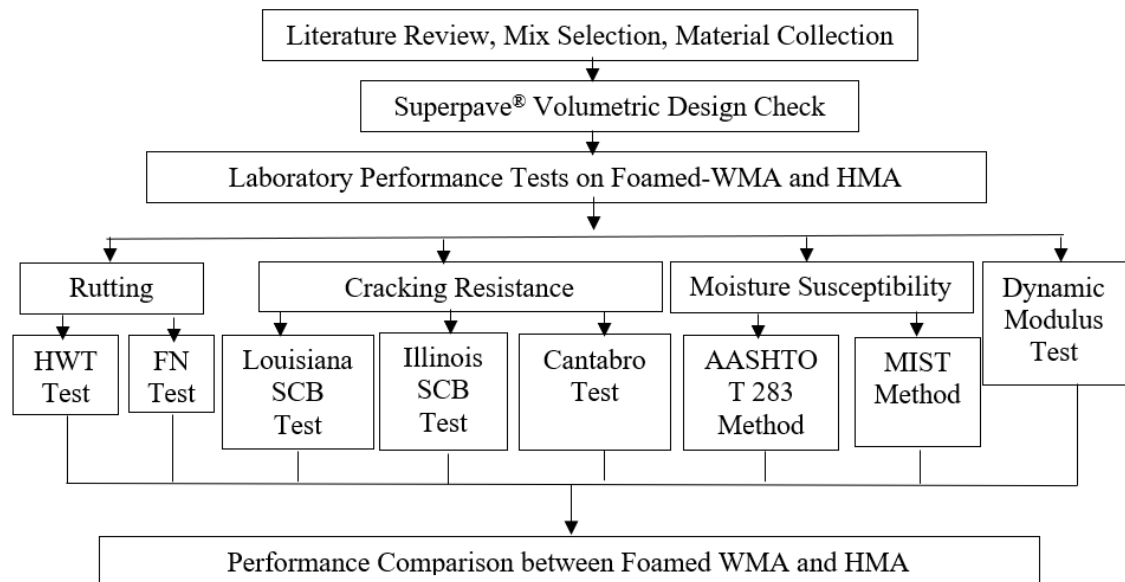


Figure 3.1 Work Flow Diagram of the Study

### **3.2 Aggregates and RAP**

Two types of aggregate gradations, a coarse S3 gradation (Nominal Maximum Aggregate Size (NMAS) = 19.0 mm) and a fine S4 gradation (NMAS = 12.5 mm), were used in this study to produce foamed WMA. In Oklahoma, the S3 and S4 aggregate gradations are typically used as intermediate and surface course mixes, respectively. The asphalt mixes with S3 aggregate gradation (called herein as S3 mixes) were prepared using 25% RAP, whereas the asphalt mixes with S4 aggregate gradation (called herein as S4 mixes) were prepared using 5% RAP, following current ODOT's practice (ODOT, 2013a). For this purpose, approximately 1,000 kg aggregates and 270 kg RAP were collected from a local asphalt plant. The collected materials were transported and stored in the University of Oklahoma Broce Civil Engineering Materials Laboratory for testing, as shown in Figure 3.2. Tables 3.1 and 3.2 present the percentages of different aggregates used for each of S3 and S4 mixes. The S3 mixes contained 10% of 1" rocks, 27% of 5/8" chips, 12% of screening, 15% of manufactured sand and 11% fine sand. On the other hand, S4 mixes contained 35% of 5/8" chips, 10% of screening, 15% of manufactured sand and 14% fine sand. The gradation curves for S3 and S4 mixes are shown in Figure 3.3.





(a)

(b)

Figure 3.2 Collection of Materials (a) Collection of Aggregates for Laboratory

Produced Asphalt Mixes (b) Storage of Collected Aggregates

Table 3.1 Aggregate Components for S3 Mixes

No.	Aggregate	Producer/ Supplier	% Used
1	1" Rock	Hanson	10
2	5/8" Chips	Hanson	27
3	3/16" Scrns.	Hanson	12
4	Man. Sand	Martin-Marietta (Davis, OK)	15
5	Sand	General Materials Inc (Oklahoma City, OK)	11
6	Fine RAP	Contractor / Project Site	25

Table 3.2 Aggregate Components for S4 Mixes

No.	Aggregate	Producer/ Supplier	% Used
1	5/8" Chips	Hanson	35
2	Man. Sand	Hanson	36
3	3/16" Scrns.	Hanson	10
4	Sand (Unlisted Source)	General Materials Inc., 63rd St.(Oklahoma City, OK)	14
5	Fine RAP	Contractor / Project Site	5

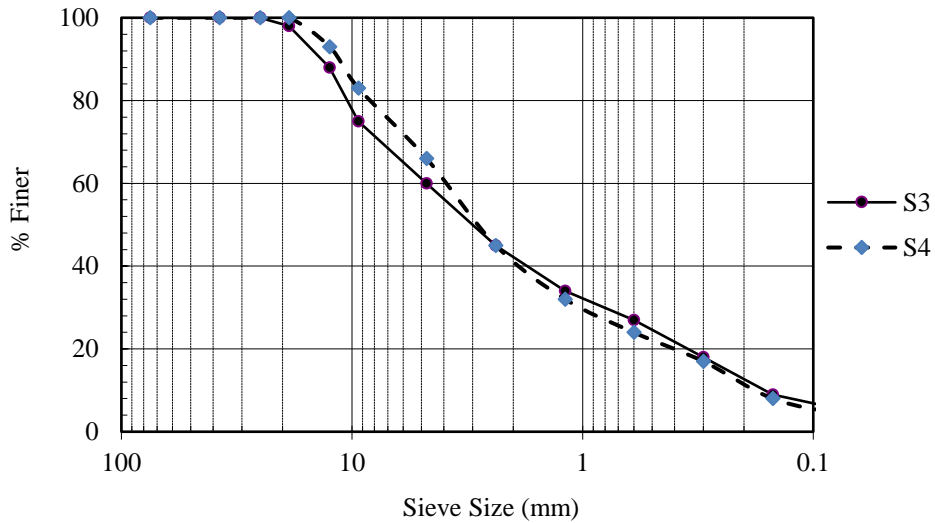


Figure 3.3 Combined Aggregate Gradation Curves (S3 Mixes and S4 Mixes)

### 3.3 Asphalt Binder

A PG 64-22 OK asphalt binder was used as the virgin binder in producing the asphalt mixes. The asphalt binder was collected from a local asphalt plant and stored at the University of Oklahoma Broce Civil Engineering Materials Laboratory. The HMA was produced by using this binder without any modification. However, for production of WMA, the collected binder was foamed using a laboratory foamer, called Accufoamer. Figure 3.4 presents a schematic diagram of the foaming mechanism for Accufoamer. As shown in Figure 3.4, the foamer has two tanks: one for asphalt binder and the other for foaming water. Both tanks are connected to separate airlines to maintain pressure precisely. The temperature and pressure used in this study to produce foamed binder were 135°C and 210 kPa, respectively. These parameters were selected based on the literature on foamed WMA and current practice followed by the local asphalt plant (Bonaquist, 2011; Malladi, 2015). Once the desired temperature and pressure are reached, the valves are then opened to produce foamed binder (Figure 3.4).

The foaming is performed by inserting pressurized water into the preheated asphalt binder (Jenkins, 2000; Van et al., 2007). During foaming, the injected water vaporizes and produces steam, which increases the volume of binder and reduces its viscosity (Van De Ven et al., 2007; Zaumanis, 2010).

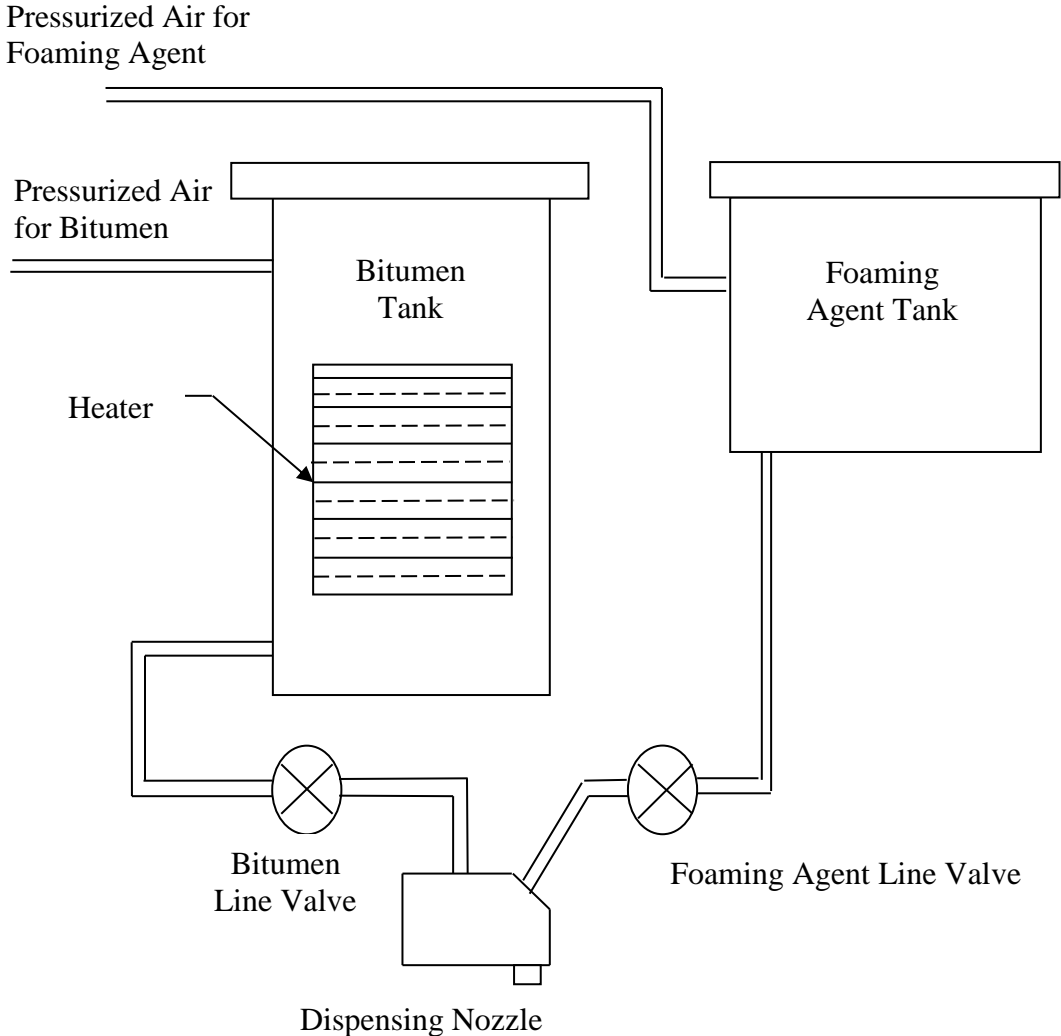


Figure 3.4 AccuFoamer Schematic Diagram (After InstroTek<sup>®</sup> Inc., 2015)

### 3.4 Asphalt Mixes

Mix design sheets for both foamed WMA S3 and WMA S4 were collected from a local asphalt plant. These mix designs were initially developed for HMA based on the

AASHTO R 35 method considering light traffic condition with anticipated Equivalent Single Axle Load (ESAL) of less than 0.3 million (AASHTO, 2013). According to the AASHTO R 35 method, the volumetric properties of HMA samples are targeted to attain air voids of four percent (AASHTO, 2013). The mixing and compaction temperatures for HMA were selected as 163°C and 149°C, respectively, based on the binder's viscosity of  $0.17 \pm 0.02$  Pa-s and  $0.28 \pm 0.03$  Pa-s, respectively (Asphalt Institute, 2016). According to AASHTO specification for light traffic condition, the number of gyration was kept at 50 for preparing the volumetric samples using Superpave® Gyrotory Compactor (SGC) (AASHTO, 2013). The same mix design methods were followed for the foamed WMA except using foamed binder and lower mixing and compaction temperatures. The mixing and compaction temperatures for foamed WMA were lowered to 135°C and 127°C, respectively. These temperatures were selected based on previous studies conducted on foamed WMA and the current practice of the local asphalt plant (Bonaquist, 2011; Malladi, 2015).

In this study, a total of eight asphalt mixes were produced in the laboratory. The characteristics of these eight mixes are summarized in Table 3.3. Mix-1 through Mix-4 were of S3 type, while Mix-5 through Mix-8 were of S4 type. Mix-1 and Mix-5 were prepared using the HMA mix design procedure, which involved higher mixing (163°C) and compaction (149°C) temperatures. These mixes used regular binder (without foaming) and are considered as control mixes. Mix-2 and Mix-6 were prepared with foamed binder in the laboratory using lower temperatures, 135°C for mixing and 127°C for compaction. The aggregates and RAP used in WMA were dried at a lower temperature (135°C) for two hours, which is commonly used in the WMA production

plant as per the mix design sheets. As reported by Jenkins et al. (2000), WMA may be produced at a much lower temperature (as low as 90°C). To evaluate the effect of reduction in mixing and compaction temperatures on volumetric properties, the mixing and compaction temperatures were reduced to 115°C and 107°C, respectively for both Mix-3 and Mix-7. The mixing and compaction temperatures for both Mix-4 and Mix-8 were further reduced to 95°C and 87°C, respectively. For all mixes, aggregates and RAP were heated at the corresponding mixing temperatures for two hours. The foamed WMA binder was produced at 135°C for all cases. As reported by Jenkins (2000), the mixing temperature is mainly controlled by the temperature of the aggregate, not by the temperature of the foamed binder. As noted earlier, the rutting, cracking and moisture-induced damage potentials of Mix-1, Mix-2, Mix-5 and Mix-6 were evaluated in the laboratory. Table 3.4 presents the corresponding test matrix. The numbers in Table 3.4, except NMAS, represent the number of samples tested for each case.

Table 3.3 Properties of the Asphalt Mixes

Mix ID	Mix Type	Mixing/ Compaction Temperatures (°C)	NMAS (mm)	Binder Type	Foamed Binder	RAP Content (%)
Mix-1	HMA S3	163/149	19	PG 64-22	No	25
Mix-2	WMA S3	135/127	19	PG 64-22	Yes	25
Mix-3	WMA S3	115/107	19	PG 64-22	Yes	25
Mix-4	WMA S3	95/87	19	PG 64-22	Yes	25
Mix-5	HMA S4	163/149	12	PG 64-22	No	5
Mix-6	WMA S4	135/127	12	PG 64-22	Yes	5
Mix-7	WMA S4	115/107	12	PG 64-22	Yes	5
Mix-8	WMA S4	95/87	12	PG 64-22	Yes	5

Table 3.4 Test Matrix for Asphalt Mixes

Mix ID	NMAS (mm)	Volumetrics Check	HWT Test	FN Test	Louisiana SCB Test	I-FIT Test	Abrasion Loss Test	DM test	TSR test	
									AASHTO T 283	MIST
Mix-1	19	6	4	3	9	4	3	3	3	3
Mix-2	19	6	4	3	9	4	3	3	3	3
Mix-3	19	3	--	--	--	--	--	--	--	--
Mix-4	19	3	--	--	--	--	--	--	--	--
Mix-5	12	3	4	3	9	4	3	3	3	3
Mix-6	12	3	4	3	9	4	3	3	3	3
Mix-7	12	3	--	--	--	--	--	--	--	--
Mix-8	12	3	--	--	--	--	--	--	--	--

### 3.5 Mix Design Volumetrics

#### 3.5.1 Volumetric Properties

As mentioned in Chapter 2, mix designs as per AASHTO R 35 method are primarily based on the volumetric properties of the asphalt mixes, which include Air Voids (AV), Voids in Mineral Aggregate (VMA), and Voids Filled with Asphalt (VFA) (AASHTO, 2013). The aggregate gradations of S3 and S4 mixes were maintained in a way to satisfy the AASHTO limits for VMA and VFA (AASHTO, 2013). A summary of the volumetric properties of the control HMA S3 mix (Mix-1) and the control HMA S4 mix (Mix-5) are summarized in Table 3.5 and Table 3.6, respectively. The optimum binder content was determined based on the four percent air voids and by satisfying the requirements for VMA and VFA. The optimum binder contents for Mix-1 and Mix-5 were found as 4.5% and 4.9% by weight of total mix, respectively, following a trial and error approach (Tables 3.5 and 3.6). The amount of binder replaced by RAP for Mix-1 and Mix-5 were found to be 31.1% and 4.1%, respectively. Also, for calculating the percent air voids of asphalt mixes, theoretical maximum specific gravity ( $G_{mm}$ ) and bulk specific gravities ( $G_{mb}$ ) of asphalt mixes were determined. The  $G_{mm}$  of loose asphalt

mixes was determined using the Rice density test in accordance with AASHTO T 209 (AASHTO, 2012). The  $G_{mm}$  value is an indicator of zero percent air voids in the asphalt mixes (theoretically feasible). On the other hand,  $G_{mb}$  is defined as the ratio of the mass of a unit volume permeable material (including both permeable and impermeable voids) to the same volume gas-free distilled water in the air at 25°C. The  $G_{mb}$  of compacted asphalt samples were determined using AASHTO T 166 method (AASHTO, 2010). About 4.8 kg of loose asphalt mixes were used to prepare compacted samples for  $G_{mb}$  tests. In the Superpave® Gyrotory Compactor (SGC), number of gyration was kept at 50 to compact the asphalt samples considering light traffic condition and to obtain a final height of  $115 \pm 5$  mm. Then, the percent air voids were calculated using the following equation:

$$\% \text{ Air Voids} = \frac{G_{mm} - G_{mb}}{G_{mm}} * 100\% \quad (3.1)$$

Table 3.5 A Summary of Volumetric Properties for Mix-1

Volumetric Properties	Trial 1	Trial 2	Trial 3	Required	At Optimum Binder Content
Maximum Specific Gravity, $G_{mm}$	2.532	2.512	2.493		2.499
Virgin Binder Type	PG 64-22	PG 64-22	PG 64-22		PG 64-22
Total Binder Content (%)	4.3	4.8	5.3		4.5
Virgin Binder Content (%)	2.9	3.4	3.9		3.1
Voids in Mineral Aggregate, VMA (%)	13.6	13.3	13.0	Minimum 13.0	13.5
Voids Filled with Asphalt, VFA (%)	69.1	80.5	92.3	70-75	71.4
Density (%)	95.8	97.4	99.0	96.0	96.0
Absorbed Binder, $P_{ba}$ (%)	0.42	0.42	0.42		0.42

Table 3.6 A Summary of Volumetric Properties for Mix-5

Volumetric Properties	Trial 1	Trial 2	Trial 3	Required	At Optimum Binder Content
Maximum Specific Gravity, $G_{mm}$	2.500	2.481	2.462		2.496
Virgin Binder Type	PG 64-22	PG 64-22	PG 64-22		PG 64-22
Total Binder Content (%)	4.8	5.3	5.8		4.9
Virgin Binder Content (%)	4.6	5.1	5.6		4.7
Voids in Mineral Aggregate, VMA (%)	14.5	14.4	14.3	Minimum 14.0	14.5
Voids Filled with Asphalt, VFA (%)	71.0	80.6	89.5	72-77	73.0
Density (%)	95.8	97.2	98.5	96.0	96.0
Absorbed Binder, $P_{ba}$ (%)	0.46	0.46	0.46		0.46

### 3.5.2 Statistical Analysis

The average percent air voids for volumetric samples of Mix-2 (WMA S3) and Mix-6 (WMA S4) were compared with Mix-1 (control HMA S3) and Mix-5 (control HMA S4), respectively. For each mix type at least three volumetric samples were prepared to check the repeatability of test results. Two-tail t-tests were conducted to identify the statistical difference of average percent air voids between WMA and HMA samples, at 95% confidence level. The optimum binder content was adjusted for WMA, if significant statistical differences were observed.

Effect of further temperature reduction was investigated using two-tail t-tests by identifying differences in percent air voids between WMA samples (Mix-3, Mix-4, Mix-7, and Mix-8) and control HMA samples (Mix-1 and Mix-5). The average percent air voids of Mix-3 and Mix-4 were compared with control Mix-1, whereas the average percent air voids of Mix-7 and Mix-8 were compared with control Mix-2. Suitable



mixing and compaction temperatures were selected for foamed WMA based on these statistical results. The details of these results are discussed in Chapter 4.

### **3.6 Laboratory Performance Tests of Asphalt Mixes**

The rutting, cracking and moisture-induced damage potential of Mix-2 and Mix-6 were compared with Mix-1 and Mix-5, respectively. To evaluate the rutting performance, the HWT and FN tests were conducted on asphalt mixes. Both Louisiana SCB and Illinois SCB test methods were used in this study to characterize fatigue cracking. Also, an empirical method (Abrasion Loss or Cantabro test) was used to identify the cracking potential of asphalt mixes. Moisture-induced damage potential of each mix was assessed using the SIP and TSR values.

#### **3.6.1 Sample Preparation**

Asphalt samples for all performance tests were prepared in the laboratory using a SGC. The target air voids were kept at  $7 \pm 0.5\%$  based on the densities typically obtained in the field. After mixing, bulk HMA was short-term aged at  $135^{\circ}\text{C}$  for 4 hours as per AASHTO R 30 in order to simulate the conditioning of plant-produced mix (AASHTO, 2002). As suggested by Bonaquist (2011), the bulk WMA mixes were short-term aged at WMA compaction temperature ( $127^{\circ}\text{C}$ ) for 2 hours only to simulate the field conditioning during WMA production. The SGC was operated in the height mode during compaction to obtain the desired air voids under a specific height. After compaction, volumetric tests were conducted to check air voids in accordance with AASHTO T 166 (AASHTO, 2010).

### **3.6.2 Laboratory Testing**

#### *3.6.2.1 Dynamic Modulus (DM) Test*

Dynamic modulus tests were conducted as per AASHTO T 378 using the Asphalt Mixture Performance Tester (AMPT) (AASHTO, 2017). For this purpose, over-size samples with a diameter of 150 mm and a height of 167.5 mm were prepared using SGC. These samples were then cored from the center to obtain specimens having a diameter of 100 mm. The cored specimens were cut at both ends using a heavy duty saw to obtain specimens with a height of 150 mm. As suggested by Chehab et al. (2000), this method produces specimen with uniform air voids in both vertical and radial directions. For each asphalt mix, three replicates were prepared for dynamic modulus testing.

The dynamic modulus tests were conducted at four different temperatures, namely 4.4, 21.1, 37.8, and 54.4°C. For each temperature, six different loading frequencies, namely 25, 10, 5, 1, 0.5 and 0.1 Hz, were used. For each specimen, the tests were performed starting from the lowest temperature to the highest and from the highest frequency to the lowest. The applied loading consisted of sinusoidal compressive (haversine-shaped) pulse. The load magnitude was adjusted based on the material stiffness, frequency and temperature, to keep the strain response within 50-150 microstrains (Tran and Hall, 2006). Although dynamic modulus tests can be performed under both confined and unconfined conditions (AASHTO, 2017), unconfined condition was used here. Finally, a master curve was created at a reference temperature of 21.1°C using the time-temperature superposition method. A sigmoidal function was

used in fitting the master curve as shown in Equation 3.2 (Singh, 2011). Details of the time-temperature superposition method are given by Singh (2011).

$$\log|E^*| = \delta + \frac{\alpha}{1 + \exp(\beta + \gamma(\log f_r))} \quad (3.2)$$

where:

$|E^*|$  = dynamic modulus (MPa);

$f_r$  = reduced frequency at reference temperature;

$\delta$  = minimum value of  $|E^*|$ ;

$\delta + \alpha$  = maximum value of  $|E^*|$ ; and

$\beta, \gamma$  = parameters describing the shape of the sigmoidal function.

General form of the shift factor is given by Equations 3.3 and 3.4.

$$a(T) = \frac{f_r}{f} \quad (3.3)$$

$$\log(f_r) = \log(a(T)) + \log(f) \quad (3.4)$$

where:

$a(T)$  = temperature shift factor;

$T$  = temperature (°C); and

$f$  = frequency at a particular temperature.

A nonlinear optimization program, namely Solver in MS-Excel, was used for solving the master curve coefficients, namely  $\alpha, \beta, \gamma, \delta$  and  $c$ . Then, a quadratic polynomial fit, given by Equation 3.5, was used to establish the shift factor-temperature relationship.

$$\log(a(T)) = mT^2 + nT + p \quad (3.5)$$

where:

$T$  = temperature ( $^{\circ}\text{C}$ ); and

$m, n, p$  = polynomial fitting curve coefficients.

Table 3.7 was proposed by Witczak (2005) to check the statistical accuracy of the above-mentioned models. In this method, the  $S_e/S_y$  (standard error of estimate/standard deviation) and correlation coefficient ( $R^2$ ) are used to evaluate the statistical fitness of master curve models and shift factor equations. According to goodness of fit, the models can be classified into five groups, namely excellent, good, fair, poor, and very poor, as listed in Table 3.7.

Table 3.7 Model Evaluation Criteria (Witczak, 2005)

Rating	$R^2$	$S_e/S_y$
Excellent	$\geq 0.90$	$\leq 0.35$
Good	0.70 - 0.89	0.36 - 0.55
Fair	0.40 - 0.69	0.56 - 0.75
Poor	0.20 - 0.39	0.76 - 0.90
Very Poor	$\leq 0.19$	$\geq 0.90$

### 3.6.2.2 Louisiana Semi-Circular Bend (SCB) Test

To rank asphalt mixes based on cracking resistance, several state DOTs are currently using the Semi-Circular Bend (SCB) test (Barman et al., 2018). This test method is relatively new and there is no uniform standard followed by state DOTs across the country (Barman et al., 2016). In this study, the Louisiana SCB tests were conducted as per ASTM D 8044 (ASTM, 2013). In this method, the fracture resistance of asphalt mixes is evaluated based on the elasto-plastic fracture mechanics concept using critical strain energy release rate (Wu et al., 2005; Kim et al., 2012a). These tests were conducted on half-disk-shaped specimens having a diameter of 150 mm and a thickness of 50 mm. At first, samples having a diameter of 150 mm and a height of 120 mm were prepared using a SGC. Then each sample was saw cut to produce four half

circle specimens with a diameter of 150 mm and a thickness of 50 mm. The Louisiana SCB tests were conducted on specimens with three different notch depths, namely 25.4, 31.8, and 38.0 mm. For each notch depth, three replicate specimens were tested to check the repeatability of test results.

This method characterizes the cracking resistance of asphalt mixes at an intermediate temperature (25°C in this study) in terms of critical strain energy release rate or *J-integral* ( $J_c$ ), defined by Equation 3.6. A higher *J-integral* value represents a specimen with higher resistance to fatigue cracking (Kim et al., 2012a).

$$J_c = - \left( \frac{1}{b} \right) \frac{dU}{da} \quad (3.6)$$

where:

$J_c$  = critical strain energy release rate (kJ/m<sup>2</sup>);

$b$  = SCB specimen thickness (m);

$a$  = notch depth (m); and

$U$  = strain energy (area under stress-strain curve) (N-m).

As shown in Figure 3.5, specimens were loaded monotonically at 0.5 mm/min using a three-point flexural apparatus (Kim et al., 2012a). Figure 3.6 illustrates the procedure for computation of  $J_c$  using average strain energy. In this method, average strain energy up to failure was considered. The rate of change in average strain energy with respect to notch depths was then determined using the slope of average strain energy ( $U$ ) vs. notch depth ( $a$ ) line. The rate of change was divided by the thickness of the specimen ( $b$ ) to obtain the  $J_c$  value (Figure 3.6).

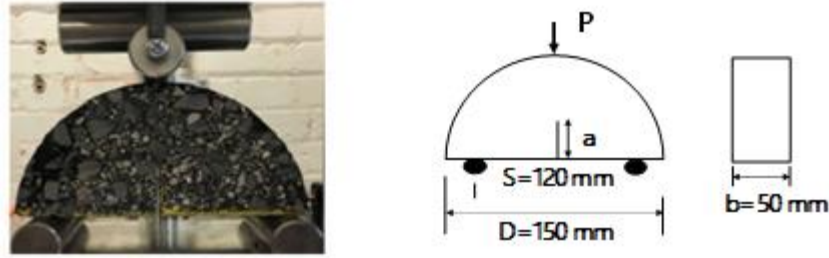


Figure 3.5 Test Setup for Semi-Circular Bend (SCB) Testing

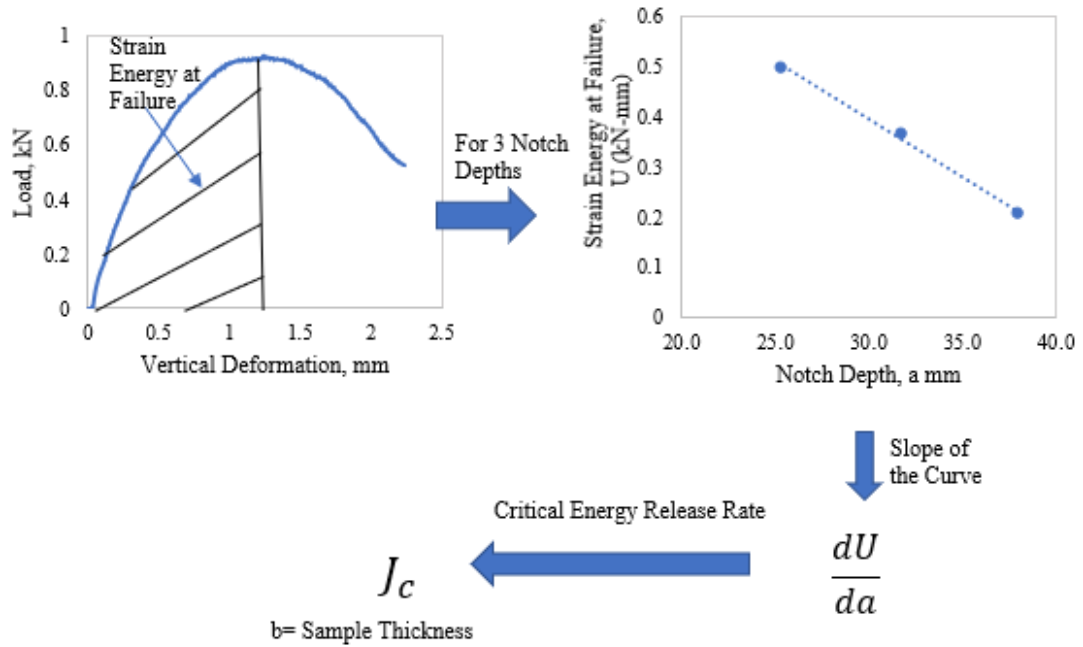


Figure 3.6 Computation of  $J_c$  Using SCB Test Results (After Kim et al., 2012a)

### 3.6.2.3 Illinois Flexibility Index (I-FIT) Test

In addition to Louisiana SCB test, in this study Illinois SCB test method, also called I-FIT test, was used to evaluate the cracking potential of asphalt mixes. This test was conducted according to AASHTO TP 124 (AASHTO, 2016). This method uses only one notch depth (15 mm) and a much faster loading rate (50 mm/min). Sample preparation was similar to that used in the Louisiana SCB method, except the notch width was much smaller ( $1.50 \pm 0.05$  mm), as per Al-Qadi et al. (2015). A special saw

was used to create this notch. The prepared specimens were tested at 25°C. The test results were presented in terms of Flexibility Index (FI), which accounted for post-crack performance (Al-Qadi et al., 2015). In this method, the total area under the load-displacement curve was considered in calculating FI, as shown in Figure 3.7. The determination of FI also depends on post-peak slope ( $m$ ) and critical displacement ( $u_i$ ). The post-peak slope is defined as the slope at the inflection point after peak load in the load-displacement diagram (Figure 3.7). The displacement at which post-peak slope intersects the displacement axis is termed critical displacement ( $u_i$ ). As noted by Al-Qadi et al. (2015), the FI can be expressed by Equation 3.7.

$$FI = A * \frac{G_{fa}}{abs(m)} \quad (3.7)$$

where:

A = unit conversion factor (0.01);

$G_{fa}$  = total fracture energy (Joules/m<sup>2</sup>);

Abs = absolute value; and

$m$  = post-peak slope (kN/mm).

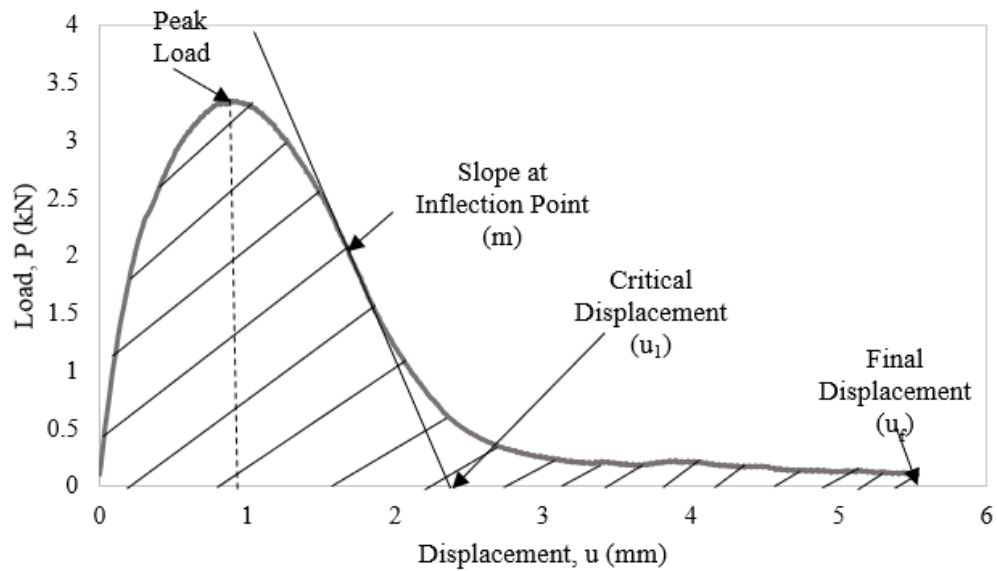


Figure 3.7 A Typical Outcome of the Illinois-SCB Test (After Al-Qadi et al., 2015)

#### 3.6.2.4 Abrasion Loss Test (Cantabro Test)

In addition to Louisiana SCB and Illinois SCB tests, Abrasion Loss Test (commonly known as Cantabro Test) was used to evaluate cracking resistance of asphalt mixes. These tests were conducted in accordance with AASHTO TP 108 (AASHTO, 2016). At least three replicate samples were prepared for verifying the reproducibility of test results. Each of these samples had a diameter of 150 mm, a height of  $115 \pm 5$  mm, and an air void of  $7 \pm 0.5\%$ .

The prepared samples were tested using the Los Angeles Abrasion machine without the steel balls. Before conducting the test, the samples were conditioned at  $25^{\circ}\text{C}$  for 4 hours. The drum of the Los Angeles machine was turned 300 times at 30 to 33 rev/min. Figure 3.8 represents the abrasion loss sample before and after the test. The percent abrasion Mass Loss ( $ML$ ) was calculated using Equation 3.8. The recommended maximum abrasion loss suggested by NCAT for asphalt mixes was 20% (NCAT, 2017).



$$ML = \frac{W_1 - W_2}{W_1} * 100 \quad (3.8)$$

where:

$W_1$  = initial mass of the sample (g); and

$W_2$  = final mass of the sample (g).

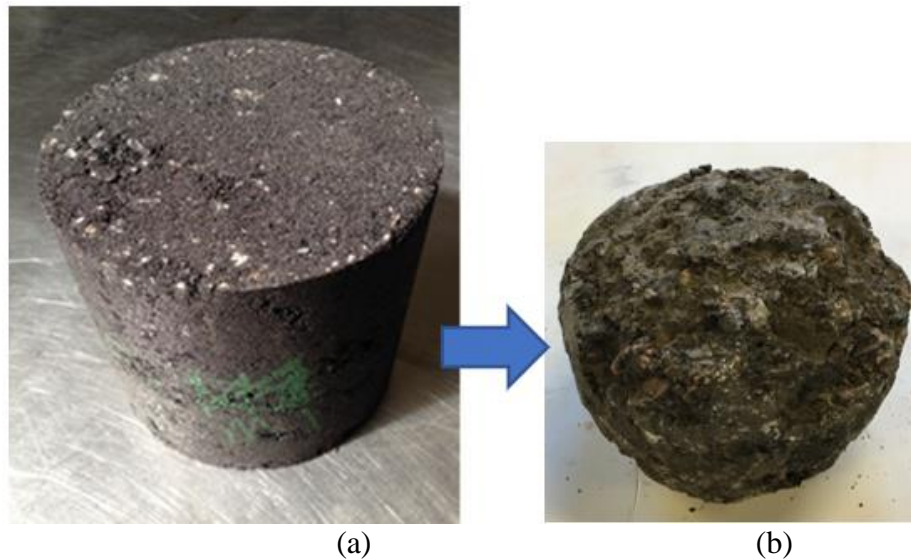


Figure 3.8 Abrasion Loss Test Sample (a) Before Testing (b) After Testing

#### 3.6.2.5 Hamburg Wheel Tracking (HWT) Test

Hamburg Wheel Tracking (HWT) tests were conducted as per AASHTO T 324 to determine the rutting susceptibility and moisture-induced damage potential of asphalt mixes (AASHTO, 2014c). Cylindrical samples with a diameter of 150 mm and a height of 60 mm were prepared in the laboratory. Two samples were taken for each HWT test and the end of each sample was saw-cut to match the mold (Figure 3.9). In AASHTO T 324, HWT tests are conducted at 50°C, a wheel passing frequency of 52 passes/minute and a wheel load of 705 N. The average linear speed of the wheel was approximately 1.1 km/hour. and the wheel traveled approximately 230 mm before reversing direction of movement. The test was automatically terminated after reaching a maximum rut depth of 20 mm or 20,000 wheel passes, whichever reached first. Deformations were

measured along the length of the wheel path at 11 equally spaced points. The rut depths at the three mid-points (5<sup>th</sup>, 6<sup>th</sup>, and 7<sup>th</sup> points) of the sample were considered in determining the average rut depth. For each mix, two sets (four in total) samples were tested to check the repeatability of results. Some noise was observed when the steel wheel traversed on the rutted sample. Lu and Harvey (2006) proposed Equations 3.9, 3.10 and 3.11 to calculate the moving averages to eliminate such noise in HWT testing.

$$\bar{d}_t = 0.40d_t + 0.25d_{t+1} + 0.15d_{t+2} + 0.10d_{t+3} + 0.10d_{t+4} \quad (1 \leq t \leq 5) \quad (3.9)$$

$$\begin{aligned} \bar{d}_t = & 0.05d_{t-5} + 0.05d_{t-4} + 0.075d_{t-3} + 0.075d_{t-2} + 0.15d_{t-1} + 0.20d_t + \\ & 0.15d_{t+1} + 0.075d_{t+2} + 0.075d_{t+3} + 0.05d_{t+4} + 0.05d_{t+5} \\ & (5 < t < 19,995) \end{aligned} \quad (3.10)$$

$$\begin{aligned} \bar{d}_t = & 0.40d_t + 0.25d_{t-1} + 0.15d_{t-2} + 0.10d_{t-3} + 0.10d_{t-4} \\ & (19,995 \leq t \leq 20,000) \end{aligned} \quad (3.11)$$

where:

$d$  = rut depth; and

$t$  = number of wheel passes.



Figure 3.9 HWT Saw-Cut Molded Sample After Testing

The post-compaction deformation, creep slope, stripping slope, and Stripping Inflection Point (SIP) were determined manually, as shown in Figure 3.10, from the HWT test results. The initial densification of asphalt pavement due to the movement of traffic was indicated by the post-compaction deformation. Yildirim and Kennedy (2002) suggested the rut depth at 1,000 wheel passes as the post-compaction point. The primary deformation under repeated loading is presented by this zone. After post-compaction zone, the rut depth increased linearly with number of wheel passes up to certain point. The secondary deformation under repeated loading is represented by this zone. The slope of this secondary zone is commonly known to be creep slope. After secondary deformation, a rapid increase in rut depth was observed with the increase in wheel passes. This rapid deformation of HWT sample is attributed to tertiary deformation. The slope of tertiary zone is commonly known as stripping slope. The moisture-induced damage potential of asphalt mixes is measured by this stripping slope. A steeper slope indicates a higher possibility of moisture damage for asphalt pavements. The intersection between the stripping slope and creep slope is presented by the SIP. The SIP can be defined as the number of repeated load cycles after which an abrupt increase in rut depth is observed in the HWT test due to stripping of binder from the aggregate (Brown et al., 2009).

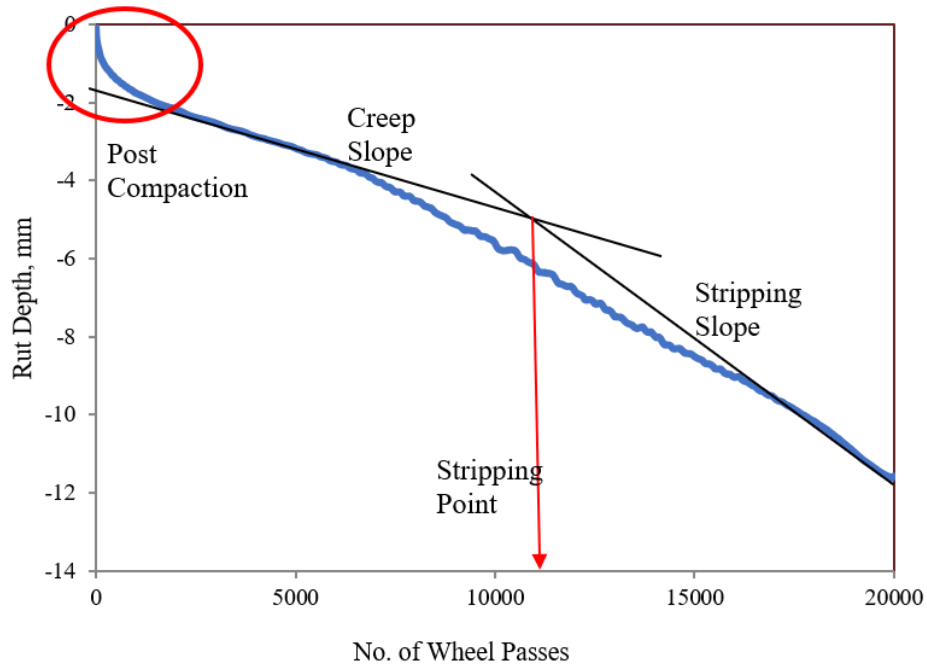


Figure 3.10 Results Showing Rut Depth vs Number of Wheel Passes

#### 3.6.2.6 Flow Number (FN) Test

The Flow Number (FN) test was conducted according to AASHTO T 378 using the AMPT machine (AASHTO, 2017). The FN test was conducted on the same specimen used for dynamic modulus test, as the specimen was not loaded beyond the elastic range in dynamic modulus test (AASHTO, 2017).

The FN test specimens were subjected to a 0.1 second repeated haversine axial compressive loading pulse followed by a 0.9 second rest period. The test was conducted at unconfined state with a contact stress of 30 kPa and repeated axial stress of 600 kPa. The temperature used for this test was 64°C which was selected based on the high-temperature Performance Grade (PG) of binder for Oklahoma. The test specimen typically experiences three stages of deformation: primary (initial consolidation of the specimen as it is loaded); secondary (creep deformation); and tertiary (shear deformation), as shown in Figure 3.11 (Copeland et al., 2010). At the primary stage, the

permanent strain rate decreases with the increase in repeated load cycles. The permanent strain rate remains constant at the secondary zone, whereas the strain rate increases in the tertiary zone of the curve. The number of cycles when tertiary deformation starts is referred to as FN (Brown et al., 2009). The test was continued up to 10,000 load cycles or until excessive tertiary deformation of the specimen. The minimum FN values suggested by AASHTO for different types of mixes and traffic loadings are shown in Table 3.8 (AASHTO, 2017). It was found that at all traffic levels, the recommended average FN value for WMA was relatively lower compared to HMA. For example, the minimum recommended FN values for HMA and WMA at more than 30 million ESALs are 740 and 415, respectively.

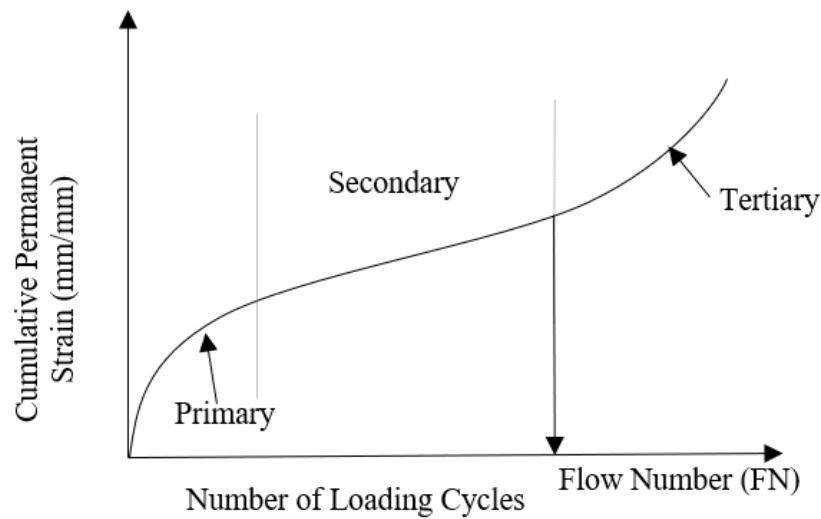


Figure 3.11 Typical Test Results for FN Tests (After Copeland et al., 2010)

Table 3.8 Minimum Average FN Requirements (AASHTO, 2017)

Traffic Level, million ESALs	HMA minimum average FN	WMA minimum average FN
<3	-	-
3 to <10	50	30
10 to <30	190	105
≥30	740	415

### 3.6.2.7 Indirect Tensile Strength Ratio (TSR) Test

Several researchers have used TSR as a potential indicator of moisture-induced damage (Solaimanian et al., 2003; Kim et al., 2012b; Shu et al., 2012). It represents the strength ratio of conditioned sample and dry sample. In this study, samples were conditioned following both AASHTO T 283 and Moisture Induced Sensitivity Test (MIST) method to evaluate the TSR values. For each case, three replicate cylindrical samples having a diameter of 150 mm and a height of  $115 \pm 5$  mm were prepared in the laboratory using SGC. The air voids of the compacted samples were maintained as  $7 \pm 0.5\%$ . The ITS test was conducted on both dry and conditioned asphalt samples according to ASTM D 6931 (ASTM, 2012). The ITS was calculated by using Equation 3.12 (ASTM, 2012).

$$S_t = \frac{2000 * P}{\pi * t * D} \quad (3.12)$$

where,

$S_t$  = Indirect Tensile Strength (kPa);

$P$  = maximum load (N);

$t$  = sample height immediately before test (mm); and

$D$  = sample diameter (mm).

The following equation was used to calculate the TSR value:

$$TSR = \frac{ITS \text{ of AASHTO T283/MIST} - \text{conditioned Samples } (ITS_{wet})}{ITS \text{ of Dry} - \text{conditioned Samples } (ITS_{dry})} \quad (3.13)$$

### 3.6.3 Moisture Conditioning

#### 3.6.3.1 AASHTO T 283 Method

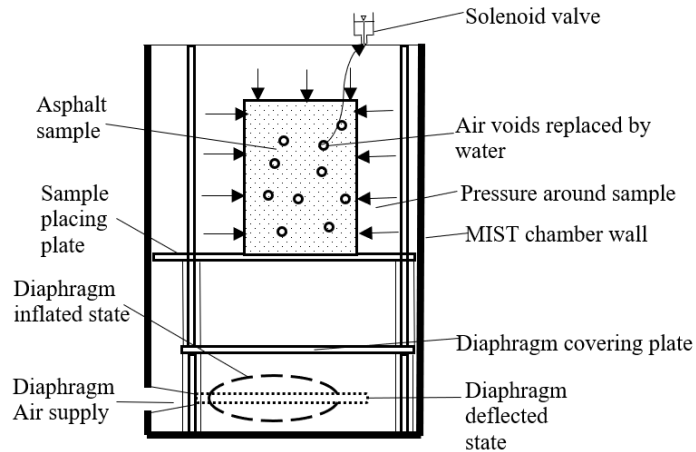
The AASHTO T 283 method was used for simulating the moisture-induced damage in the laboratory on the compacted samples before conducting the ITS test (AASHTO, 2014b). According to this procedure, samples were conditioned by saturating with water (70-80% saturation), followed by a freezing cycle ( $-18^{\circ}\text{C}$  for 16 hours) and a thawing cycle ( $60^{\circ}\text{C}$  water bath for 24 hours). The weathering effect on the asphalt sample was simulated by this conditioning method.

#### 3.6.3.2 Moisture Induced Sensitivity Test (MIST) Conditioning

MIST is a relatively new technique to simulate the generation and dissipation of pore water pressure in a saturated asphalt pavement. Initially, the ITS samples were conditioned at  $60^{\circ}\text{C}$  for 20 hours in water to simulate chemical and adhesion effects. After the adhesion phase, samples were subjected to 3,500 pressure cycles at 276 kPa to generate the effect of pore pressure buildup inside the sample according to ASTM D 7870 (ASTM, 2016). Figure 3.12 (a) presents a photographic view of MIST and Figure 3.12 (b) shows the mechanism of pore water pressure generation in the asphalt samples in MIST.



(a)



(b)

Figure 3.12 Moisture Induced Sensitivity Tester (a) Photographic Image (b) Conditioning Mechanism (After Tarefder et al., 2014)

The pore water pressure in the chamber was generated and dissipated by inflating and deflating the diaphragm of the MIST, respectively. The Solenoid valve was kept closed during the inflation of diaphragm and the pressure increased inside the chamber. Then, the Solenoid valve was opened to release the pressure and to let air bubbles pass the chamber, as shown in Figure 3.12 (b). During the inflation process, two specific phenomena took place in the MIST. Firstly, entrapped air in the asphalt sample was replaced by water. Secondly, some part of entrapped air was compressed. Then, during the deflation of diaphragm, the compressed air expanded again and replaced the water from sample pore (Tarefder et al., 2014).

### 3.7 High-Temperature Grading of Recovered RAP Binder

It was reported by Bonaquist (2011) that compaction temperature of WMA should be greater than the high-temperature PG of the extracted RAP binder to ensure sufficient active binder from the reclaimed materials. To verify this finding, the high-



temperature PG of extracted binder from the RAP used in this study was determined using a Dynamic Shear Rheometer (DSR) test (AASHTOT 315). For this purpose, the RAP binder was extracted and recovered using the AASHTO T 164 and ASTM D 5404 test procedures, respectively (AASHTO, 2014; ASTM, 2017). According to AASHTO T 164 method, the RAP was first placed in a bowl for 45 minutes with a solvent (EnSolv<sup>®</sup> EX), as shown in Figure 3.13 (a). Then, the bowl with RAP and solvent was placed in a centrifuge extractor and tightly clamped with a cover (Figure 3.13 (b)). The speed of the centrifuge extractor was then increased gradually to 3,600 rev/min to extract the solution of solvent with asphalt binder from the bowl. The centrifuge extractor was kept running until the solution stopped to flow from the bowl. The same procedure was repeated for several times (not less than three) until the extract was lighter than a light straw color (AASHTO, 2014a).

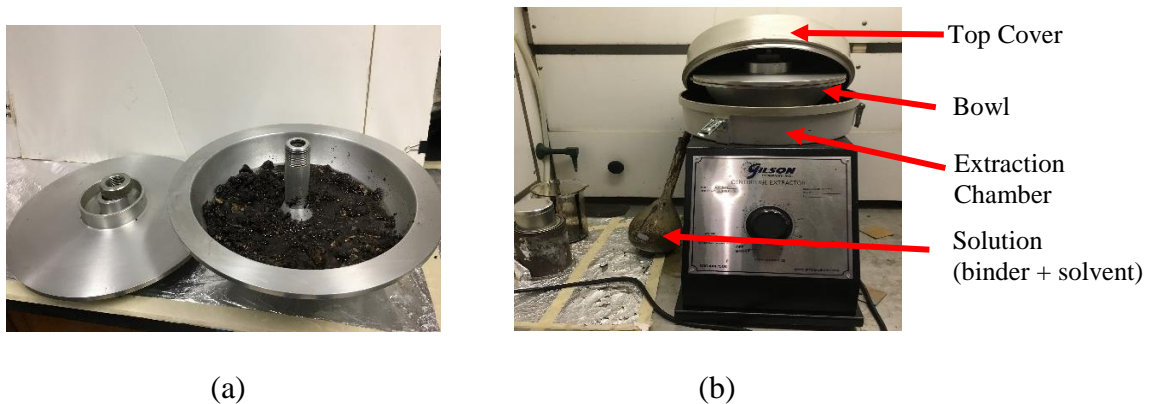


Figure 3.13 RAP Binder Extraction (a) Bowl (b) Centrifuge Extractor

The extracted solution (solvent with asphalt binder) was then placed in a rotating flask and heated in the rotary evaporator while partially immersed in an oil bath (Figure 3.14). In this process, solution was distilled under a constant vacuum and flow of Nitrogen gas. Initially, the oil bath was heated to a temperature of  $140 \pm 3^{\circ}\text{C}$  under a vacuum of  $5.3 \pm 0.7$  kPa below the atmospheric pressure. The rotation of the distillation

flask was kept as 40 rev/min. When the bulk of the solvent was distilled from the solution, the temperature of the oil bath was changed to  $165 \pm 5$  °C, the vacuum pressure was changed to  $80.0 \pm 0.7$  kPa below the atmospheric pressure, and rotation of the flask was increased to 45 rev/min to complete the distillation process. At the end of the process, the solution was distilled leaving asphalt binder in the rotating flask.

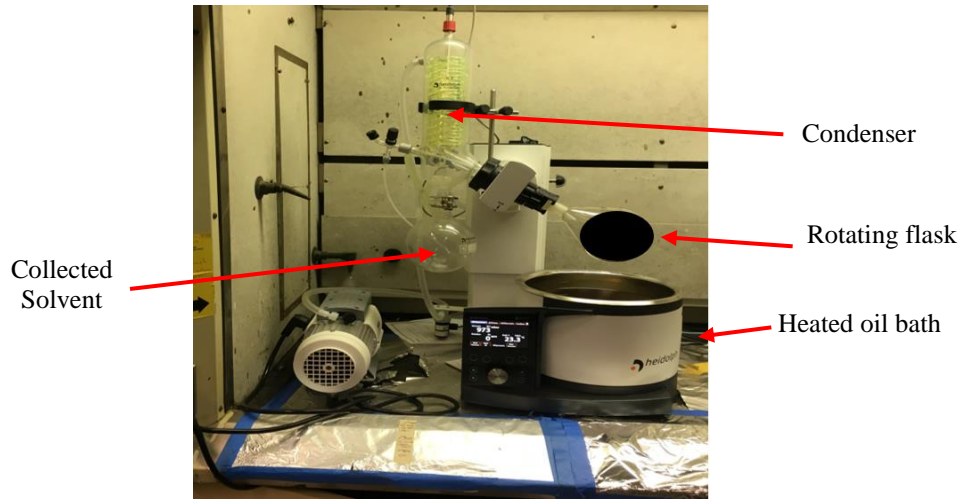


Figure 3.14 RAP Binder Recovery Using Rotary Evaporator

The high-temperature PG of the extracted RAP binder was then determined by conducting the DSR test according to AASHTO T 315 (AASHTO, 2012). This test was conducted on both unaged and Rolling Thin-Film Oven (RTFO)-aged samples at three different temperatures, namely 88°C, 94°C and 100°C. The binder conditioning after compaction of asphalt mixes was simulated by the RTFO-aging. Binder samples having a diameter of 25 mm and a thickness of 1 mm were tested under both unaged and RTFO-aged conditions. Three replicates were tested at each condition to check the variability of test results. From the DSR test results, shear modulus ( $G^*$ ), phase angle ( $\delta$ ) and rutting factor ( $G^*/\sin \delta$ ) of the binder were determined at tested temperatures. The high-temperature PG was determined based on the rutting factor ( $G^*/\sin \delta$ ) of the

binder. The following limits were used in determining the high-temperature PG of the extracted RAP binder: 1.0 kPa for unaged condition and 2.2 kPa for RTFO-aged condition.

## **CHAPTER**

# **4**

## **VOLUMETRIC PROPERTIES OF FOAMED WMA CONTAINING RAP**

### **4.1 Introduction**

As noted earlier, the volumetric properties of foamed WMA containing RAP were determined in this study using AASHTO R 35 asphalt mix design method and compared with their HMA counterparts (AASHTO, 2013). For this purpose, the volumetric properties of two control HMA mixes (Mix-1 and Mix-5) and six foamed WMA mixes (Mix-2, Mix-3, Mix-4, Mix-6, Mix-7 Mix-8) were determined. As noted in Chapter 3, these mixes were designed for light traffic with Equivalent Single Axle Load (ESAL) < 0.3 million (AASHTO, 2013). Consequently, the number of gyration in SGC was kept at 50 (AASHTO, 2013). The volumetric properties of both foamed WMA and HMA are presented in this chapter.

### **4.2 Current Foamed WMA Mix Design Practice**

As mentioned in Chapter 3, the foamed WMA mixes (Mix-2 and Mix-6) were mixed and compacted at 135°C and 127°C, respectively. The control HMA mixes (Mix-1 and Mix-5) were mixed and compacted at 163°C and 149°C, respectively. Same aggregate gradation, with 25% RAP, was used for both Mix-1 and Mix-2 so that their volumetric properties can be compared. The amount of RAP for Mix-5 and Mix-6 was

reduced to 5%, following ODOT's current practice for S4 mixes, and the aggregate gradation was adjusted accordingly (ODOT, 2013a).

The volumetric properties of asphalt mixes are generally dictated by the percent air voids at desired number of gyrations (Huang et al., 2005; Zhao et al., 2012). The percent air voids of the volumetric samples were calculated based on the theoretical maximum specific gravity ( $G_{mm}$ ) of asphalt mixes and bulk specific gravity ( $G_{mb}$ ) of compacted asphalt samples. For both Mix-1 and Mix-2, three  $G_{mm}$  tests were conducted to check the repeatability of results. The recommended maximum standard deviation for  $G_{mm}$  is 0.0064 for single-operator precision (AASHTO, 2012). The  $G_{mm}$  for Mix-1 containing 25% RAP was found to be 2.499 with a standard deviation of 0.001. As can be seen from Table 4.1, the same  $G_{mm}$  value (2.499) was observed for Mix-2 with a standard deviation of 0.001. Therefore, the standard requirement was satisfied by both Mix-1 and Mix-2 (AASHTO, 2012). Also, because the same aggregate gradations and RAP content were used in both mixes, the same  $G_{mm}$  values were found for both mixes. Similar  $G_{mm}$  values were also reported for both Zeolite and Sasobit-based WMA compared to HMA with the same limestone aggregate gradation by Hurley and Prowell (2005, 2006). An identical  $G_{mm}$  value of 2.544 was reported for both WMA with Zeolite and HMA (Hurley and Prowell, 2006). For Sasobit-based WMA, a  $G_{mm}$  value of 2.545 was found for asphalt mixes with the same aggregate gradation (Hurley and Prowell, 2006).

Table 4.1 and Figure 4.1 present the details on percent air voids for Mix-1 and Mix-2 samples. For each mix, six samples were compacted to check the repeatability of percent air voids or compaction level for the specified number of gyrations. The average

percent air voids were found as 4.2% for both mixes. The corresponding standard deviations for Mix-1 and Mix-2 were found to be 0.1% and 0.2%, respectively. The statistical difference in percent air voids between Mix-1 and Mix-2 was identified by performing a two-tail t-test. A summary of the t-test result is presented in Table 4.2. The p-value obtained from the statistical test was found to be 0.58, which is greater than 0.05. Therefore, it is evident that the difference in percent air voids between Mix-1 and Mix-2 is insignificant, at 95% confidence level. Similar volumetric properties for both HMA and WMA were reported by Bonaquist (2011), when absorbed binder content is less than one percent. In that study, asphalt mixes containing up to 40% RAP was considered and absorbed binder content was kept less than one percent for both HMA and WMA. For S3 mixes (Mix-1 and Mix-2), the percent of absorbed binder was found to be 0.42%, which is less than 1.00% (Table 3.5). Any increase in coating ability of binder due to foaming process is expected to counteract the lowering of mixing and compaction temperatures for WMA (Jones et al., 2010; Bonaquist, 2011). Therefore, compaction efforts required for both HMA (Mix-1) and foamed WMA (Mix-2) samples are expected to be similar. Several previous studies have reported similar finding (Hurley and Prowell, 2006; Wielinsk et al., 2009; Jones et al., 2010; WSDOT, 2012; Xiao et al., 2012; Malladi, 2015). It was reported that surface mixes with granite aggregate and PG 64-22 binder required similar compaction effort for both foamed WMA and control HMA (Malladi, 2015). Also, Jones et al. (2010) found that WMA with Rediset<sup>TM</sup> additives could be mixed and compacted at 35°C lower temperature than HMA to show similar compactability compared to HMA.

Table 4.1 Percent Air Voids for Mix-1 and Mix-2

Mix ID	Weight in Air, $W_d$ (gm)	Weight in Saturated Surface Dry, $W_{ssd}$ (gm)	Weight in Water, $W_{water}$ (gm)	Maximum Specific Gravity $G_{mm}$	Air Voids Content (%)	Average Air Voids Content (%)	Standard Deviation (%)
Mix-1	4801.8	4814.1	2810.8	2.499	4.1	4.2	0.1
	4802.2	4813.4	2811.5		4.0		
	4800.2	4815.3	2809.4		4.2		
	4800.3	4815.7	2809.5		4.3		
	4802.8	4815.9	2813.7		4.0		
	4801.2	4815.8	2808.1		4.3		
Mix-2	4800.8	4817.2	2819.2	2.499	3.9	4.2	0.2
	4803.6	4819.0	2810.9		4.3		
	4800.4	4818.2	2814.6		4.1		
	4817.5	4833.2	2815.2		4.5		
	4798.3	4819.4	2811.3		4.4		
	4801.0	4819.3	2815.0		4.2		

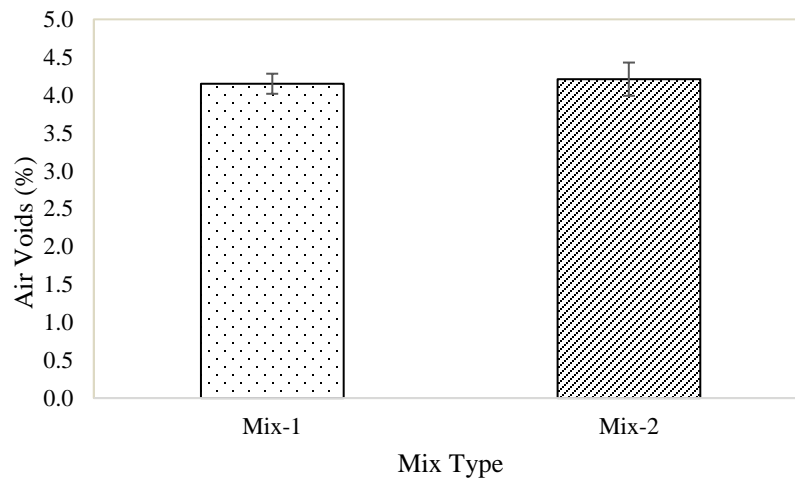


Figure 4.1 Percent Air voids for Mix-1 and Mix-2

Table 4.2 t-Test Results at 95% Confidence Level

	Mix-1	Mix-2
Mean	4.2	4.2
t Stat	-0.573	
**P(T<=t) two-tail	0.58	

\*\*P greater than 0.05 = insignificant difference

While using RAP in WMA, the blending of aged binder from RAP and new binder may be hindered due to the lower mixing and compaction temperatures of WMA than HMA (Bonaquist, 2011). To ensure adequate blending of aged and virgin binders, the compaction temperature of WMA should be greater than the high-temperature PG of RAP (Bonaquist, 2011). From DSR test results presented in Table 4.3, the high-temperature PG of the RAP binder used in this study was found to be 94.1°C. Because the volumetric samples of Mix-2 were compacted at a higher temperature (127.0°C) than the high-temperature PG of the RAP binder (94.1°C), proper blending of aged and new binder was expected for foamed WMA. Therefore, it is expected that the difference in percent air voids between Mix-1 and Mix-2 samples would be insignificant, as was the case here. Hence, it is postulated that the foamed WMA S3 containing 25% RAP can be designed as per AASHTO R 35 (AASHTO, 2013), when mixing and compaction temperatures are kept at 135°C and 127°C, respectively.

Table 4.3 High-Temperature PG of Recovered RAP Binder

Aging Condition	Temperature (°C)	$ G^* /\sin \delta$ (kPa)	Superpave <sup>®</sup> Requirement $ G^* /\sin \delta$ (kPa)	PG Temperature (°C)	Continuous High-Temperature PG (°C)
Unaged	88	2.80	1.0	96.7	94.1
	94	1.37			
	100	0.69			
RTFO-aged	88	4.55	2.2	94.1	
	94	2.23			
	100	1.10			

A similar trend in percent air voids was observed for the S4 mixes (Mix-5 and Mix-6) containing 5% RAP (Table 4.4 and Figure 4.2). The  $G_{mm}$  value for both S4 mixes was found to be 2.496. The average percent air voids for both Mix-5 and Mix-6



were observed as 4.5%. For both mixes, three volumetric samples were compacted to check repeatability. To check the repeatability of test results, the average percent voids of at least three volumetric samples were recommended by AASHTO (AASHTO, 2013). The standard deviations of percent air voids for Mix-5 and Mix-6 were 0.1% and 0.2%, respectively. Table 4.5 presents the t-test results for differences in percent air voids between Mix-5 and Mix-6. The p-value obtained from this test was 0.98, which was much higher than 0.05. Comparatively, for S4 mixes the p-value (0.98) was higher than that for S3 mixes (0.58). A lower amount of RAP used in S4 mixes is believed to give a higher p-value, as the variability in the mix properties increases with an increase in RAP content (Jones, 2008). The percent absorbed binder was found to be 0.46% for both Mix-5 and Mix-6, which is less than 1.00% (Table 3.6). Moreover, the compaction temperature (127.0°C) for Mix-6 was greater than the high-temperature PG of extracted RAP binder (94.1°C). Therefore, similar volumetric properties were expected for both Mix-5 and Mix-6 because of adequate blending of aged binder with the virgin binder. Similar findings were reported by other researchers (Hurley and Prowell, 2006; Wielinsk et al., 2009; Jones et al., 2010; Bonaquist, 2011; WSDOT, 2012; Xiao et al., 2012; Malladi, 2015).

Table 4.4 Percent Air Voids for Mix-5 and Mix-6

Mix ID	Weight in Air, $W_d$ (gm)	Weight in Saturated Surface Dry, $W_{ssd}$ (gm)	Weight in Water $W_{water}$ (gm)	Max. Sp. Gravity $G_{mm}$	Air Voids Content (%)	Average Air Voids Content (%)	Standard Deviation (%)
Mix-5	4796.1	4808.4	2797.6	2.496	4.4	4.5	0.1
	4799.0	4810.6	2794.0		4.7		
	4797.4	4810.3	2799.5		4.4		
Mix-6	4797.1	4804.3	2795.0	2.496	4.4	4.5	0.2
	4799.0	4810.3	2793.0		4.7		
	4797.2	4811.2	2799.5		4.5		

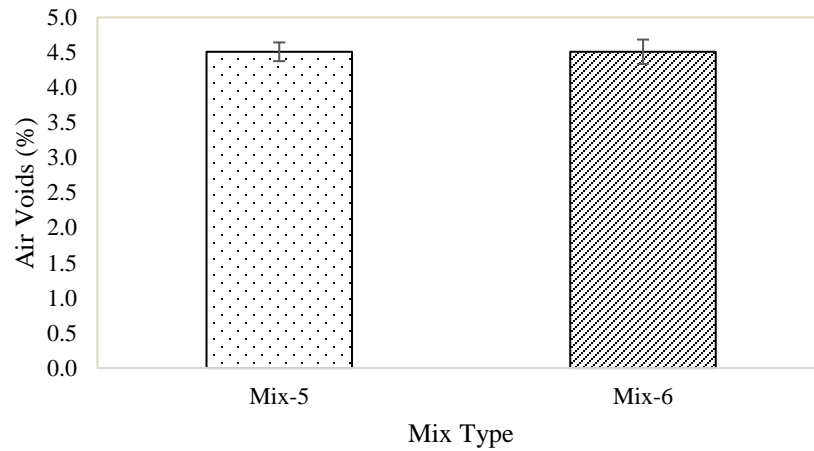


Figure 4.2 Percent Air voids for Mix-5 and Mix-6

Table 4.5 t-Test Results at 95% Confidence Level

	Mix-5	Mix-6
Mean	4.5	4.5
t Stat	-0.03	
**P(T<=t) two-tail	0.98	

\*\*P greater than 0.05 = insignificant difference

### **4.3 Reduction in Mixing and Compaction Temperatures**

The mixing and compaction temperatures of foamed WMA were further lowered from the current WMA practice to check the variation in percent air voids compared to control HMA. The same aggregate gradation and RAP content (25%) was used for producing Mix-3 and Mix-4 as in the case of Mix-1. Mix-7 and Mix-8, however, were produced using aggregate gradation and RAP content (5%) similar to that of Mix-5. For each case, three volumetric samples were compacted to check the repeatability of percent air voids. For Mix-3 and Mix-7, both mixing and compaction temperatures were lowered by 20°C (i.e., to 115°C and 107°C, respectively). For Mix-4 and Mix-8, both mixing and compaction temperatures were lowered further by 20°C to 95°C and 87°C, respectively, to check their effect on the blending of binders and coating ability. For all samples produced at lower temperatures than used in practice (i.e., mixing at 135°C and compaction at 127°C), uncoated aggregates were observed after mixing and compaction, as shown in Figures 4.3(a) and 4.3(b). These figures indicate potential for weak bond between aggregate and binder, and difficulty in compaction or achieving desired air voids at 50 number of gyration. Increased RAP content in Mix-3 and Mix-4 made compaction more difficult.



Figure 4.3 Uncoated Volumetric Samples at Lower Mixing and Compaction Temperatures (a) After Mixing and (b) After Compaction

Figure 4.4 presents the results for average percent air voids for all S3 mixes (Mix-1, Mix-2, Mix-3, and Mix-4) containing 25% RAP. Both Mix-1 and Mix-2 exhibited essentially identical volumetric properties. The percent air voids were found to increase with further reduction in mixing and compaction temperatures for foamed WMA. To identify statistical differences in air voids between Mix-1 and WMA with reduced mixing and compaction temperatures (Mix-3 and Mix-4) two-tail t-tests were performed. The results are summarized in Table 4.6. The p-values observed for Mix-3 and Mix-4 were  $2.936e-04$  and  $3.679e-07$ , respectively, compared to Mix-1. These p-values were much lower than 0.05 for both cases indicating that the percent air voids of mixes with reduced mixing and compaction temperatures were significantly different than those of the control HMA, at 95% confidence level. Therefore, it can be concluded that the mixing and compaction temperatures significantly control the volumetric properties of foamed WMA.

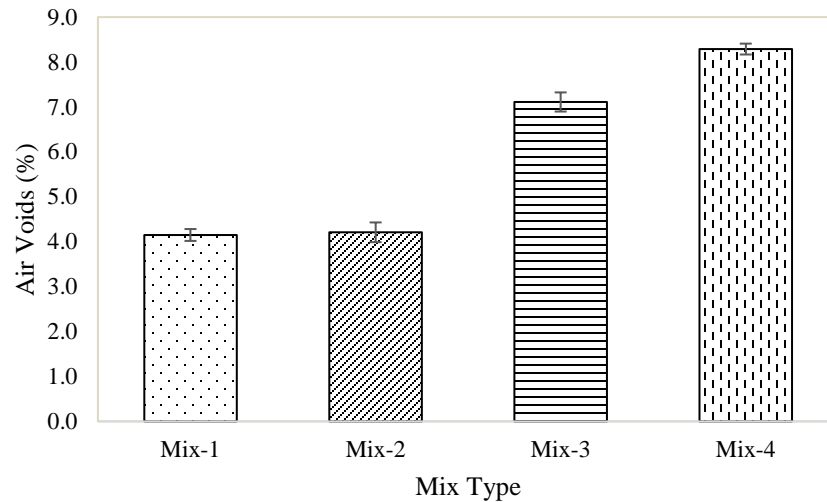


Figure 4.4 Percent Air Voids for S3 Mixes

Table 4.6 A Summary of Statistical Results for S3 Mixes

Mix ID	Mix Type	RAP Content (%)	Mixing/ Compaction Temperature (°C)	Average Air Voids (%)	p-Value (Two-Tail t-Test)	Difference at 95% Confidence Level
Mix-1	HMA	25	163/149	4.2	Control Mix	
Mix-2	WMA	25	135/127	4.2	0.58	Insignificant
Mix-3	WMA	25	115/107	7.1	2.936e-04	Significant
Mix-4	WMA	25	95/87	8.3	3.679e-07	Significant

Also, differences in percent air voids of Mix-4 samples became more significant compared to Mix-1 samples when the mixing and compaction temperatures were reduced by 40°C (from the current WMA practice), while keeping the amount of RAP content unchanged (25%). As pointed out earlier, this is likely caused by the lack of proper blending of the RAP binder with the virgin binder. For S3 mixes with 25% RAP content, about 31% of the total binder was expected from RAP. As the compaction temperature (87.0°C) for Mix-4 was lower than the high-temperature PG of the extracted RAP binder (94.1°C), proper blending of the RAP binder with the virgin binder was likely not achieved. Irrespective of the mixing and compaction temperatures, the foamed binder was produced at 135°C and aggregates were heated at 95°C for Mix-

4. It is likely that this large difference (40°C) in temperature between foamed binder and aggregates resulted in improper mixing. According to Bowering and Martin (1976), to ensure proper mixing between foamed WMA binder and aggregate the maximum temperature difference should not exceed 23°C. At a higher temperature difference, the foams in the binder collapse more rapidly due to quick heat transfer when they come in contact with aggregates (Jenkins et al.,1999).

A similar trend in percent air voids of foamed WMA S4 mixes was observed, as compared to control HMA S4 mix. Figure 4.5 presents the percent air voids for all S4 mixes (Mix-5, Mix-6, Mix-7, and Mix-8) containing 5% RAP. The results of the statistical tests are summarized in Table 4.7. The p-values found for Mix-7 and Mix-8 were 1.75e-05 and 1.571e-05, respectively. These p-values are much lower than 0.05 for both cases, which indicates that percent air voids of mixes with reduced mixing and compaction temperatures are significantly different than those of the control HMA, at 95% confidence level. An increase in percent air voids was observed with a decrease in compaction and mixing temperatures because of difficulty in compaction due to insufficient coating. Also, the difference in percent air voids between Mix-5 and Mix-8 became larger, as expected. This was because of lower compaction temperature (87.0°C) for Mix-8 than the high-temperature PG of RAP binder (94.1°C). Also, the foamed WMA binder was produced at 135°C while aggregates were heated at 95°C for Mix-8. This temperature difference (40°C) was more than 23°C recommended by Bowering and Martin (1976) necessary for coating and compaction.

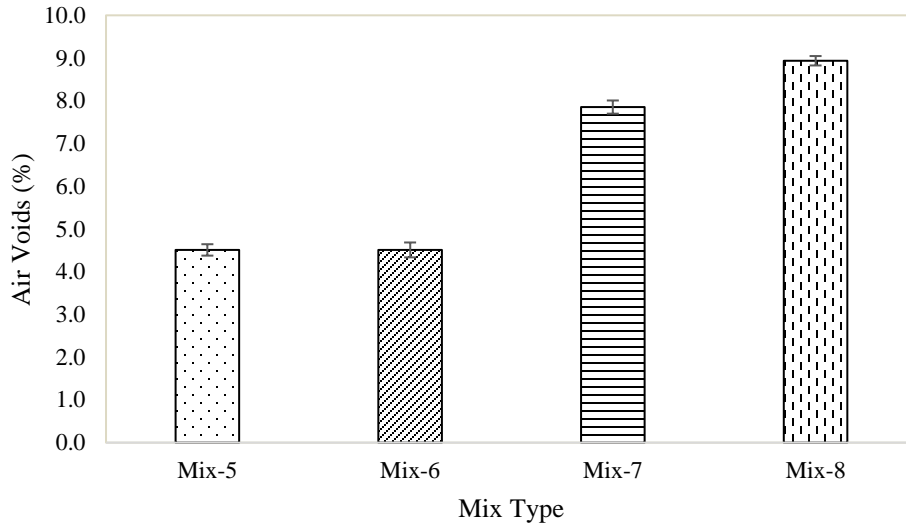


Figure 4.5 Percent Air Voids for S4 Mixes

Table 4.7 A Summary of Statistical Results for S4 Mixes

Mix ID	Mix Type	RAP Content (%)	Mixing/ Compaction Temperature (°C)	Average Air Voids (%)	p-Value (Two-Tail t-Test)	Difference at 95% Confidence Level
Mix-5	HMA	5	163/149	4.5	Control Mix	
Mix-6	WMA	5	135/127	4.5	0.98	Insignificant
Mix-7	WMA	5	115/107	7.9	1.75e-05	Significant
Mix-8	WMA	5	95/87	8.9	1.571e-05	Significant

#### 4.4 Summary

The volumetric properties of foamed WMA and HMA were discussed in this chapter. It was found that the foaming process involved in WMA increases the coating ability of the binder. This increase in coating ability of binder counteracted the lowering of mixing and compaction temperatures for WMA. As a result, the control HMA and foamed WMA produced at mixing and compaction temperatures used in practice exhibited similar volumetric properties. However, statistically significant differences in percent air voids were observed for further reduction in mixing and compaction temperatures, at 95% confidence level. Reduction in mixing and compaction

temperatures beyond certain level results in improper mixing between aggregates and foamed binder. Also, while incorporating RAP in the WMA, the high-temperature PG of RAP binder is expected to play an important role in ensuring proper blending between aged and virgin binder. It was found that the compaction temperature of WMA needs to be higher than the high-temperature PG of extracted RAP binder to obtain enough active binder from RAP. Furthermore, the temperature difference between foamed binder and aggregates should not exceed certain level during mixing to avoid rapid collapse of foam when it comes in contact with aggregates.



## **CHAPTER**

# **5**

## **LABORATORY PERFORMANCE OF WMA CONTAINING RAP**

### **5.1 Introduction**

As discussed in Chapter 4, volumetric properties of WMA were similar to those of HMA when the foamed WMA was mixed (135°C) and compacted (127°C) at temperatures currently used in practice. However, further reduction in the mixing and compaction temperatures of foamed WMA mixes (Mix-3, Mix-4, Mix-7 and Mix-8) showed statistically significant difference in volumetric properties compared to those of control HMA mixes. Therefore, only performance of foamed WMA (i.e., Mix-2 and Mix-6) mixed at 135°C and compacted at 127°C was tested in the laboratory and compared to their HMA counterparts (i.e., Mix-1 and Mix-5). Specifically, performance of these mixes was evaluated with respect to dynamic modulus, rutting, cracking and moisture-induced damage. The results are presented and discussed in this chapter.

### **5.2 Dynamic Modulus Test**

As mentioned in Chapter 3, dynamic modulus tests were conducted in accordance with AASHTO T 378 (AASHTO, 2017). Dynamic modulus values were used to develop master curves with respect to reduced frequencies, as discussed in Chapter 3. The model parameters for dynamic modulus master curves for both HMA

and WMA are shown in Table 5.1 at a reference temperature of 21.1°C. The correlation coefficients ( $R^2$ ) were found to be greater than 0.90 for all mixes. Also, the  $S_e/S_y$  (standard error of estimate/standard deviation) values were found to be lower than 0.35. Based on the criteria suggested by Witczak (2005), the goodness-of-fit statistics for these master curve models can be considered “excellent” (Table 3.7). Therefore, the sigmoidal function discussed in Chapter 3 could be used effectively to develop the dynamic modulus master curve. Also, temperature shift factor parameters for all cases are summarized in Table 5.2. Based on the correlation coefficients of shift factor, the master curve models are also rated as “excellent.”

Table 5.1 Dynamic Modulus Master Curve Model Parameters

Mix Type	Dynamic Modulus Model Parameters					Goodness-of-fit Statistics		
	$\alpha$	$\delta$	$\beta$	$\gamma$	$c$	$R^2$	Se/Sy	Rating
Mix-1	3.494	1.188	-0.663	-0.325	9583.851	0.992	0.068	Excellent
Mix-2	3.948	0.664	-0.745	-0.308	9583.848	0.996	0.085	Excellent
Mix-5	3.597	0.993	-0.612	-0.330	9583.996	0.992	0.066	Excellent
Mix-6	3.293	1.185	-0.495	-0.371	9583.860	0.996	0.079	Excellent

Table 5.2 Dynamic Modulus Master Curve Shift Factor Model Parameters

Mix Type	Shift Factor Parameters			Goodness-of-fit Statistics	
	$m$	$n$	$p$	$R^2$	Rating
Mix-1	0.0003	-0.125858	2.50517	1.00	Excellent
Mix-2	0.0003	-0.125858	2.50517	1.00	Excellent
Mix-5	0.0003	-0.125860	2.50521	1.00	Excellent
Mix-6	0.0003	-0.125859	2.50517	1.00	Excellent

The dynamic modulus master curves for S3 mixes (Mix-1 and Mix-2) are shown in Figure 5.1. The corresponding master curves for S4 mixes (Mix-5 and Mix-6) are shown in Figure 5.2. An increase in dynamic modulus values was observed with the increase in frequency and decrease in testing temperature. These results are compatible with expectations as an increase in testing frequency and/or a decrease in temperature

increases the stiffness of asphalt mixes (Flintsch et al., 2007; Tashman and Elangovan, 2008; Singh et al., 2011; Ghabchi, 2014).

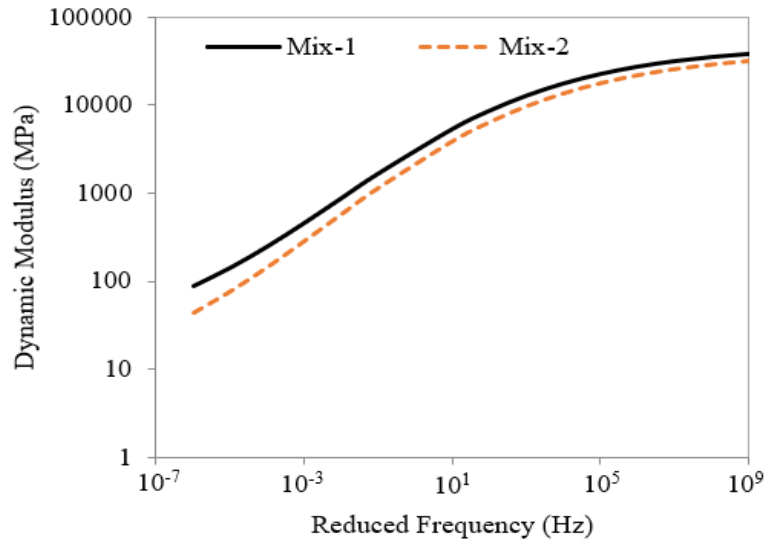


Figure 5.1 Master Curve for Mix-1 and Mix-2 at a Reference Temperature of 21.1°C

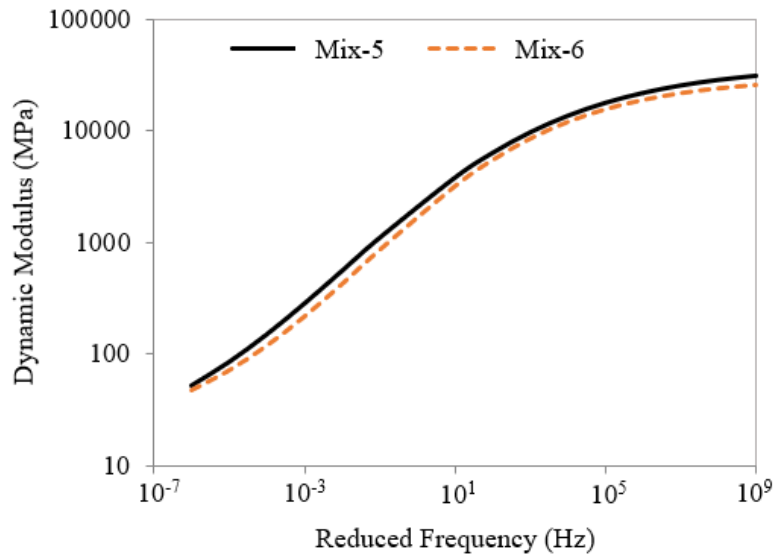


Figure 5.2 Master Curve for Mix-5 and Mix-6 at a Reference Temperature of 21.1°C

From Figures 5.1. and 5.2, it is evident that both HMA and WMA showed a similar trend. However, for a given reduced frequency, the dynamic modulus values for WMA were smaller compared to their HMA counterparts. For example, at 10<sup>-4</sup> Hz reduced frequency predicted dynamic modulus values for Mix-1 (control HMA S3) and

Mix-2 (WMA S3) were found to be 249 MPa and 147 MPa, respectively. Therefore, 41% lower dynamic modulus value was observed for Mix-2 compared to Mix-1 at  $10^{-4}$  Hz reduced frequency. A similar trend was observed for S4 mixes. The predicted dynamic modulus values for Mix-5 (control HMA S4) and Mix-6 (WMA S4) at  $10^{-4}$  Hz reduced frequency were 151 MPa and 120 MPa, respectively. Thus, about 21% lower dynamic modulus value was observed for Mix-6 compared to Mix-5 at  $10^{-4}$  Hz reduced frequency. As noted previously, a lower degree of aging in WMA is expected to produce softer mixes compared to HMA (Hurley and Prowell, 2006; Alhasan et al., 2014; Malladi, 2015). Several other researchers have reported lower dynamic modulus values for WMA compared to HMA (Copeland et al., 2010; Goh and You, 2011b; Ghabchi, 2014; Pandey, 2016). About 19% lower mean dynamic modulus value was reported by Goh and You (2011b) for porous WMA compared to porous HMA at  $-5^{\circ}\text{C}$  reference temperature. A lower dynamic modulus can cause more rutting in case of WMA (Ghabchi, 2014). Also, a lower stiffness may result in increased cracking resistance for foamed WMA compared to HMA (Ghabchi, 2014).

From these figures it is evident that both S3 mixes containing 25% RAP had higher dynamic modulus values compared to S4 mixes containing 5% RAP. For instance, at  $10^{-4}$  Hz reduced frequency dynamic modulus values for Mix-1 and Mix-5 were found to be 249 MPa and 151 MPa, respectively. Therefore, 39% lower dynamic modulus value was observed for Mix-5 compared to Mix-1 at  $10^{-4}$  Hz reduced frequency. A similar trend was followed by foamed WMA. About 18% lower dynamic modulus value was observed for Mix-6 compared to Mix-2 at  $10^{-4}$  Hz reduced frequency. As reported by Pandey (2016), higher RAP contents lead to stiffer mixes and

higher dynamic modulus, which supports the results obtained from this study. Also, the differences in the dynamic modulus values between Mix-1 and Mix-2 were more pronounced at lower reduced frequencies (Figure 5.1). With increased reduced frequency, the differences in dynamic modulus values between Mix-1 and Mix-2 samples were found to reduce. The differences in dynamic modulus values between Mix-1 and Mix-2 were found to decrease from 41% to 24% for reduced frequency  $10^{-4}$  Hz to  $10^4$  Hz. This was logical because lower reduced frequency was associated with higher temperature according to the time-temperature superposition principle. Similar observations were made by Ghabchi (2014). As reported by Ghabchi (2014), at a higher reduced frequency aggregate structure is believed to govern the mix properties, especially for coarser mixes. For finer mixes (S4 mixes), both HMA and WMA samples were found to exhibit a similar trend at all levels of frequencies. The differences in dynamic modulus values between S4 mixes were 14% and 21% at reduced frequency  $10^4$  Hz and  $10^{-4}$  Hz, respectively. Therefore, effect of aged binder from RAP on the dynamic modulus master curve was insignificant when the RAP content was low (5% in this case). The dynamic modulus values generated in this study can be used in the M-EPDG software for predicting rutting and cracking.

### **5.3 Fatigue Cracking Resistance**

Fatigue cracking is one of the common distresses in asphalt pavements due to repeated traffic loading (Colombier, 1997; Baek J., 2010; Moreno and Rubio, 2013). As discussed in Chapter 2, different agencies are currently using different test methods to characterize fatigue resistance of asphalt mixes during the design stage (Barman et al., 2018). As noted earlier, the Louisiana SCB, I-FIT and Abrasion Loss or Cantabro tests

were used in this study to identify the cracking potential of asphalt mixes. These results are presented next.

### 5.3.1 Louisiana SCB Test

The Louisiana SCB tests were conducted in accordance with the ASTM D 8044 test method (ASTM, 2013). As mentioned in Chapter 3, samples with three different notch depths (namely 25.4 mm, 31.8 mm and 38.0 mm) and a loading rate of 0.5 mm/min were used in this testing.

Figure 5.3 presents the variation of average strain energy at failure with respect to notch depths for S3 mixes. The repeatability of test results was checked in terms of Coefficient of Variation (COV) of average strain energy. For each notch depth at least three specimens were tested. The COV of average strain energy was found to be less than 15% for each set of samples (Table 5.3). These COV values were smaller than those (maximum 21%) reported by Arshadi et al. (2017). It is evident from Figure 5.3 that the average strain energy decreases with the increase in notch depths for both mixes, as expected. The reduction in effective loading area with increasing notch depth is believed to decrease the average strain energy (Kim et al., 2012a; Khan, 2016; Saeidi and Aghayan, 2016). For all notch depths, Mix-2 (WMA S3) exhibited higher average strain energy than that of Mix-1 (HMA S3). For example, at 25.4 mm notch depth, the average strain energy at failure for Mix-1 and Mix-2 were found to be 0.33 Joules and 0.50 Joules, respectively.

Table 5.3 Coefficient of Variance (%) at Different Notch Depths for S3 Mixes

Mix Type	Notch Depth, mm		
	25.4	31.8	38.0
Mix-1	9	4	3
Mix-2	13	14	12

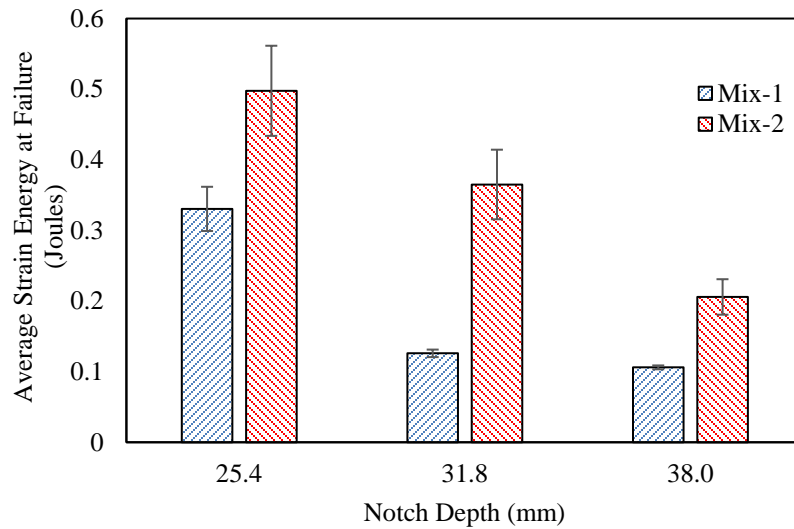


Figure 5.3 Average Strain Energy at Failure for Mix-1 and Mix-2

As noted by Kim et al. (2012a), samples with a higher average strain energy may not exhibit higher cracking resistance. Instead, the strain energy release rate ( $J_c$ ) is a better indicator of cracking resistance of asphalt mixes. For Mix-2, a higher  $J_c$  value was observed compared to that of Mix-1 (Figure 5.4). Therefore, a foamed WMA containing 25% RAP is expected to show a higher cracking resistance than that of HMA. As noted earlier, lower mixing and compaction temperatures for WMA are expected to produce softer mixes due to reduced aging (Hurley and Prowell, 2006; Alhasan et al., 2014; Malladi, 2015). Softer mixes may result in a higher cracking resistance for WMA (Kim et al., 2012a; Zhao et al., 2013; Dong et al., 2017; Ghabchi et al., 2019). Several other researchers have reported exactly opposite findings (Lee et al., 2009; Hill et al., 2012b; Valdes-Vidal et al., 2018). According to these researchers WMA is expected to exhibit lower cracking resistance than HMA. They attributed the presence of moisture at lower temperature in foamed WMA for this observation (Hill et al., 2012b). A combination of factors such as ambient moisture in aggregate, type of aggregate, amount of RAP, sources of RAP, age of RAP, type and amount of virgin

binder can be responsible for opposing findings. According to ASTM D 8044, a  $J_c$  value of 0.5 to 0.60 kJ/m<sup>2</sup> ensures sufficient cracking resistance (ASTM, 2013). It is evident from Figure 5.4 that both Mix-1 and Mix-2 had lower  $J_c$  values than the minimum required. Mix-2 did not satisfy the minimum requirement only by a small margin (0.03 kJ/m<sup>2</sup>).

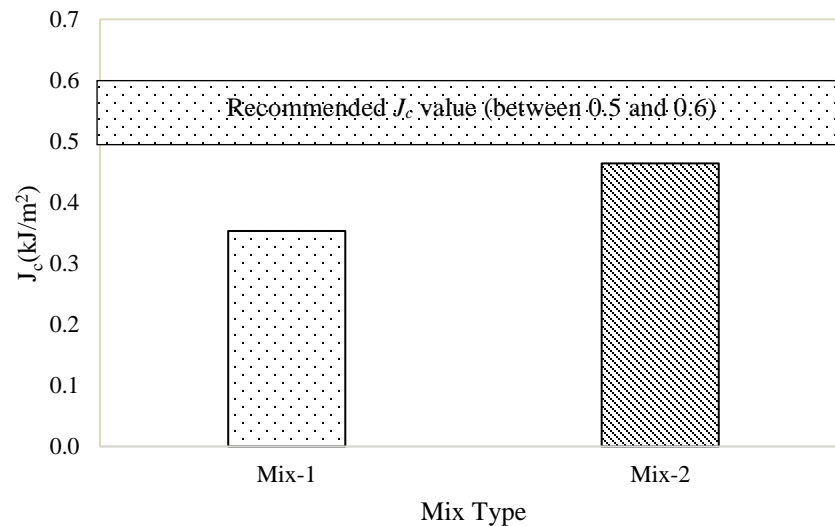


Figure 5.4  $J_c$  Values for Mix-1 and Mix-2

A similar trend in the cracking resistance was observed for S4 mixes containing 5% RAP (Figures 5.5 and 5.6). Figure 5.5 presents the variation in average strain energy with notch depths for Mix-5 (HMA S4) and Mix-6 (WMA S4). The average strain energy was found to decrease with increasing notch depth for both mixes due to reduction in loading area (Kim et al., 2012a; Khan, 2016; Saeidi and Aghayan, 2016). As can be seen from Table 5.4, the COV for average strain energy was found to be less than 15% for all notch depths. Also, the  $J_c$  value exhibited by Mix-6 was 0.60 kJ/m<sup>2</sup>, which met the ASTM D 8044 minimum requirement (ASTM, 2013) (Figure 5.6). However, the minimum  $J_c$  requirement was not met by the tested samples of Mix-5. Based on these results, foamed WMA containing 5% RAP showed a higher fatigue



resistance than the corresponding HMA. Several other researchers have also reported higher fatigue resistance for WMA compared to HMA (Kim et al., 2012a; Zhao et al., 2013; Yu et al., 2016; Dong et al., 2017; Rani et al., 2019). However, Jones et al. (2010) and Bonaquist (2011) reported similar cracking resistance for both HMA and WMA when using same aggregates and same binder (performance grade-wise). Lee et al. (2009), Hill et al. (2012b) and Valdes-Vidal et al. (2018) reported lower fatigue resistance for foamed WMA compared to HMA containing RAP. As noted above, various factors could be responsible for opposing findings. Based on the aforementioned results, the WMA used in this study are expected to show better fatigue resistance compared to their HMA counterparts.

Table 5.4 Coefficient of Variance (%) at Different Notch Depths for S4 Mixes

Mix Type	Notch Depth, mm		
	25.4	31.8	38.0
Mix-5	7	11	12
Mix-6	12	15	9

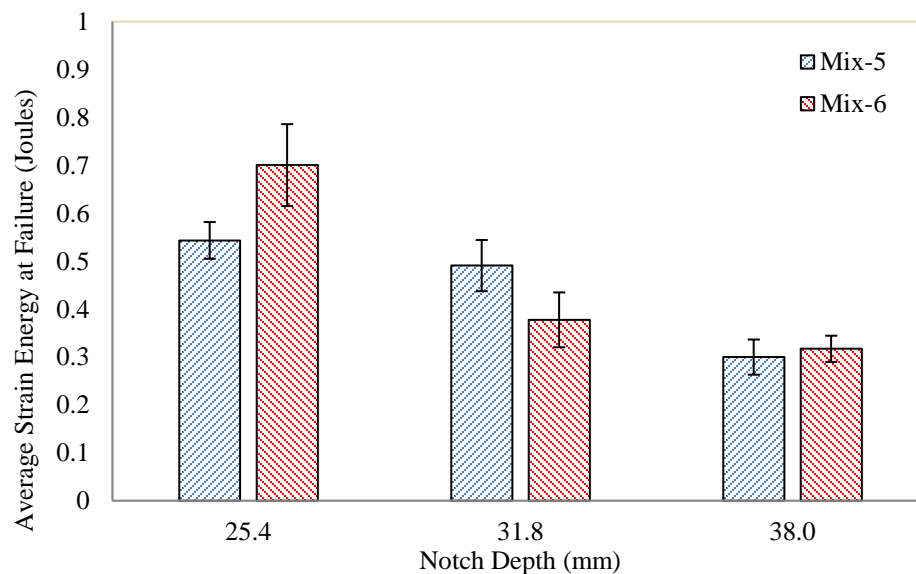


Figure 5.5 Average Strain Energy at Failure for Mix-5 and Mix-6

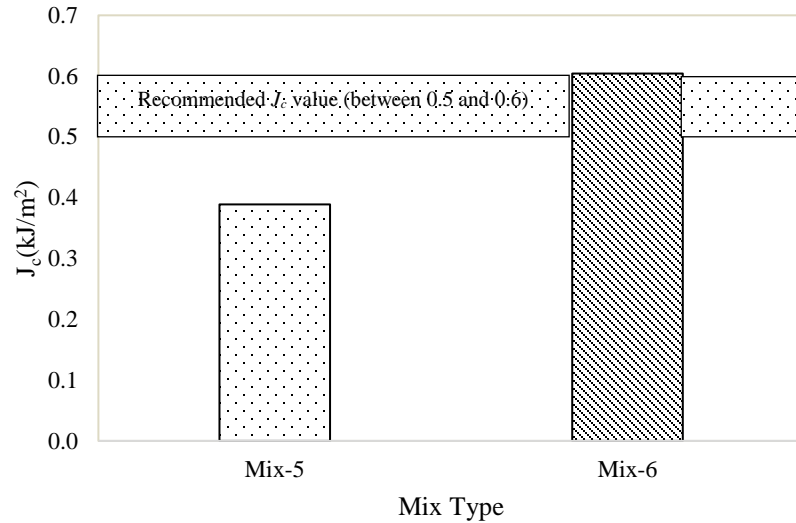


Figure 5.6  $J_c$  Values for Mix-5 and Mix-6

A comparison of  $J_c$  values shows that S4 mixes were found to exhibit higher cracking resistance than S3 mixes. This may be attributed to significantly higher RAP content (25%) of S3 mixes than S4 mixes (5%). According to McDaniel et al. (2000), Huang et al. (2004) and Ghabchi et al. (2016), incorporation of RAP up to a certain limit has a positive effect on the cracking resistance of asphalt mixes. Also, finer mixes (S4 mixes) are expected to show a higher resistance to fatigue than coarser mixes (S3 mixes) due to different crack propagation mechanisms (Barman et al., 2018). In case of a coarser mix, crack generally propagates within the mastic (composed of asphalt binder, filler and fine aggregate fraction) resulting in lower fracture energy. For a finer mix, however, cracks generally propagate through the aggregate, as shown in Figure 5.7 (Barman et al., 2018). As a result, S4 mixes can exhibit higher cracking resistance than S3 mixes.

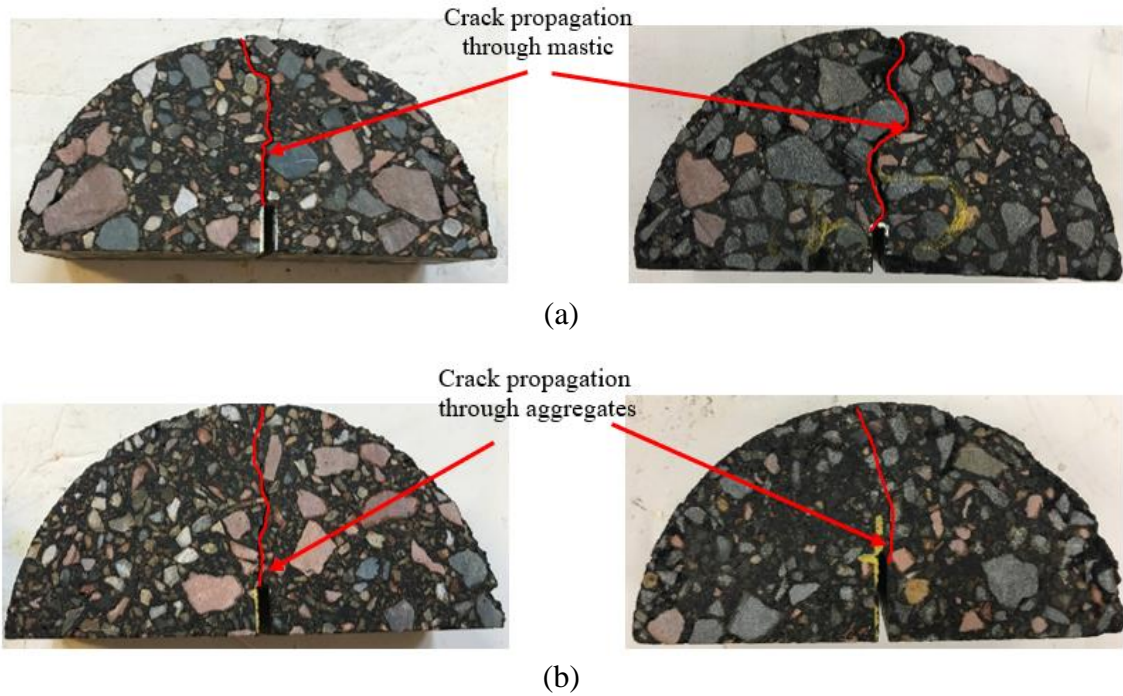


Figure 5.7 Cracking Mechanism for (a) S3 Mixes (b) S4 Mixes

### 5.3.2 I-FIT or Illinois SCB Test

As described in Chapter 3, Illinois SCB or I-FIT tests were performed according to the AASHTO TP 124 test method and used to evaluate the fatigue cracking resistance of asphalt mixes (AASHTO, 2016). In this method, a much higher loading rate (50 mm/min) was used than the Louisiana SCB test method (0.5 mm/min). It was observed that the cracks were more prominent in case of I-FIT than in case of the Louisiana SCB test method due to rapid loading (Figure 5.8).

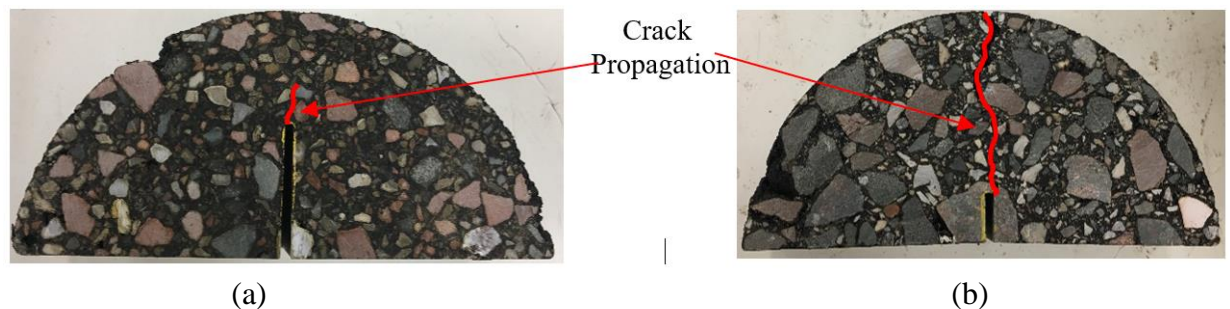
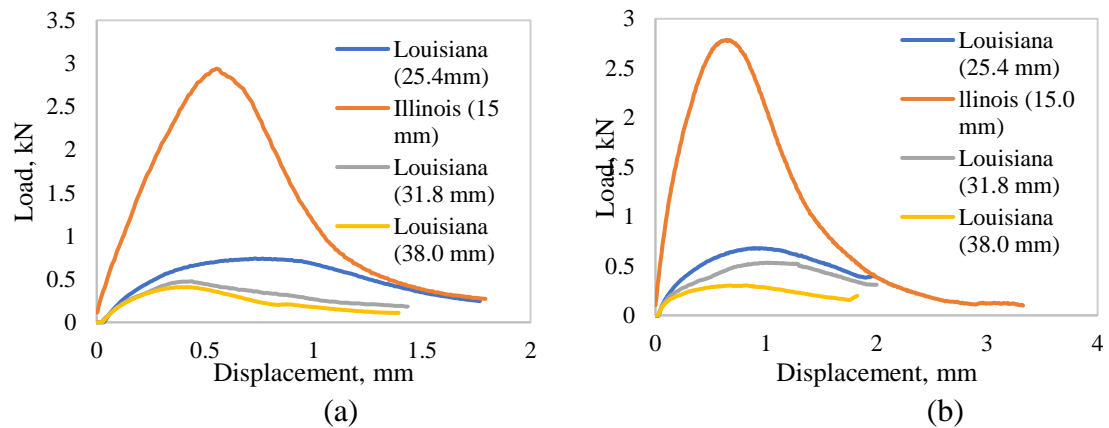


Figure 5.8 SCB Tested Specimens (a) Louisiana SCB (b) I-FIT

Figure 5.9 shows the load-displacement diagrams for typical Louisiana SCB and I-FIT specimens. A higher peak load and stiffer slope were observed for I-FIT samples compared to the Louisiana SCB samples for all mixes. On the contrary, the load-displacement curves for the Louisiana SCB tested samples were found to be flatter indicating a more ductile behavior than I-FIT for all samples tested here. This is primarily caused by a higher loading rate for I-FIT than that of the Louisiana SCB method. According to Khan (2016), the elastic component of a viscoelastic material becomes greater with the increase in loading rate. Also, the area under the load-displacement curve for the I-FIT method was larger than the corresponding area in Louisiana SCB method for all notch depths. Based on these observations a higher toughness can be expected for the I-FIT samples, which is attributed to smaller induced crack length (15.0 mm) for the I-FIT samples compared to the Louisiana SCB samples (Kim et al., 2012a; Khan, 2016; Saeidi and Aghayan, 2016).



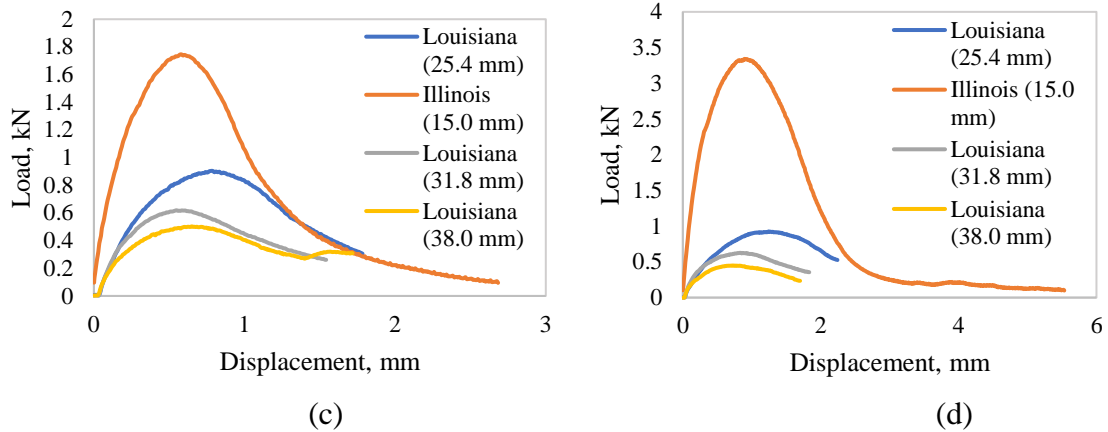


Figure 5.9 Load-Displacement Diagram for Louisiana SCB and I-FIT Tested Specimens

(a) Mix-1 (b) Mix-2 (c) Mix-5 (d) Mix-6

As discussed in Chapter 3, Flexibility Index (FI), based on the load-displacement curve in the I-FIT method, is used as an indicator of cracking resistance of asphalt mixes. Asphalt mixes with higher FI values are expected to show better cracking resistance (AASHTO, 2016; Ozer et al., 2016). Also, a higher FI value indicates a ductile material and vice versa. In this study, four I-FIT samples were tested for each mix type to obtain the average FI value for each mix. A similar trend in the cracking resistance was found from the I-FIT results, when compared with the Louisiana SCB results. The foamed WMA exhibited a higher cracking resistance compared to the HMA (Figures 5.10 and 5.11). The average FI value for Mix-1 was found to be 2.4 with a standard deviation of 0.6. The corresponding average FI value for Mix-2 was 4.3 with a standard deviation of 0.7. Also, the average FI values for Mix-5 and Mix-6 were 3.8 and 9.2 with standard deviations of 0.8 and 1.0, respectively. Therefore, Mix-2 and Mix-6 showed higher FI values compared to Mix-1 and Mix-5, respectively. A lower degree of aging in WMA is expected to increase their cracking resistance (Hurley and Prowell, 2006; Alhasan et al., 2014; Malladi, 2015).

The recommended minimum FI value to ensure cracking resistance varies from state to state (Ozer et al., 2016). According to Ozer et al. (2016), asphalt mixes with FI values greater than 6.7 may be classified as “best performing,” while mixes with FI values less than 2.0 may be considered “poor performing.” Mixes with FI values between these limits are expected to exhibit “intermediate performance.” Based on these criteria, Mix-6 can be classified as “best performing,” while the other three mixes are expected to exhibit “intermediate performance” with respect to cracking resistance.

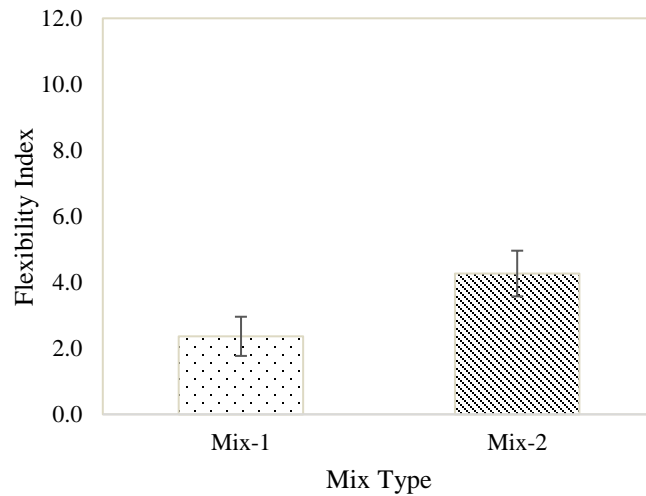


Figure 5.10 Flexibility Index for Mix-1 and Mix-2

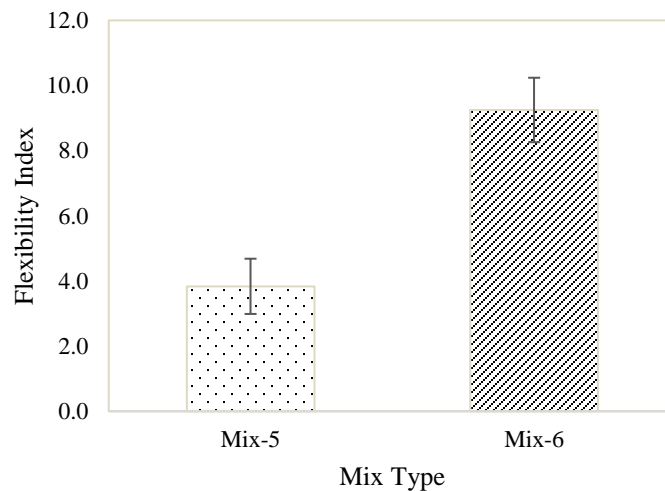


Figure 5.11 Flexibility Index for Mix-5 and Mix-6

As in the case of Louisiana SCB test results, S4 mixes were found to exhibit higher FI values compared to the S3 mixes. This may be attributed to increased brittleness of asphalt mixes with incorporation of high amount of RAP in S3 mixes (25%) compared to S4 mixes (5%) (Shu et al., 2008; Guo et al., 2014; Lu and Saleh, 2016). Also, a coarser aggregate gradation for S3 mixes is believed to be responsible for the propagation of cracking within the mastic, as shown in Figure 5.7.

### **5.3.3 Abrasion Loss Test**

As noted in Chapter 3, Abrasion Loss Test (commonly known as Cantabro test) was performed in this study according to the AASHTO TP 108 test method and used as an additional indicator of fatigue cracking resistance (AASHTO, 2016). A higher mass loss indicates a lower fatigue cracking resistance and vice versa (AASHTO, 2016). Figure 5.12 shows the percent abrasion loss for Mix-1 and Mix-2. For each mix type three specimens were tested to check the reproducibility of test results. The average abrasion loss for Mix-1 and Mix-2 were found to be 29% and 17%, respectively. The standard deviations for Mix-1 and Mix-2 were found to be 2.6% and 3.9%, respectively. Therefore, Mix-2 exhibited higher fatigue cracking resistance than Mix-1. A lower degree of aging for WMA is expected to result in an increase in cracking resistance (Hurley and Prowell, 2006; Alhasan et al., 2014; Malladi, 2015). It is seen that the abrasion loss test results follow a similar trend as the Louisiana SCB and I-FIT test results for S3 mixes. Therefore, this test method may be considered as an alternative to scan asphalt mixes for their fatigue cracking resistance during the mix design stage. Jones et al. (2010) and Bonaquist (2011) reported similar fatigue cracking resistance for both HMA and WMA with the same aggregate and binder PG. These findings are

different from those of the present study.

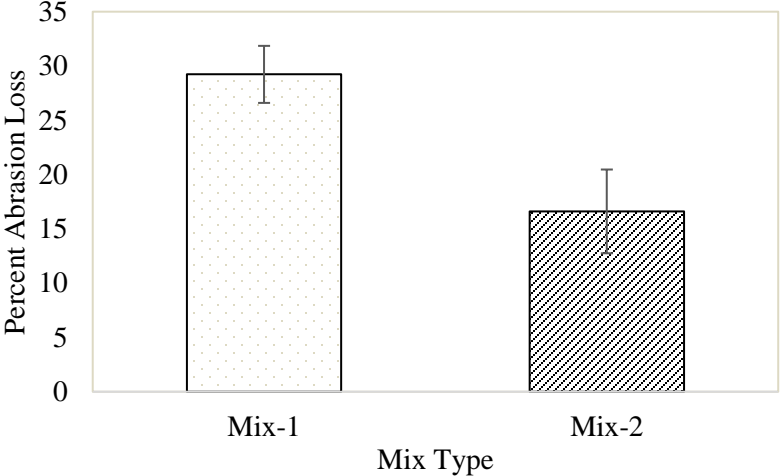


Figure 5.12 Percent Abrasion Loss for Mix-1 and Mix-2

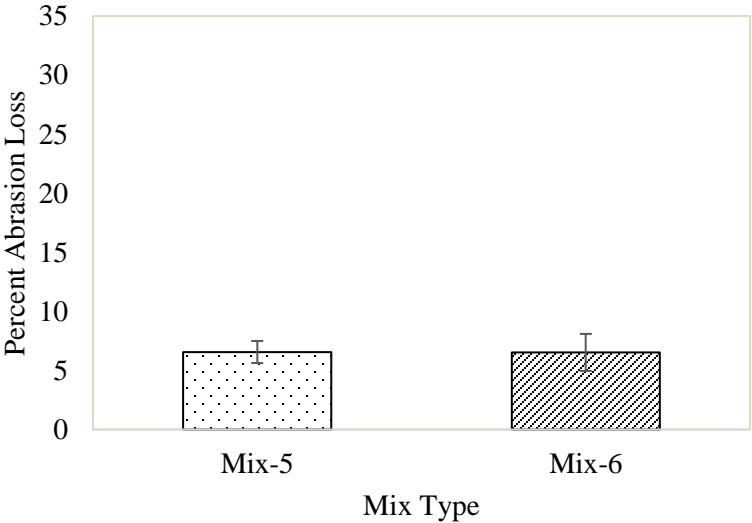


Figure 5.13 Percent Abrasion Loss for Mix-5 and Mix-6

The same average abrasion loss (7%) for both Mix-5 and Mix-6 samples was found, as shown in Figure 5.13. The standard deviations for Mix-5 and Mix-6 were found to be 0.9% and 1.6%, respectively. Based on these results, similar fatigue cracking resistance is expected for both S4 mixes. Jones et al. (2010) and Bonaquist (2011) reported similar cracking resistance for HMA and WMA with the same aggregate and binder. In the present study, Mix-6 was found to exhibit a higher cracking



resistance than Mix-5 in both Louisiana SCB and I-FIT tests. The Abrasion Loss Test is an empirical test with no clear mechanistic basis for simulation of fatigue cracking. This test method was originally developed for accessing the abrasion loss of asphalt mixes (AASHTO, 2016). The adhesive bonding between aggregates and binder under impact load is mainly evaluated in this test method (Shaowen and Shanshan, 2011). In case of S4 (finer) mixes higher binder content (4.9%) was used compared to S3 (coarser) mixes (4.5%), which is believed to improve the adhesion between aggregates and binder. Therefore, both S4 mixes were found to exhibit similar percent abrasion loss (7%). However, the effect of abrasion is more prominent in case of S3 mixes due to a lower amount of binding material. Therefore, Mix-1 was found to exhibit higher abrasion loss than Mix-2. Also, both Louisiana SCB and I-FIT tests are mechanistic-based test methods for evaluating fatigue cracking resistance. Therefore, Abrasion Loss test may not be a good test for screening of fine mixes (S4 here) for fatigue cracking. A relatively higher mass loss observed for S3 mixes compared to S4 mixes can be attributed to increased RAP content (Shu et al., 2008; Guo et al., 2014; Lu and Saleh, 2016; Saeidi and Aghayan, 2016). Both S3 mixes did not satisfy the NCAT abrasion loss requirement of 20%, whereas S4 mixes satisfied the requirement (NCAT, 2017).

#### **5.3.4 Ranking of Asphalt Mixes Based on Fatigue Cracking Resistance**

Table 5.5 presents the ranking of all four mixes (Mix-1, Mix-2, Mix-5, and Mix-6) based on their resistance to fatigue cracking. The rating was conducted on a scale of 1 to 4, where 1 represents the best performing and 4 represents the worst performing asphalt mix with respect to fatigue cracking resistance. It was found that the Louisiana SCB, I-FIT and dynamic modulus values at  $10^{-4}$  Hz reduced frequency ranked the

fatigue cracking resistance of asphalt mixes in similar orders. However, Abrasion Loss test could not differentiate between the fatigue cracking resistance of Mix-5 and Mix-6. Therefore, the Louisiana SCB and I-FIT tests are found to characterize the cracking resistance of asphalt mixes consistently. Although the Abrasion Loss Test is relatively easy to conduct, it could not characterize the fatigue resistance of some asphalt mixes.

Based on the Louisiana SCB and I-FIT test results, Mix-6 was found to exhibit the highest resistance to fatigue cracking followed by Mix-2, Mix-5, and Mix-1. From these results one could conclude that a foamed WMA with fine aggregate gradation and low RAP content is expected to perform well relative to fatigue. The cracking resistance reduces with coarser aggregate gradation and increased RAP content beyond certain level.

Table 5.5 Ranking of Asphalt Mixes based on Fatigue Cracking performance

Mix Type	Louisiana SCB	I-FIT	Abrasion Loss Tests	Dynamic Modulus
Mix-1	4	4	4	4
Mix-2	2	2	3	2
Mix-5	3	3	1	3
Mix-6	1	1	1	1

## 5.4 Rutting Performance

The permanent deformation or rutting is an important factor for the longevity of the asphalt pavement. During the hot summer months, this becomes more crucial as binder losses its viscosity. At that moment, the moving traffic load is mainly supported by the mineral aggregate structure (Brown et al., 2009). Different researchers have taken different approaches to identify the rutting potential of asphalt mixes (Miller et al., 1995; Cooley et al., 2000; Kandhal and Cooley, 2002). In this study, both HWT and FN tests were used to evaluate the rutting resistance of asphalt mixes.

#### 5.4.1 Hamburg Wheel Tracking (HWT) Test

In this study, the HWT tests were conducted as per AASHTO T 324 to evaluate the rutting resistance of asphalt mixes (AASHTO, 2014c). Figures 5.14 and 5.15 present the HWT fitted graphs obtained in this study for S3 and S4 mixes, respectively. As discussed in Chapter 3, fitted curve was plotted based on the equations suggested by Lu and Harvey (2006). It is evident from these figures that for both cases, control HMA was found to show higher rutting resistance compared to foamed WMA containing an identical amount of RAP. The rut depths at 1,000, 5,000, 10,000, 15,000, and 20,000 passes for all mixes are presented in Table 5.6. The test data indicated that for similar number of wheel passes, higher rut depths were observed in WMA samples compared to HMA samples, and this difference became increasingly dominant at higher numbers of passes. The rut depth at 20,000 wheel passes for Mix-1 and Mix-2 were found to be 3.5 mm and 6.2 mm, respectively. Also, a relatively higher rut depth (11.2 mm) was observed for Mix-6 compared to Mix-5 (3.3 mm). The rut depth in a HWT sample is expected to be controlled by the percent air voids of the sample during preparation (Yildirim and Kennedy, 2002). However, similar average percent air voids were observed for both HMA and WMA samples prepared for HWT testing (Table 5.6). Furthermore, as discussed in Chapter 3, several rutting parameters namely post-compaction deformation, creep slope, stripping slope, and Stripping Inflection Point (SIP) were determined from the HWT test results and presented in Table 5.7. The initial densification of asphalt pavement due to the movement of traffic was indicated by the post-compaction deformation. The rut depth at 1,000 wheel passes was suggested as the post-compaction point by Yildirim and Kennedy (2002). From Table 5.7, it is evident

that WMA showed higher post-compaction deformation compared to HMA. Also, distinct SIPs for both Mix-2 and Mix-6 were found at 17,100 and 12,000 wheel passes, respectively. However, for HMA, no defined SIP was observed for both mixes. Therefore, HMA was expected to exhibit a higher resistance to moisture-induced damage.

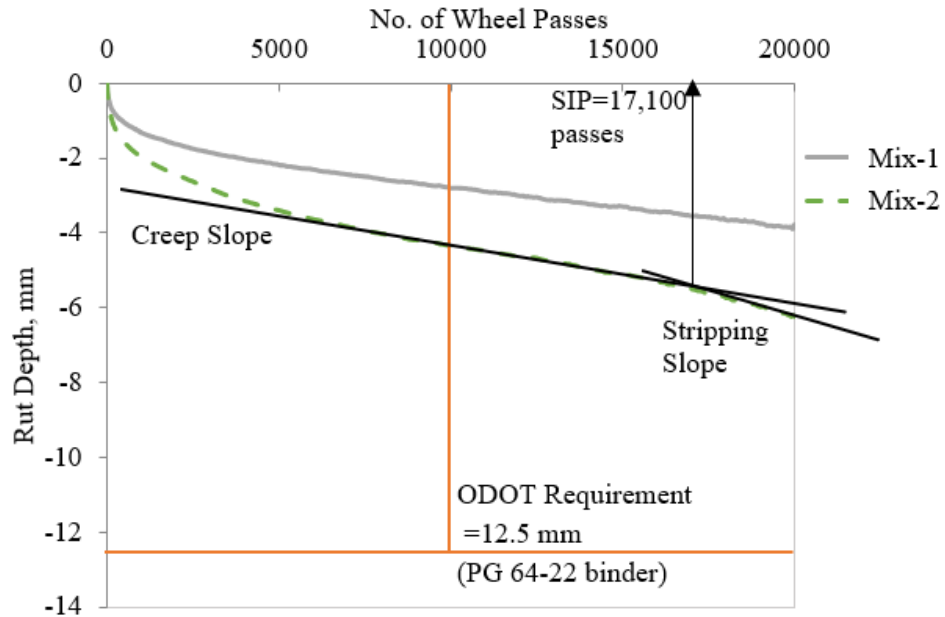


Figure 5.14 Comparison of HWT graphs for Mix-1 and Mix-2

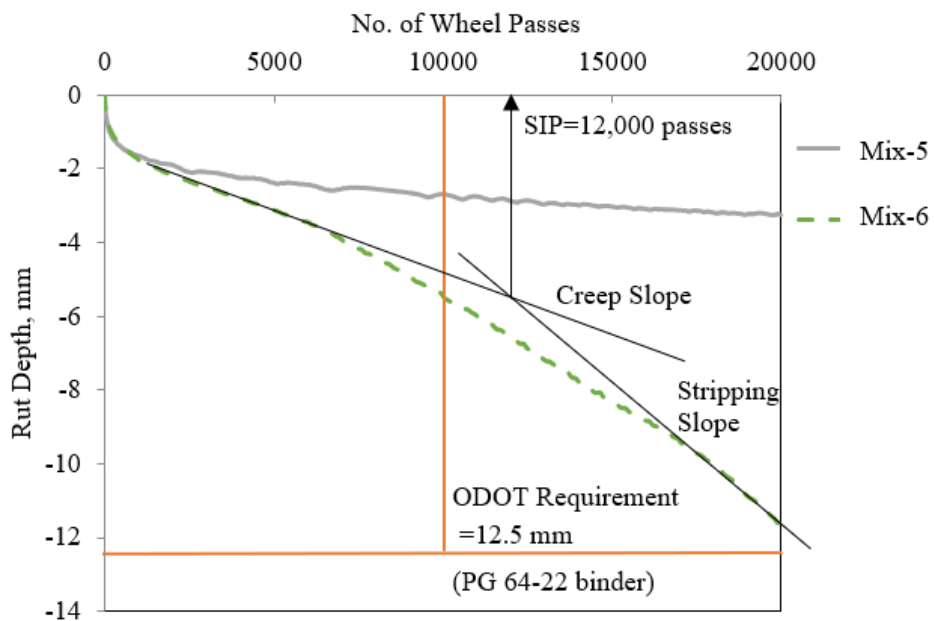


Figure 5.15 Comparison of HWT graphs for Mix-5 and Mix-6

Table 5.6 Rut Depths (mm) for Foamed WMA and HMA at Different Numbers of Wheel Passes

MIX ID	Average % Air Voids	RAP content (%)	Wheel passes				
			1,000	5,000	10,000	15,000	20,000
Mix-1	6.8	25	1.1	1.7	2.2	2.7	3.5
Mix-2	6.8	25	2.0	3.4	4.3	5.1	6.2
Mix-5	6.9	5	1.7	2.4	2.7	3.0	3.3
Mix-6	7.0	5	1.8	3.1	5.4	8.3	11.2

Table 5.7 Performance Parameters Obtained from HWT Tests

MIX ID	Average % Air Voids	HWT indices					
		Post-compaction (mm)	Creep slope (mm/passes)	Inverse Creep slope (passes/mm)	Stripping inflection point (passes)	Stripping slope (mm/passes)	Inverse Stripping slope (passes/mm)
Mix-1	6.8	1.06	0.000100	10,000	N/A	N/A	N/A
Mix-2	6.8	1.98	0.000150	6,667	17,100	0.000417	2,400
Mix-5	6.9	1.58	0.000067	15,000	N/A	N/A	N/A
Mix-6	7.0	1.76	0.000339	2,946	12,000	0.000756	1,324

Also, the inverse creep slope for Mix-2 was found to be 6,667 passes/mm, whereas for Mix-1 this inverse slope was 10,000 passes/mm (Table 5.7). Therefore, about two times higher resistance to creep was observed for Mix-1 than Mix-2. In addition, Mix-5 was found to exhibit about five times higher resistance (15,000 passes/mm) compared to Mix-6 (2,946 passes/mm). Therefore, foamed WMA exhibited more susceptibility to rutting compared to HMA. Similar observations for WMA were also reported by several other researchers (Hill, 2011; Bonaquist, 2011; Ali et al., 2013; Mo et al., 2012; Zhao et al., 2013; Yu et al., 2016; Rahman et al., 2018; Ghabchi et al., 2019). A lower rutting resistance for foamed WMA was reported by Zhao et al. (2013) compared to HMA. In that study, RAP content as high as 40% was considered in

evaluating the rutting resistance. The stiffness of foamed WMA is expected to reduce at a lower degree of aging as shown in the dynamic modulus test results, which increases the rutting potential for foamed WMA. However, an insignificant difference in the rutting performance of HMA and WMA was reported by several other researchers (Jones, 2004; Prowell et al., 2007; Wielinski et al., 2009). A higher density was expected for foamed WMA compared to HMA due to better compactability, which may counteract the lower aging effect with respect to the rutting resistance (Prowell et al., 2007; Wielinski et al., 2009). As noted earlier, several factors such as aggregate gradation, quality of RAP, type and amount of virgin binder can be responsible for opposing findings. Based on the findings presented herein, the WMA is expected to show lower rutting resistance compared to HMA. However, both HMA and WMA satisfied ODOT's minimum requirement of 12.5 mm rut depth at 10,000 wheel passes for PG 64-22 grade binder (ODOT, 2011).

From Tables 5.6 and 5.7, it is evident that higher rutting resistance was shown by S3 mixes compared to S4 mixes. For Mix-2 rut depth observed at 10,000 wheel passes was 4.3 mm, whereas at the same wheel passes, 5.4 mm of rut depth was observed for Mix-6. Also, inverse creep slope increased from 2,946 passes/mm to 6,667 passes/mm for Mix-6 to Mix-2 indicating a higher rutting resistance. Furthermore, Mix-1 also showed higher rutting resistance than Mix-5. The rut depths for Mix-1 and Mix-5 at 10,000 passes were found to be 2.2 mm and 2.7 mm, respectively. The incorporation of a high percentage of RAP in S3 mixes (25%) compared to S4 mixes (5%) is believed to have increased the rutting resistance due to addition of aged binder from RAP. Similar findings for the increase in RAP content were reported by several other

researchers (Shu et al., 2008; Hong et al., 2010; Zhao et al., 2013; Guo et al., 2014; Dong et al., 2017; Rahman et al., 2018). As reported by Dong et al. (2017), the increase in rutting resistance with an increase in RAP content was more dominant in HMA compared to WMA. In their study, up to 80% virgin binder replacement by RAP aged binder was studied. However, insignificant improvement in the rutting resistance with the increase in RAP content was reported by Daniel and Lachance (2005), Shah et al. (2007), and Apeageyi et al. (2011). It was reported that for asphalt mixes with lower high-temperature PG virgin binder (PG 58 to lower), addition of RAP may adversely affect the rutting resistance (Apeageyi et al., 2011). Although in this study, PG 64-22 virgin binder was used in producing asphalt mixes. The future studies can explore other binder types to evaluate the effect of RAP in rutting resistance of asphalt mixes. Overall, based on the findings presented herein, an increase in RAP content was expected to increase the rutting resistant of asphalt mixes.

#### **5.4.2 Flow Number (FN) Test**

The Flow Number (FN) test was conducted as per AASHTO T 378 to evaluate the rutting resistance of asphalt mixes (AASHTO, 2017). The asphalt mix with a higher FN value is expected to show higher resistance to rutting (Witczak et al., 2002; Copeland et al., 2010; Zhao et al., 2013; Roy et al., 2015; Chaturabong, 2016). Figures 5.16 and 5.17 show the FN test results for S3 mixes and S4 mixes, respectively. For each mix type, three specimens were tested to check the repeatability of test results. The COVs for Mix-1 and Mix-2 were found to be 4.6% and 19.5%, respectively. Also, the COVs for Mix-5 and Mix-6 were found to be 14.2% and 21.7%, respectively. The recommended COVs by AASHTO T 378 for mixes with NMAS of 19 mm and 12.5

mm are 58.5% and 43.1%, respectively (AASHTO, 2017). Therefore, the COV requirements were satisfied for both S3 and S4 mixes. Also, it was found from Figures 5.16 and 5.17 that both WMA showed lower FN values compared to their HMA counterparts. The average FN values for Mix-1 and Mix-2 were found to be 167 and 59, respectively. A similar trend was followed by S4 mixes. The average FN values for Mix-5 and Mix-6 were found to be 107 and 16, respectively. Therefore, lower resistance to rutting is expected for WMA compared to HMA. A similar observation was reported by several other researchers (Hill, 2011; Bonaquistet et al., 2011; Hossain et al., 2012; Ali et al., 2013; Zhao et al., 2013; Yu et al., 2016; Rahman et al., 2018). Also, as discussed in Table 3.8, no minimum requirement of FN value has been mentioned by AASHTO for both HMA and WMA for light traffic condition (ESALs < 0.3 million) (AASHTO, 2017).

S3 mixes were found to exhibit higher FN values compared to S4 mixes. Therefore, S3 mixes are expected to show higher rutting resistance due to incorporation of high percentage of RAP (Shu et al., 2008; Hong et al., 2010; Zhao et al., 2013; Guo et al., 2014; Dong et al., 2017; Rahman et al., 2018).

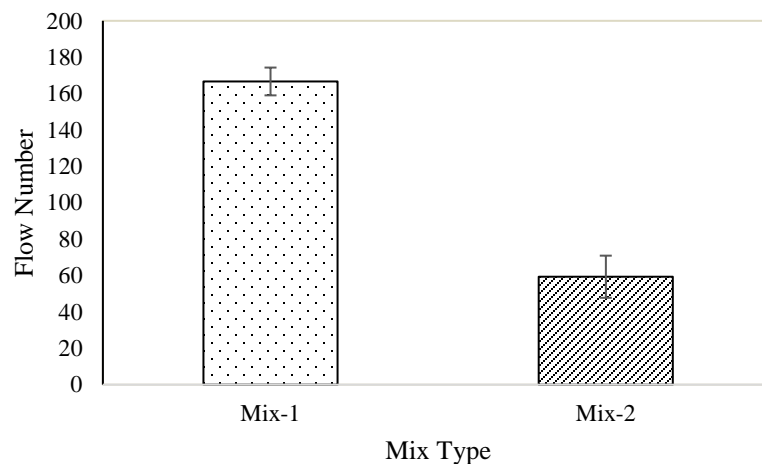


Figure 5.16 Comparison of FN for Mix-1 and Mix-2



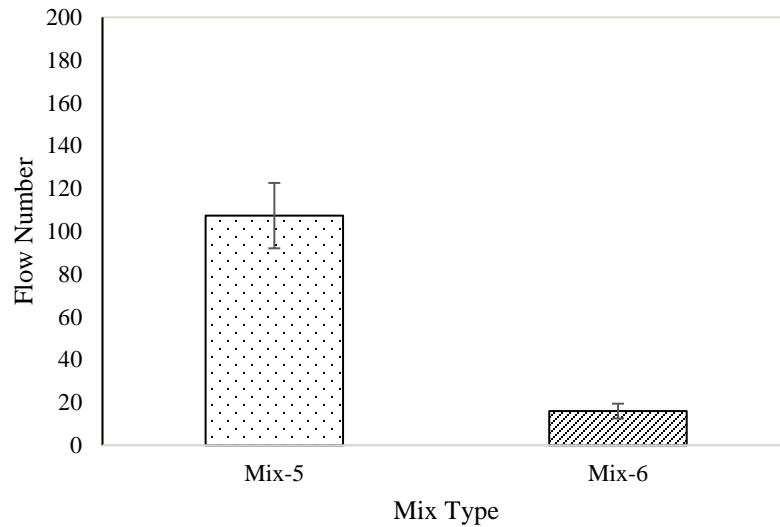


Figure 5.17 Comparison of FN for Mix-5 and Mix-6

### 5.4.3 Ranking of Asphalt Mixes Based on Rutting Performance

Table 5.8 presents the ranking of asphalt mixes based on various rutting parameters. The rating was conducted on a scale of 1 to 4, where 1 represents the best performing and 4 represents the worst performing asphalt mix. From HWT test data, rut depth at 10,000 wheel passes, inverse creep slope (passes/mm) and SIP were considered to rank the asphalt mixes. The ODOT's rut depth limit at 10,000 wheel passes for asphalt mixes having a PG 64-22 binder was used in this ranking (ODOT, 2011). Also, dynamic modulus value at  $10^{-4}$  Hz reduced frequency and 21.1°C reference temperature was considered in ranking the rutting resistance of asphalt mixes. The ranking of asphalt mixes based on the FN value is included in Table 5.8.

It is evident from Table 5.8 that foamed WMA was found to exhibit a lower rutting resistance compared to control HMA. Based on the rut depth, FN and dynamic modulus, Mix-1 exhibited the highest resistance to rutting, followed by Mix-5, Mix-2, and Mix-6. However, Mix-5 showed the highest rutting resistance, followed by Mix-1,

Mix-2, and Mix-6 when using inverse creep slope for ranking. The finer aggregate gradation is believed to decrease the rutting potential for S4 mixes compared to S3 mixes. This is mainly attributed to a higher degree of aggregate segregation within the sample for coarser mixes (Krutz and Sebaaly, 1993; Hand and Epps, 2001; Sebaaly et al., 2004; Kim et al., 2009; Golalipour et al., 2012). The high RAP content, on the contrary, increases the rutting resistance for S3 mixes compared to S4 mixes. Therefore, these two opposing factors (aggregate gradation and RAP content) were found to rank Mix-1 and Mix-5 differently, while considering different parameters.

Table 5.8 Ranking of Asphalt Mixes Based on Rutting Resistance

Mix Type	Dynamic Modulus	HWT Indices			Average FN
		Rut Depth at 10,000 Wheel Passes (mm)	Inverse Creep Slope (passes/mm)	SIP	
Mix-1	1	1	2	1	1
Mix-2	3	3	3	3	3
Mix-5	2	2	1	1	2
Mix-6	4	4	4	4	4

It is evident from the laboratory test results that foamed WMA is expected to exhibit lower rutting resistance compared to their HMA counterparts. However, a field study conducted by Wielinski et al. (2009) suggested that both HMA and WMA performed equally in the arid Southern California climate and subjected to heavy traffic loads. Sargand et al. (2011) and Prowell et al. (2007) also reported similar field rutting performance for both WMA and HMA. It is believed that long-term field investigations are required to evaluate the actual rutting resistance of foamed WMA compared to control HMA.

## **5.5 Moisture-Induced Damage**

The reduction in mixing and compaction temperatures and injection of water during the foaming process are believed to increase the moisture-induced damage potential for foamed WMA (Hurley and Prowell, 2005; Hurley and Prowell, 2006; Prowell et al., 2007; Wasiuddin et al., 2007; Ali et al., 2013; Xu et al., 2017). There are several test methods available to evaluate the moisture-induced damage potential of asphalt mixes. Among all methods, the SIP from the HWT test results and TSR from the ITS test are most commonly used moisture susceptibility parameters (Kim et al., 2012b; Abuawad et al., 2015). In this study, SIP and TSR were used to identify the moisture-induced damage potential of asphalt mixes.

### **5.5.1 Stripping Infection Point (SIP)**

As discussed earlier, no distinct SIP was observed for both HMA mixes (Figures 5.14 and 5.15). However, SIPs were found for both foamed WMA mixes. The SIPs for Mix-2 and Mix-6 were found at 17,100 and 12,000 wheel passes, respectively. The possibility of moisture-induced damage in the foamed WMA samples is indicated by SIP. After that point, the rate of rut depth increased rapidly due to the intrusion of moisture in the specimen. For instance, the resistance to rutting reduced from 6,667 passes/mm to 2,400 passes/mm after the SIP for Mix-2. A similar trend was observed for Mix-6. Therefore, foamed WMA was found to exhibit more moisture-induced damage potential compared to HMA. The partially dried aggregates at a lower mixing temperature and injection of water vapor are believed to increase the moisture-induced damage potential for foamed WMA (Hurley and Prowell, 2005; Hurley and Prowell, 2006; Prowell et al., 2007; Wasiuddin et al., 2007; Kim et al., 2012b, Ali et al., 2013;

Xu et al., 2017). A higher moisture-induced damage was observed for WMA compared to HMA while considering both AASHTO T 283 test and SCB test results by Kim et al. (2012b). However, insignificant difference between the moisture-induced damage potential of WMA and HMA was reported by some other researchers (Punith et al., 2012; Xiao et al., 2012; Hailesilassie et al., 2015; Rani, 2018). It was suggested that as long as the mixing temperature of foamed WMA is high enough to ensure the dissipation of water, both HMA and WMA can show similar moisture-induced damage potential (Punith et al., 2012; Xiao et al., 2012; Hailesilassie et al., 2015). In this study, aggregates and RAP were dried for two hours at WMA mixing temperature (135°C) before adding foamed binder, which is commonly followed in the WMA production plant. Therefore, increasing drying period for aggregates and RAP may lower moisture-induced damage potential for foamed WMA (Ali et al., 2013)

The SIP found for Mix-2 was at higher wheel passes (17,100) compared to Mix-6 (12,000). Also, a higher inverse stripping slope was observed for Mix-2 (2,400 passes/mm) compared to Mix-6 (1,324 passes/mm) indicating a higher resistance to stripping due to increase in RAP content. Therefore, the addition of aged binder from RAP is believed to have a positive effect on the moisture-induced damage resistance of asphalt mixes due to stronger bonding between RAP aggregate and binder. Similar findings for moisture-induced damage potential were also reported by several other researchers (Zhao et al., 2012; Shu et al., 2012; Hill et al., 2012a; Rahman et al., 2019). For both Evotherm and Sasobit-based WMA, addition of RAP was found to decrease the moisture-induced damage potential (Hill et al., 2012a). In their study, up to 45% RAP content was considered for evaluating the effect of RAP on moisture-induced

damage. On the contrary, an increase in moisture-induced damage potential with increased RAP content was reported by Moghadas et al. (2014) and Guo et al. (2014). It was suggested that the increase in viscosity of the asphalt binder due to an increase in RAP content may cause insufficient binder coating on aggregates (Moghadas et al., 2014; Guo et al., 2014). Therefore, weak bonding between aggregate and binder may produce asphalt mixes with more moisture-induced damage potential (Moghadas et al., 2014; Guo et al., 2014).

### **5.5.2 AASHTO T 283 Method**

The AASHTO T 283 method, commonly known as freeze-thaw method, was used to determine the moisture-induced damage potential of asphalt mixes (AASHTO, 2014b). Figure 5.18 presents the ITS test results with freeze-thaw conditioned TSR values ( $TSR_{F-T}$ ) for S3 mixes. As mentioned in Chapter 3, TSR is the ratio between freeze-thaw conditioned (moist conditioned) ( $ITS_{F-T}$ ) and dry ( $ITS_{dry}$ ) ITS values. The average  $ITS_{dry}$  and  $ITS_{F-T}$  values for Mix-1 were found to be 2,381 kPa and 2,009 kPa with standard deviations of 104 kPa and 100 kPa, respectively. Also, the average  $ITS_{dry}$  and  $ITS_{F-T}$  values for Mix-2 were found to be 2,596 kPa and 2,054 kPa with standard deviations of 117 kPa and 194 kPa, respectively. Therefore, Mix-2 was found to exhibit a higher ITS than Mix-1 under both dry and moist conditions. Also, the  $TSR_{F-T}$  value observed for Mix-2 was slightly lower (0.79) compared to Mix-1 (0.84). Furthermore, Mix-1 satisfied ODOT's current requirement for  $TSR_{F-T}$  of 0.80, whereas Mix-2 did not satisfy the requirement by a small margin (0.01). Therefore, a slightly higher moisture-induced damage potential for foamed WMA is expected compared to HMA due to partially dried aggregates and incorporation of water in the foaming process (Hurley

and Prowell, 2005; Prowell et al., 2007; Ali et al., 2013; Xu et al., 2017; Rahman et al., 2019).

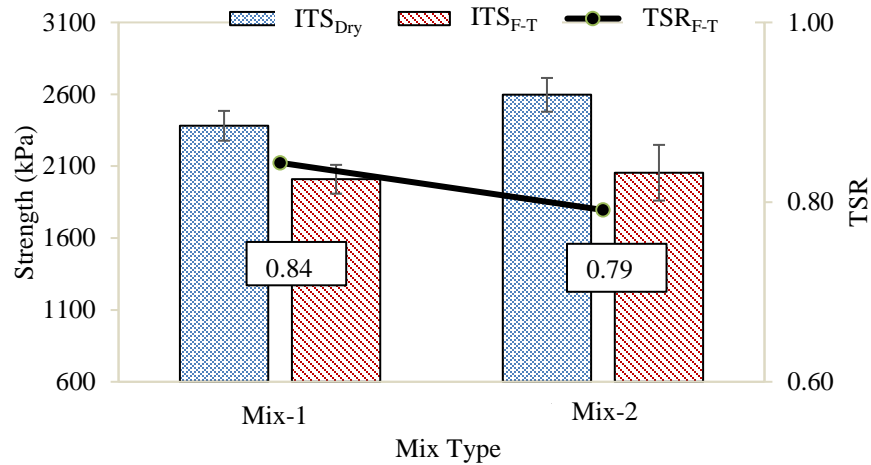


Figure 5.18 Indirect Tensile Strength (ITS<sub>dry</sub> and ITS<sub>F-T</sub>) and TSR (TSR<sub>F-T</sub>) Values for S3 mixes (AASHTO T 283 method)

Figure 5.19 presents the ITS test results with freeze-thaw conditioned TSR values (TSR<sub>F-T</sub>) for S4 mixes. The average ITS<sub>dry</sub> and ITS<sub>F-T</sub> values for Mix-5 were found to be 2,367 kPa and 1,897 kPa with standard deviations of 70 kPa and 50 kPa, respectively. Also, the average ITS<sub>dry</sub> and ITS<sub>F-T</sub> values for Mix-6 were found to be 2,206 kPa and 1,681 kPa with standard deviations of 23 kPa and 38 kPa, respectively. Therefore, a lower ITS was found for Mix-6 compared to Mix-5. The presence of moisture at lower WMA mixing temperature was believed to cause lower ITS values for Mix-6 (Hill et al., 2012a). Also, the TSR<sub>F-T</sub> value observed for Mix-6 was slightly lower (0.76) compared to Mix-5 (0.80). Furthermore, Mix-6 mix did not satisfy ODOT's current specification for moisture-induced damage (0.80), whereas Mix-5 satisfied the requirement. A higher moisture-induced damage potential for foamed WMA compared to HMA was also reported by other researchers due to partially dried aggregates and

incorporation of water in the foaming process (Hurley and Prowell, 2005; Prowell et al., 2007; Ali et al., 2013; Xu et al., 2017).

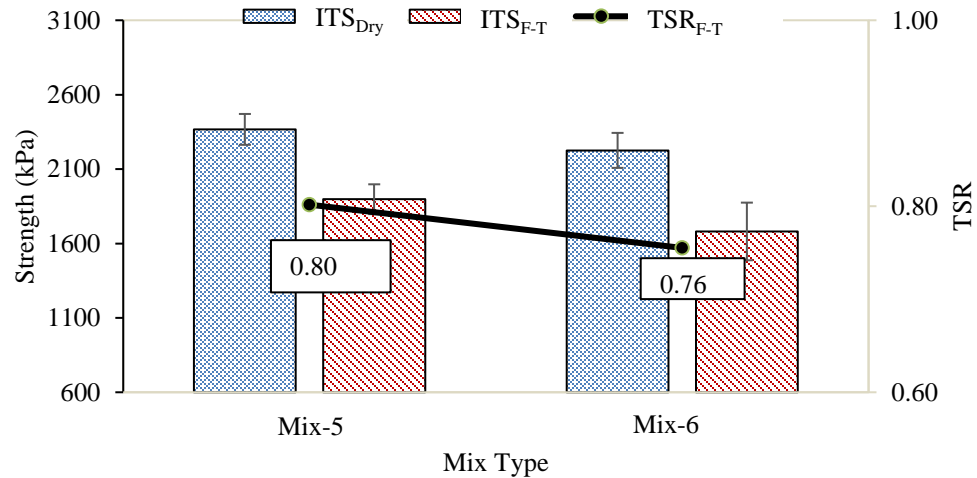


Figure 5.19 Indirect Tensile Strength (ITS<sub>dry</sub> and ITS<sub>F-T</sub>) and TSR (TSR<sub>F-T</sub>) Values for Mix-5 and Mix-6 (AASHTO T 283 method)

### 5.5.3 MIST Conditioning

In this study, the MIST conditioning was also used as per ASTM D 7870 to evaluate the moisture-induced damage potential of asphalt mixes (ASTM, 2016). Figures 5.20 and 5.21 show the ITS test results and MIST conditioned TSR values (TSR<sub>MIST</sub>) for S3 and S4 mixes, respectively. A significant reduction in ITS value was observed for both Mix-2 and Mix-6 after MIST conditioning. A lower TSR<sub>MIST</sub> value of 0.68 was observed for Mix-2 compared to control Mix-1 (0.94) after MIST conditioning. Also, a TSR<sub>MIST</sub> value of only 0.60 was observed for Mix-6, whereas Mix-5 exhibited a higher TSR<sub>MIST</sub> value of 0.91. Therefore, MIST conditioning followed a similar trend in screening the moisture-induced damage potential of asphalt mixes compared to SIP and TSR<sub>F-T</sub> parameters. Furthermore, higher TSR<sub>MIST</sub> values

were found for S3 mixes compared to S4 mixes due to increased RAP amount (Zhao et al., 2012; Shu et al., 2012; Hill et al., 2012a).

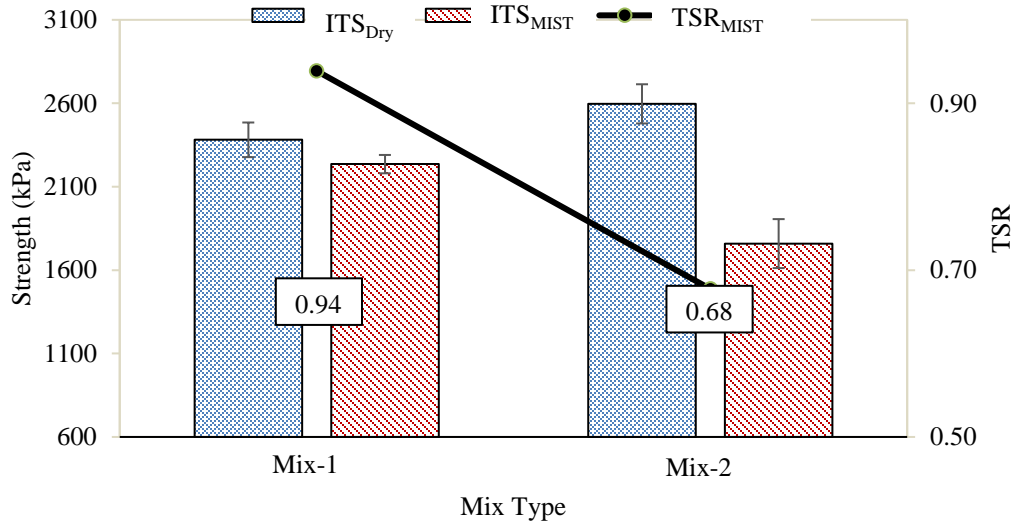


Figure 5.20 Indirect Tensile Strength (ITS<sub>dry</sub> and ITS<sub>MIST</sub>) and TSR<sub>MIST</sub> Values for Mix-1 and Mix-2 (MIST Conditioning)

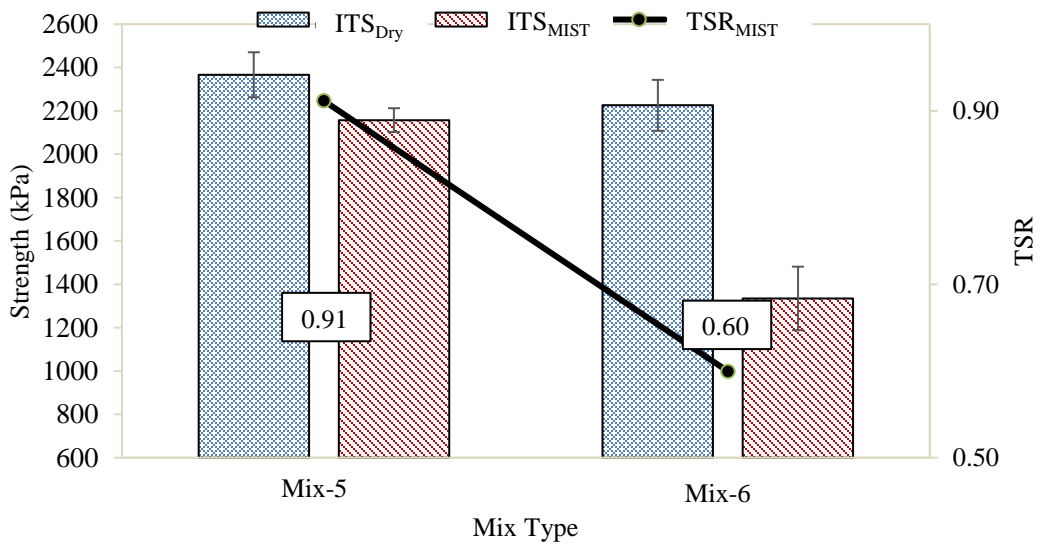


Figure 5.21 Indirect Tensile Strength (ITS<sub>dry</sub> and ITS<sub>MIST</sub>) and TSR<sub>MIST</sub> Values for Mix-5 and Mix-6 (MIST Conditioning)



In this study, MIST conditioning was found to screen the moisture-induced damage potential of WMA from HMA more distinctly compared to AASHTO T 283 conditioning method. In AASHTO T 283 method, environmental degradation of asphalt sample was simulated by one freeze-thaw cycle without considering traffic and cyclic pore pressure effects (AASHTO, 2014b). On the other hand, the generation and dissipation of pore water pressure in saturated pavement due to vehicular movement is simulated in the MIST conditioning process. In MIST, the stripping of asphalt mixes was caused by this generation of pore water pressure (Tarefder and Ahmad, 2014; Weldegiorgis and Tarefder, 2015). Therefore, several researchers have suggested using MIST conditioning in evaluating the moisture-induced damage potential of asphalt mixes (Mallick et al., 2005; Chen and Huang, 2008; Tarefder and Ahmad, 2014; Weldegiorgis and Tarefder, 2015).

#### **5.5.4 Visual Rating of Fractured Faces**

The fractured faces of the asphalt samples after ITS tests were examined to visually rank the moisture-induced damage potential of asphalt mixes according to AASHTO T 283 (AASHTO, 2014b). The rating was conducted on a scale of 1 to 4, where 1 represents no moisture-induced damage and 4 represents severe moisture-induced damage potential. Tables 5.9 and 5.10 represent a photographic view of fracture faces for S3 and S4 mixes, respectively. Both HMA mixes were rated as 1 based on visual inspection, which indicates no moisture-induced damage. On the other hand, WMA mixes were rated as 2 indicating low moisture-induced damage potential due to the presence of stripping at the fractured faces. Also, severe stripping of binder from aggregates was not observed for any of those mixes. Furthermore, stripping was

more dominantly observed for MIST conditioned samples compared to freeze-thaw conditioned samples due to application of cyclic loading in MIST conditioning.

Table 5.9 Fractured Faces of Asphalt Mixes, and Visual Ratings of TSR Test for Mix-1  
and Mix-2






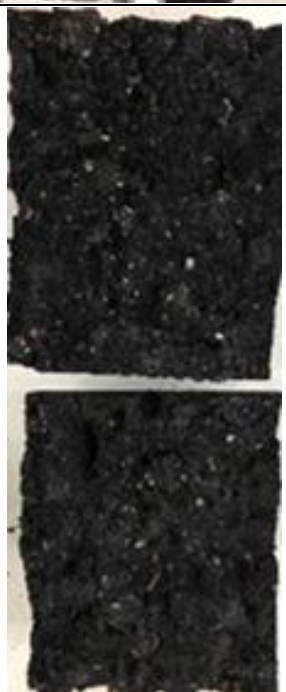







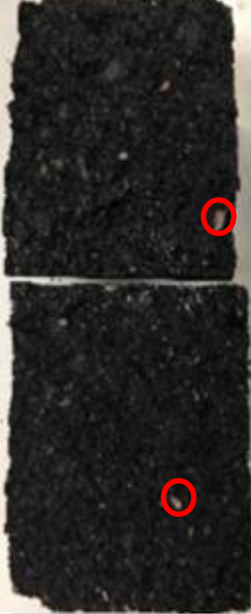








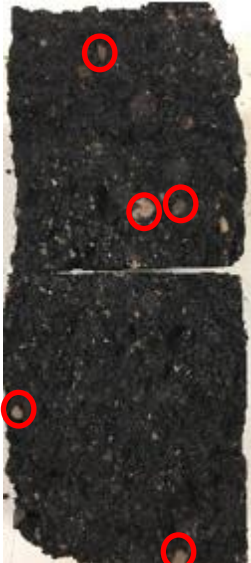






Mix Type	Fractured Section			Visual Inspection Rating of Stripping
	Tested in Dry Condition	AASHTO T 283 Method	MIST Condition	
Mix-1		 	 	1
Mix-2		 	 	2

Table 5.10 Fractured Faces of Asphalt Mixes, and Visual Ratings of TSR Test for Mix-5 and Mix-6

Mix Type	Fractured Section			Visual Inspection Rating of Stripping
	Tested in Dry Condition	AASHTO T 283 Method	MIST Condition	
Mix-5		  Stripping of Binder	    Stripping of Binder	1
Mix-6		    Stripping of Binder	       Stripping of Binder	2

### 5.5.5 Ranking of Asphalt Mixes Based on Moisture-Induced Damage Potential

Table 5.11 shows the ranking of asphalt mixes using different parameters obtained from HWT and TSR test results. A similar ranking of moisture-induced damage potential for asphalt mixes was found based on different test parameters. No distinct SIP was observed for HMA in the HWT test results. Therefore, the same rank was assigned for both Mix-1 and Mix-5. On the other hand, both TSR values followed a similar trend in ranking the asphalt mixes. Based on the TSR values, Mix-1 exhibited the highest resistance to moisture-induced damage followed by Mix-5, Mix-2, and Mix-6. Therefore, foamed WMA technology is expected to produce higher moisture susceptible mixes due to the lowering of mixing and compaction temperatures. Ali et al. (2013) suggested a longer drying period for aggregates in case of WMA to allow the entrapped water to escape. The moist aggregates increased the potential of moisture-induced damage for foamed WMA due to inadequate aggregate coating in presence of water (Ali et al., 2013). Also, an increase in RAP content was found to be beneficial for moisture-induced damage resistance due to stronger bond between the aged binder and aggregates.

Table 5.11 Ranking of Asphalt Mixes Based on Moisture-Induced Damage Resistance

Mix Type	HWT Test	ITS test		
	SIP	TSR <sub>F-T</sub>	TSR <sub>MIST</sub>	Visual Inspection
Mix-1	1	1	1	1
Mix-2	3	3	3	2
Mix-5	1	2	2	1
Mix-6	4	4	4	2

Furthermore, the field moisture-induced damage potential of WMA may be different from the laboratory performance. Kim et al. (2012b) reported similar field

performance for both HMA and WMA in the early stage (three years after placement) of the pavement. However, long-term field investigation is required to evaluate the actual moisture resistance of WMA. A field study conducted by Martin (2014) suggested that, after summer aging in the field, the moisture-induced damage potential of WMA was found to increase rapidly.

## **5.6 Summary**

The fatigue cracking, rutting and moisture-induced damage potentials of foamed WMA compared to control HMA are discussed in this chapter. The foamed WMA containing RAP was found to exhibit lower stiffness compared to HMA in the dynamic Modulus test. This is attributed to a lower degree of aging at lower mixing and compaction temperatures for foamed WMA. Also, an increase in RAP content was found to increase the stiffness of asphalt mixes due to incorporation of aged binder from RAP. The stiffer asphalt mixes are expected to exhibit lower fatigue cracking resistance and higher rutting resistance. Therefore, foamed WMA was found to show higher fatigue cracking resistance compared to HMA in Louisiana SCB and I-FIT tests. A similar trend in the fatigue cracking resistance was observed for coarser mixes in the Abrasion Loss Test. However, this test method could not screen the fatigue cracking resistance of finer mixes. Therefore, instead of Abrasion Loss Test, Louisiana SCB or/and I-FIT test may be conducted in screening the cracking resistance of asphalt mixes. Furthermore, coarser mixes were found to show lower fatigue cracking resistance compared to finer mixes due to higher RAP content and crack propagation mechanism. In case of rutting, the foamed WMA containing RAP showed lower resistance compared to their HMA counterparts, as expected from dynamic modulus

values. This is mainly attributed to reduced aging for foamed WMA. Also, the coarser mixes were found to show higher rutting resistance compared to finer mixes due to increase in RAP content. Furthermore, the foamed WMA was found to exhibit more moisture-induced damage potential compared to HMA containing RAP. The partially dried aggregates at a lower mixing temperature and use of water in the foaming process are believed to increase the moisture susceptibility for foamed WMA. The presence of moisture is expected to affect the bonding between aggregates and binder in the foamed WMA. The MIST conditioning was found to screen the asphalt mixes more distinctly compared to AASHTO T 283 method due to the application of cyclic loads during conditioning process. However, all test parameters ranked the asphalt mixes in a similar way. Also, increase in RAP content was found to lower moisture-induced damage potential due to strong bonding between RAP aggregate and binder. Overall, use of RAP in WMA was found beneficial so far as rutting and moisture-induced damage are concerned, but detrimental to cracking resistance.

## CHAPTER

# 6

## CONCLUSION AND RECOMMENDATIONS

### 6.1 Conclusions

In this study, the volumetric properties, rutting resistance, cracking resistance and moisture-induced damage potential of foamed WMA containing RAP were evaluated and compared with HMA counterparts. The important findings of this study are given below:

1. The foamed WMA technique was found to increase fatigue cracking resistance, rutting potential and moisture-induced damage potential of asphalt mixes. The addition of RAP in WMA, on the contrary, was expected to reduce fatigue cracking resistance, rutting potential and moisture-induced damage potential of asphalt mixes. Therefore, a suitable combination of foamed WMA technique and RAP may counteract each other's effects.
2. While incorporating RAP, compaction temperature greater than high-temperature PG of RAP was reported to exhibit similar volumetric properties for WMA compared to HMA. However, in this study, the mixing and compaction temperatures of the mix, along with the high-temperature PG of RAP, was found to govern the volumetric properties of the foamed WMA containing RAP. Significant differences in the percent air voids between foamed WMA and HMA mixes were observed while mixing and compacting at temperatures lower



than practice temperatures but higher than high-temperature PG of RAP. Other pertinent findings from this study are summarized in the following sections.

### **6.1.1 Volumetric Properties**

1. In this study, foamed WMA was produced using the same mix design procedure as traditional HMA, except that lower mixing (135°C) and compaction (127°C) temperatures were used for the foamed mixes. The mixing and compaction temperatures used for the HMA were 163°C and 149°C, respectively. It was found that both fine and coarse WMA mixes exhibited similar percent air voids as HMA mixes. The corresponding p-values for the fine and coarse mixes were 0.98 and 0.58, respectively, indicating insignificant differences in air voids for both foamed WMA and HMA, at 95% confidence level. The reduction in mixing and compaction temperatures for foamed WMA did not cause any coating and compaction problems.
2. To identify the effect of further lowering of mixing and compaction temperatures, foamed WMA was produced at temperatures that were 20°C and 40°C lower than the temperatures used in practice. For both cases uncoated aggregates were observed after mixing and compaction. The degree of uncoated aggregates increased with the lower temperatures. Statistically significant differences in percent air voids were observed at 95% confidence level as compared to HMA for both cases.
3. A reduction of 40°C in both mixing and compaction temperatures from the current WMA practice was found to produce mixes with higher statistical differences in percent air voids compared to control HMA. Reduction of

compaction temperature (87°C) below the high-temperature PG (94°C) of the extracted RAP binder was found to be responsible for inadequate compaction and thus, significant difference in percent air voids. Therefore, while incorporating RAP in WMA, the compaction temperature should be greater than the high-temperature PG of extracted RAP binder to ensure required active binder from RAP.

## **6.1.2 Laboratory Performance**

### *6.1.2.1 Dynamic Modulus Test*

1. Relatively low dynamic modulus values were found for foamed WMA compared to HMA. Therefore, foamed WMA exhibited relatively lower stiffness compared to control HMA. The reduced degree of aging at low mixing and compaction temperatures is believed to lower stiffness for WMA. The differences in dynamic modulus values between WMA and HMA were found to be more dominant for coarser mixes at lower reduced frequencies due to incorporation of high amount of RAP (25%).
2. An increase in RAP content was found to increase the dynamic modulus values due to the addition of aged and stiffer binder in the asphalt mixes. Therefore, it can be concluded that increase in RAP content increases the stiffness of asphalt mixes.

### *6.1.2.2 Cracking Properties*

1. The Louisiana SCB and I-FIT tests were found to follow a similar trend in screening asphalt mixes for cracking resistance. A higher  $J_c$  and FI index were observed for foamed WMA than HMA indicating higher cracking

resistance. A higher fatigue resistance of foamed WMA was expected due to a lower stiffness found in the dynamic modulus testing.

2. The percent loss in the abrasion test was found to provide inconsistent results compared to the Louisiana SCB and I-FIT tests for fine mixes. Although this test is easy to conduct, it may not screen mixes for their fatigue resistance. Lack of a strong mechanistic basis could be attributed to such inconsistencies. SCB test methods (both Louisiana and I-FIT) provided consistent results indicating that these test methods can be used for screening of both WMA and HMA for fatigue cracking resistance.
3. Incorporation of RAP was found to increase the stiffness of asphalt mixes, which resulted in a lower fatigue resistance. Also, the finer mixes showed higher cracking resistance than coarser mixes due to differences in crack propagation mechanisms. For finer mixes crack was found to propagate through the aggregates, whereas crack mostly propagated through the mastic for coarser mixes.

#### *6.1.2.3 Rutting Properties*

1. It was found that foamed WMA exhibited lower rutting resistance than HMA with identical RAP content. This was attributed to lower stiffness of WMA as indicated by dynamic modulus values. However, both fine and coarse WMA satisfied ODOT's current provision for rut depth of 12.5 mm at 10,000 wheel passes in HWT test (ODOT, 2011).
2. It was found that both HWT and FN tests screened the rutting resistance of asphalt mixes in a similar way. HMA mix with high RAP content showed the

best rutting performance, whereas foamed WMA with lower RAP content was ranked the worst. This was expected as foamed WMA with low RAP content exhibited lower stiffness in the dynamic modulus test.

3. The coarser mixes were found to exhibit higher rutting resistance than finer mixes due to increased RAP content. Incorporation of aged and stiffer binder from RAP was found to increase the rutting resistance of asphalt mixes.

#### *6.1.2.4 Moisture-Induced Damage Potential*

1. Distinct SIPs for both WMA coarse and fine mixes were observed at about 17,100 and 12,000 wheel passes, respectively. However, no SIP was observed for the HMA. Therefore, foamed WMA may exhibit higher moisture-induced damage potential than HMA, in presence of moisture.
2. A relatively low TSR value was observed for foamed WMA compared to HMA for both AASHTO T 283 and MIST conditioning methods, indicating higher moisture-induced damage potential for WMA. The MIST method was found to screen asphalt mixes more distinctly compared to the AASHTO T 283 method due to the application of cyclic loads during the conditioning process.
3. The lower mixing and compaction temperatures for WMA may result in partially dried aggregates. Also, water used in the foaming process for WMA may adversely affect the bonding between aggregates and binder. Therefore, foamed WMA exhibited higher moisture-induced damage potential compared to HMA.
4. It was found that incorporation of RAP in the asphalt mixes increased the moisture-induced damage resistance. The stronger bond between aged binder

and aggregates of RAP is expected to reduce moisture-induced damage potential.

## **6.2 Recommendations**

Based on the limitations of this study, the following recommendations are made:

1. The RAP content up to 25% was considered in this study. The effect of higher RAP content in foamed WMA could be considered in a future study.
2. The WMA using foaming process was considered in this study. Therefore, the laboratory and field performance of other WMA, namely chemical and organic can be verified in the future study.
3. In this study, two commonly used asphalt mixes for intermediate and surface courses in Oklahoma were considered for laboratory performance evaluation of foamed WMA. It is recommended that addition intermediate and surface course mixes can be considered for future studies.
4. In this study, percent air voids were considered to check the volumetric properties of WMA and HMA. In the future, optimum binder content and absorbed binder content can be varied to identify the mix design related issues of foamed WMA.
5. The field performance of WMA may be different than the laboratory performance. Therefore, both short-term and long-term field performance of foamed WMA can be evaluated in the future.

## References

1. AASHTO TP 10 (1993). "Standard Test Method for Thermal Stress Restrained Specimen Tensile Strength." *American Association of State Highway and Transportation Officials*, Washington, D.C.
2. AASHTO (2004). "Guide for Mechanistic-Empirical Design of New and Rehabilitated Pavement Structures." *American Association of State and Highway Transportation Officials, Final Report 1-37A prepared for National Cooperative Highway Research Program (NCHRP)*, Washington, D.C.
3. AASHTO R 30 (2002). "Standard Practice for Mixture Conditioning of Hot Mix Asphalt (HMA)." *American Association of State Highway and Transportation Officials*, Washington, D.C.
4. AASHTO R 35 (2013). "Standard Practice for Superpave Volumetric Design for Asphalt Mixtures." *American Association of State Highway and Transportation Officials*, Washington, D.C.
5. AASHTO TP 108 (2016). "Standard Practice for Abrasion Loss of Asphalt Mixture Specimens." *American Association of State Highway and Transportation Officials*, Washington, D.C.
6. AASHTO TP 124 (2016). "Determining the Fracture Potential of Asphalt Mixtures Using Semicircular Bend Geometry (SCB) at Intermediate Temperature." *American Association of State Highway and Transportation Officials*, Washington, D.C.
7. AASHTO T 164 (2014a). "Standard Method of Quantitative Extraction of Asphalt Binder from Hot Mix Asphalt (HMA)." *American Association of State and Highway Transportation Officials*, Washington, D.C.
8. AASHTO T 166 (2010). "Standard Method of Test for Bulk Specific Gravity of Compacted Hot-Mix Asphalt Using Saturated Surface-Dry Specimens." *American Association of State and Highway Transportation Officials*, Washington, D.C.
9. AASHTO T 209 (2012). "Theoretical Maximum Specific Gravity ( $G_{mm}$ ) and Density of Hot Mix Asphalt (HMA)." *American Association of State and Highway Transportation Officials*, Washington, D.C.

10. AASHTO T 283 (2014b). “Standard Practice for Resistance of Compacted Asphalt Mixtures to Moisture-Induced Damage.” *American Association of State Highway and Transportation Officials*, Washington, D.C.
11. AASHTO T 324 (2014c). “Standard Method of Test for Hamburg Wheel-Track Testing of Compacted Hot Mix Asphalt (HMA).” *American Association of State Highway and Transportation Officials*, Washington, D.C.
12. AASHTO T 378 (2017). “Standard Method of Test for Determining the Dynamic Modulus and Flow Number for Asphalt Mixtures Using the Asphalt Mixture Performance Tester (AMPT).” *American Association of State Highway and Transportation Officials*, Washington, D.C.
13. Abbas, A. R., and Ali, A. (2011). “Mechanical Properties of Warm Mix Asphalt Prepared Using Foamed Asphalt Binders.” *Executive Summary Report (No. FHWA/OH-2011/6)*. Ohio. Dept. of Transportation.
14. Abuawad, I. M., Al-Qadi, I. L., and Trepanier, J. S. (2015). “Mitigation of Moisture Damage in Asphalt Concrete: Testing Techniques and Additives/Modifiers Effectiveness.” *Construction and Building Materials*, Vol. 84, pp. 437-443.
15. Alhasan, A.A., Abbas, A.R., Nazzal, M., Dessouky, S., Ali, A., Kim, S.S. and Powers, D. (2014). “Low-Temperature Characterization of Foamed Warm-Mix Asphalt Produced by Water Injection.” *Transportation Research Record: Journal of the Transportation Research Board*, Vol. 2445, pp. 1–11.
16. Ali, A., Abbas, A., Nazzal, M., Alhasan, A., Roy, A. and Powers, D. (2013). “Effect of Temperature Reduction, Foaming Water Content, and Aggregate Moisture Content on Performance of Foamed Warm Mix Asphalt.” *Construction and Building Materials*, Vol. 48, pp. 1058–1066.
17. Ali, S.A. (2016). “Rheological Properties of Polymer and RAP Modified Asphalt Binders Using Multiple Stress Creep and Recovery Method.” *MS Thesis*, University of Oklahoma, Norman, OK, USA.
18. Al-Qadi, I. L., Ozer, H., Lambros, J., El Khatib, A., Singhvi, P., Khan, T., and Doll, B. (2015). “Testing Protocols to Ensure Performance of High Asphalt Binder Replacement Mixes Using RAP and RAS.” *Illinois Center for Transportation/Illinois Department of Transportation*, pp. 1-191.

19. Apeageyi, A. K., Diefenderfer, B. K., and Diefenderfer, S. D. (2011). "Rutting Resistance of Asphalt Concrete Mixtures that contain Recycled Asphalt Pavement." *Transportation Research Record: Journal of the Transportation Research Board, Vol. 2208(1)*, pp. 9-16.
20. Arshadi, A., Ghabchi, R., Ali S.A., Barman, M., Zaman, M., and Commuri, S. (2017). "Cracking Resistance of Warm Mix Asphalt Containing Recycled Asphalt Materials (RAP and RAS)." *Transportation Research Board Annual Meeting, January 8-12, 2017, Washington, D.C.*
21. Asphalt Institute (2016). "Determining Lab Mixing and Compaction Temperatures for Binders." 2696 Research Park Drive Lexington, KY 40511-8480.  
<http://www.asphaltinstitute.org/engineering/determining-lab-mixing-compaction-temperatures-binders/>  
(Accessed Date: 7.6.2019)
22. ASTM D 5404 (2017). "Standard Test Method for Recovery of Asphalt from Solution Using the Rotary Evaporator Cracking Resistance Using the Semi-Circular Bend Test (SCB) at Intermediate Temperature." *American Society for Testing and Materials, West Conshohocken, PA, 19428-2959, U.S.A.*
23. ASTM D 6931 (2012). "Standard Test Method for Indirect Tensile (IDT) Strength of Bituminous Mixtures." *American Society for Testing and Materials, West Conshohocken, PA, 19428-2959, U.S.A.*
24. ASTM D 7870 (2016). "Standard Practice for Moisture Conditioning Compacted Asphalt Mixture Specimens by Using Hydrostatic Pore Pressure." *American Society for Testing and Materials, West Conshohocken, PA, 19428-2959, U.S.A.*
25. ASTM D 8044 (2013). "Standard Test Method for Evaluation of Asphalt Mixture Cracking Resistance Using the Semi-Circular Bend Test (SCB) at Intermediate Temperature." *American Society for Testing and Materials, West Conshohocken, PA, 19428-2959, U.S.A.*
26. Baek J. (2010). "Modeling Reflective Cracking Development in Hot-Mix Asphalt Overlays and Quantification of Control Techniques." *Ph.D. Dissertation, University of Illinois at Urbana-Champaign, Urbana, Illinois.*



27. Barman, M., Arshadi, A., Ghabchi, R., Singh, D., Zaman, M., and Commuri, S. (2016). "Recommended Fatigue Test for Oklahoma Department of Transportation." *Report No. FHWA-OK-16-05*, pp. 10-14
28. Barman, M., Ghabchi, R., Singh, D., Zaman, M., and Commuri, S. (2018). "An Alternative Analysis of Indirect Tensile Test Results for Evaluating Fatigue Characteristics of Asphalt Mixes." *Construction and Building Materials, Vol. 166*, pp. 204–213.
29. Biligiri, K., Kaloush, K., Mamlouk, M., and Witczak, M. (2007). "Rational Modeling of Tertiary Flow for Asphalt Mixtures." *Transportation Research Record: Journal of the Transportation Research Board, Vol. 2001*, pp. 63-72.
30. Biligiri, K. P., Said, S., and Hakim, H. (2012). "Asphalt Mixtures." *International Journal of Pavement Research and Technology, Vol. 5(4)*, pp. 209-217.
31. Bonaquist, R. (2011). "Mix Design Practices for Warm Mix Asphalt." *NCHRP Report 691, National Cooperative Highway Research Program*, Washington, D.C.
32. Bowering, R. H., and Martin, C. L. (1976). "Foamed Bitumen Production and Application of Mixtures Evaluation and Performance of Pavements." *In Association of Asphalt Paving Technologists Proc (Vol. 45)*.
33. Brown, D. C. (2008). "Warm Mix: the Lights are Green." *HMAT: Hot Mix Asphalt Technology, Vol. 13(1)*, pp. 20-32.
34. Brown, E. R., Kandhal, P. S., Roberts, F. L., Kim, Y. R., Lee, D. Y., and Kennedy, T. W. (2009). "Hot Mix Asphalt Materials, Mixture Design, and Construction." *NAPA Research and Education Foundation, 3<sup>rd</sup> edition*, pp. 210-215.
35. Bueche, N., (2009). "Warm Asphalt Bituminous Mixtures with Regards to Energy, Emissions and Performance." *Young Researchers Seminar (YRS), June 3 to 9, 2009, LAVOC-CONF- 2010-002*, Torino, Italy.
36. Butz, T., Rahimian, I., and Hildebrand, G. (2001). "Modification of Road Bitumen with the Fischer-Tropsch Paraffin Sasobit." *Journal of Applied Asphalt Binder Technology, Vol.1 (2)*, pp. 70-86.
37. Chaturabong, P. (2016). "Mechanisms of Asphalt Mixture Rutting Failure in the Hamburg Wheel Tracking Test and the Potential for Replacing the Flow Number Test." *PhD Thesis*, The University of Wisconsin-Madison.

38. Chaturabong, P., and Bahia, H.U. (2017). "Mechanisms of Asphalt Mixture Rutting in the Dry Hamburg Wheel Tracking Test and the Potential to be Alternative Test in Measuring Rutting Resistance." *Construction and Building Materials*, Vol. 146, pp. 175-182.
39. Chehab, G., O'Quinn, R. E., and Kim, Y. R. (2000). "Specimen Geometry Study for Direct Tension Test Based on Mechanical Tests and Air Void Variation in Asphalt Concrete Specimens Compacted by Superpave Gyrotory Compactor." *Journal of Transportation Research Record: Journal of the Transportation Research Board*, No. 1723, *Journal of the Transportation Research Board*, Washington, D.C., pp. 125–132.
40. Chen, X., and Huang, B. (2008). "Evaluation of Moisture Damage in Hot Mix Asphalt Using Simple Performance and Superpave Indirect Tensile Tests." *Construction and Building Materials*, Vol. 22(9), pp. 1950-1962.
41. Choubane, B., Page, G., and Musselman, J. (2000). "Suitability of Asphalt Pavement Analyzer for Predicting Pavement Rutting." *Transportation Research Record: Journal of the Transportation Research Board*, Vol. 1723, pp. 107-115.
42. Chowdhury, A., and Button, J. W. (2008). "A Review of Warm Mix Asphalt." (No. SWUTC/08/473700-00080-1). College Station, TX: Texas Transportation Institute, the Texas A & M University System, pp. 11-12.
43. Colombier, G. (1997). "Cracking in Pavements: Nature and Origin of Cracks." In: *Vanelstraete A, Franckien L. editors, Prevention of reflective cracking in pavements – RILEM Report 18*, pp. 1–15.
44. Cooley, L. A., Kandhal, P. S., Buchanan, M. S., Fee, F., and Epps, A. (2000). "Loaded Wheel Testers in The United States: State of The Practice." *Transportation Research Circular, E-C016*, Transportation Research Board, Washington, DC, pp. 1-15.
45. Copeland, A., D'Angelo, J., Dongre, R., Belagutti, S., and Sholar, G. (2010). "Field Evaluation of High Reclaimed Asphalt Pavement-Warm-Mix Asphalt Project in Florida: Case Study." *Transportation Research Record: Journal of the Transportation Research Board*, Vol. 2179, pp. 93-101.
46. Coree, B., Ceylan, H., and Harrington, D. (2005). "Implementing the Mechanistic-Empirical Pavement Design Guide: Implementation Plan." In *Trans Project Reports*. 51.

[http://lib.dr.iastate.edu/intrans\\_reports/51](http://lib.dr.iastate.edu/intrans_reports/51)

(Accessed: 4.29.18)

47. Corte, J. F. (2001). "Development and Uses of Hard-grade Asphalt and of High Modulus Asphalt Mixes in France." *Transportation Research Board: Transportation Research Circular, Vol. 503*, pp. 12-31.
48. D'Angelo, J., Harm, E., Bartoszek, J., Baumgardner, G., Corrigan, M., Cowser, J., and Prowell, B. (2008). "Warm-mix Asphalt: European Practice." (No. FHWA-PL-08-007). United States. Federal Highway Administration. Office of International Programs.
49. Daniel, J. S., and Lachance, A. (2005). "Mechanistic and Volumetric Properties of Asphalt Mixtures with Recycled Asphalt Pavement." *Transportation Research Record: Journal of the Transportation Research Board, Vol. 1929(1)*, pp. 28-36.
50. Dave, E.V., Song S.H., Buttlar W.G., and Paulino G.H. (2007). "Reflective and Thermal Cracking Modeling of Asphalt Concrete." In: Loizos, Scarpas, Al-Qadi, editors, *Advanced Characterization of Pavement and Soil Engineering Materials Conference*, Athens, Greece, pp. 1241–1252.
51. Dinis-Almeida, M., Castro-Gomes, J., and Antunes, M.D.L. (2012). "Mix Design Considerations for Warm Mix Recycled Asphalt with Bitumen Emulsion." *Construction and Building Materials, Vol. 28*, pp. 687–693.
52. Dong, F., Yu, X., Xu, B. and Wang, T. (2017). "Comparison of High Temperature Performance and Microstructure for Foamed WMA and HMA with RAP Binder." *Construction and Building Materials, Vol. 134*, pp. 594–601.
53. Doyle, J.D., and Howard, I.L. (2011). "Evaluation of The Cantabro Durability Test for Dense Graded Asphalt." *In Geo-Frontiers Conference: Advances in Geotechnical Engineering*, pp. 4563-4572.
54. Federal Highway Administration, (1997). Publication Number: FHWA-RD-97-148 "User Guidelines for Waste and Byproduct Materials in Pavement Construction." <https://www.fhwa.dot.gov/publications/research/infrastructure/structures/97148/rap131.cfm>  
(Accessed: 4.29.18)
55. Flintsch, G. W., Loulizi, A., Diefenderfer, S. D., Diefenderfer, B. K., and Galal, K. A. (2008). "Asphalt Material Characterization in Support of Mechanistic–Empirical

- Pavement Design Guide Implementation in Virginia.” *Transportation Research Record: Journal of the Transportation Research Board*, Vol. 2057(1), pp. 114-125.
56. Francken, L. (1977). “Permanent Deformation Law of Bituminous Road Mixes in Repeated Triaxial Compression.” *In Volume I of proceedings of 4th International Conference on Structural Design of Asphalt Pavements*, Ann Arbor, Michigan, August 22-26, 1977.
  57. Gandhi, T., Akisetty, C., and Amir Khanian, S. (2009). “Laboratory Evaluation of Warm Asphalt Binder Aging Characteristics.” *International Journal of Pavement Engineering*, Vol. 10, pp. 353–359.
  58. Ghabchi, R. (2014). “Laboratory Characterization of Recycled and Warm Mix Asphalt for Enhanced Pavement Applications.” *PhD Thesis*, University of Oklahoma, Norman, OK, USA.
  59. Ghabchi, R., Barman, M., Singh, D., Zaman, M., and Mubarak, M.A. (2016). “Comparison of Laboratory Performance of Asphalt Mixes Containing Different Proportions of RAS and RAP.” *Construction and Building Materials*, Vol. 124, pp. 343-351.
  60. Ghabchi, R., Zaman, M., Arshadi, A., Rahman, M.A., and Barman, M. (2019). “Development of Special Provision for Mix Design of Foamed WMA Containing RAP.” *Final report to be Submitted to Southern Plains Transportation Center, Project SPTC15.1-31*, 80 pages.
  61. Grebenshikov, S., and Prozzi, J. (2011). “Enhancing Mechanistic-Empirical Pavement Design Guide Rutting-Performance Predictions with Hamburg Wheel Tracking Results.” *Transportation Research Record: Journal of the Transportation Research Board*, Vol. 2226, pp. 111-118.
  62. Goh, S. W., and You, Z. (2011a). “Evaluation of Warm Mix Asphalt Produced at Various Temperatures through Dynamic Modulus Testing and Four Point Beam Fatigue Testing.” *Proceedings of the GeoHunan international conference—pavements and materials: recent advances in design, testing, and construction*, Hunan, China, *Geotechnical Special Publication*, Vol. 212, pp. 123-30.

63. Goh, S. W., and You, Z. (2011b). "Mechanical Properties of Porous Asphalt Pavement Materials with Warm Mix Asphalt and RAP." *Journal of Transportation Engineering*, Vol. 138(1), pp. 90-97.
64. Golalipour, A., Jamshidi, E., Niazi, Y., Afsharikia, Z., and Khadem, M. (2012). "Effect of Aggregate Gradation on Rutting of Asphalt Pavements." *Procedia-Social and Behavioral Sciences*. Vol. 53, pp. 440-449.
65. Guo, N., You, Z., Zhao, Y., Tan, Y. and Diab, A. (2014). "Laboratory Performance of Warm Mix Asphalt Containing Recycled Asphalt Mixtures." *Construction and Building Materials*, Vol. 64, pp. 141–149.
66. Hailesilassie, B. W., Hugener, M., and Partl, M. N. (2015). "Influence of Foaming Water Content on Foam Asphalt Mixtures." *Construction and Building Materials*, Vol. 85, pp. 65-77.
67. Hand, A. J., and Epps, A. L. (2001). "Impact of Gradation Relative to Superpave Restricted Zone on Hot-Mix Asphalt Performance." *Transportation research record: Journal of the Transportation Research Board*, Vol. 1767(1), pp. 158-166.
68. Hill, B. (2011). "Performance Evaluation of Warm Mix Asphalt Mixtures Incorporating Reclaimed Asphalt Pavement." *PhD Thesis*, University of Illinois at Urbana-Champaign, Champaign, IL.
69. Hill, B., Behnia, B., Buttlar, W. G., and Reis, H. (2012a). "Evaluation of Warm Mix Asphalt Mixtures Containing Reclaimed Asphalt Pavement through Mechanical Performance Tests and an Acoustic Emission Approach." *Journal of Materials in Civil Engineering*, Vol. 25(12), pp. 1887-1897.
70. Hill, B., Behnia, B., Hakimzadeh, S., Buttlar, W. G., and Reis, H. (2012b). "Evaluation of Low-Temperature Cracking Performance of Warm-Mix Asphalt Mixtures." *Transportation Research Record: Journal of the Transportation Research Board*, Vol. 2294(1), pp. 81-88.
71. Hong, F., Chen, D. H., and Mikhail, M. M. (2010). "Long-Term Performance Evaluation of Recycled Asphalt Pavement Results from Texas: Pavement Studies Category 5 Sections from the Long-Term Pavement Performance Program." *Transportation Research Record: Journal of the Transportation Research Board*, Vol. 2180(1), pp. 58-66.

72. Hossain, Z., Zaman, M., O'Rear, E. A., and Chen, D. H. (2012). "Effectiveness of Water-Bearing and Anti-Stripping Additives in Warm Mix Asphalt Technology." *International Journal of Pavement Engineering, Vol. 13(5)*, pp. 424-432.
73. Hossain, Z., Zaman, M., Solanki, P., Ghabchi, R., Singh, D., Adje, D., and Lewis, S. (2013). "Implementation of MEPDG for Asphalt Pavement with RAP." *Final Report, Report No. OTCREOS10.1-45-F*, University of Oklahoma, Norman, OK.
74. Huang, B., Li, G., Vukosavljevic, D., Shu, X., and Egan, B. K. (2005). "Laboratory Investigation of Mixing Hot-Mix Asphalt with Reclaimed Asphalt Pavement." *Transportation Research Record: Journal of the Transportation Research Board, Vol. 1929(1)*, pp. 37-45.
75. Huang, B., Xiang, S., and Zuo, G. (2013). "Using Notched Semi Circular Bending Fatigue Test to Characterize Fracture Resistance of Asphalt Mixtures." *Construction and Building Materials, Vol. 109*, pp. 78–88.
76. Huang, B., Zhang, Z., Kingery, W., and Zuo, G. (2004). "Fatigue crack Characteristics of HMA Mixtures Containing RAP." *In Proceeding 5th Int. Conf. on Cracking in Pavements, RILEM*, pp. 631-638.
77. Huang, Y.H. (2004). "Pavement Analysis and Design." *Pearson Education, Inc., 2nd Edition*, Upper Saddle River, NJ 0745 8.
78. Hurley, G. C., and Prowell, B. D. (2005). "Evaluation of Sasobit for Use in Warm Mix Asphalt." *NCAT report, Vol. 5(6)*, pp. 1-27.
79. Hurley, G., and Prowell, B.D. (2006). "Evaluation of Potential Process for Use in Warm Mix Asphalt." *Journal of the Association of Asphalt Paving Technologist, Vol. 75*, pp. 41-90.
80. Hurley, G., Prowell, B., and Kvasnak, A. (2010). "Wisconsin Field Trial of Warm Mix Asphalt Technologies: Construction Summary." *Research Report NCAT 10-04*, National Center for Asphalt Technology, Auburn, AL.
81. Illinois Center for Transportation (ICT) (2007). "Reclaimed Asphalt Pavement – A Literature Review." *Illinois Center for Transportation, R27-11*.  
<http://hdl.handle.net/2142/46007>  
(Accessed Date: 4.1.2018)
82. InstroTek® Inc. (2015). "User Guide AccuFoamer™."

[https://cdn.shopify.com/s/files/1/1245/4913/files/AccuFoamer\\_3-Manual-04-09-2015.pdf](https://cdn.shopify.com/s/files/1/1245/4913/files/AccuFoamer_3-Manual-04-09-2015.pdf)

(Accessed Date: 1.1.2019)

83. Jenkins, K. J. (2000). "Mix Design Considerations for Cold and Half-Warm Bituminous Mixes with Emphasis of Foamed Bitumen." *PhD thesis*, Stellenbosch: Stellenbosch University.
84. Jenkins, K. J., De Groot, J., Van de Ven, M. F. C., and Molenaar, A. (1999). "Half-Warm Foamed Bitumen Treatment, a New Process." *In 7th Conference on asphalt pavements for Southern Africa (CAPSA 99)*, pp. 1-17.
85. Jenq, Y.S., Perng, J.D. (1991). "Analysis of Crack Propagation in Asphalt Concrete Using Cohesive Crack Model." *Transportation Research Record: Journal of the Transportation Research Board, Vol. 1317*, pp. 90-99.
86. Jiang, W., Zhang, X., and Li, Z. (2013). "Simulation Test of The Dynamic Water Pressure of Asphalt Concrete." *Journal of Highway and Transportation Research and Development (English Edition), Vol. 7(1)*, pp. 23-27.
87. Jones, W. (2004). "Warm mix asphalt-a state-of-the-art review." *Australian Asphalt Pavement Association Advisory Note, 17*, 20-26 Sabre Drive, Port Melbourne, Australia, VIC 3207.
88. Jones, C. L. (2008). "Summit on Increasing RAP Use in Pavements Sate's Perspective." *Presented at MoreRap Conference*, North Carolina Department of Transportation, Auburn, AL.
89. Jones, D., Tsai, B. W., Signore, J. M., and University of California (System) (2010). "Warm-mix asphalt study: laboratory test results for AkzoNobel Rediset™ WMX." *Pavement Research Center*, University of California.
90. Kaloush, K. E., Witczak, M. W., and Sullivan, B. W. (2003). "Simple Performance Test for Permanent Deformation Evaluation of Asphalt Mixtures." *In Sixth International RILEM Symposium on Performance Testing and Evaluation of Bituminous Materials, April, 2003*, RILEM Publications SARL, pp. 498-505.
91. Kandhal, P. S., and Cooley, L. A. (2002). "Evaluation of Permanent Deformation of Asphalt Mixtures Using Loaded Wheel Tester." *Asphalt Paving Technology, Vol. 71*, pp. 739-753.

92. Karlson, T. K. (2005). "Evaluation of Cyclic Pore Pressure Induced Moisture Damage in Asphalt Pavement." *M.S. thesis*, University of Florida, Gainesville, FL.
93. Kasozi, A. M., Hajj, E. Y., Sebaaly, P. E., and Elkins, J. C. (2012). "Evaluation of Foamed Warm-Mix Asphalt Incorporating Recycled Asphalt Pavement for Volumetric and Mechanical Properties." *International Journal of Pavement Research and Technology*, Vol. 5(2), pp. 75-83.
94. Kavussi, A., and Hashemian, L. (2012). "Laboratory Evaluation of Moisture Damage and Rutting Potential of WMA Foam Mixes." *International Journal of Pavement Engineering*, Vol. 13(5), pp. 415-423.
95. Khan, A. S. M. (2016). "Displacement Rate and Temperature Effect on Asphalt Concrete Cracking Potential." *MS Thesis*, University of Illinois at Urbana Champaign, USA.
96. Kheradmand, B., Muniandy, R., Hua, L.T., Yunus, R.B., and Solouki, A. (2014). "An Overview of the Emerging Warm Mix Asphalt Technology." *International Journal of Pavement Engineering*, Vol. 15:1, pp. 79-94, DOI: 10.1080/10298436.2013.839791
97. Kim, M., Mohammad, L., and Elseifi, M., (2012a). "Characterization of Fracture Properties of Asphalt Mixtures as Measured by Semicircular Bend Test and Indirect Tension Test." *Transportation Research Record: Journal of the Transportation Research Board*, Vol. 2296, pp. 115-124. DOI: 10.3141/2296-12
98. Kim Y., and Little D.N. (2005). "Development of Specification Type Test to Assess the Impact of Fine Aggregate and Mineral Filler on Fatigue Damage." *Technical Report 0-1707- 10*, Texas Transportation Institute.
99. Kim, Y. and Lee, H.D. (2006). "Development of Mix Design Procedure for Cold In-Place Recycling with Foamed Asphalt." *Journal of Materials in Civil Engineering*, ASCE, Vol. 19(11), pp. 1000-1010.
100. Kim, Y., Lee, H.D., and Heitzman, M. (2007). "Validation of New Mix Design Procedure for Cold In-Place Recycling with Foamed Asphalt." *Journal of Materials in Civil Engineering*, ASCE, Vol. 18(1), pp. 116-124.
101. Kim, Y. R., Park, H. M., Aragão, F. T. S., and Lutif, J. E. S. (2009). "Effects of Aggregate Structure on Hot-Mix Asphalt Rutting Performance in Low Traffic Volume Local Pavements." *Construction and Building materials*, Vol. 23(6), pp. 2177-2182.



102. Kim, Y. R., Zhang, J., and Ban, H. (2012b). "Moisture Damage Characterization of Warm-Mix Asphalt Mixtures Based on Laboratory-Field Evaluation." *Construction and Building Materials*, Vol. 31, pp. 204-211.
103. Kristjansdottir, O. (2014). "Warm Mix Asphalt for Cold Weather Paving." *PhD Thesis*, University of Washington, Seattle, WA.
104. Krutz, N. C., and Sebaaly, P. E. (1993). "The Effects of Aggregate Gradation on Permanent Deformation of Asphalt Concrete." *Journal of the Association of Asphalt Paving Technologists*, Vol. 62, pp. 450-473.
105. Kuna, K., Airey, G., and Thom, N. (2017). "Mix Design Considerations of Foamed Bitumen Mixtures with Reclaimed Asphalt Pavement Material." *International Journal of Pavement Engineering*, Vol. 18(10), pp. 902-915.
106. Kutay, M. E., and Aydilek, A. H. (2007). "Dynamic Effects on Moisture Transport in Asphalt Concrete." *Journal of Transportation Engineering*, Vol. 133(7), pp. 406-414.
107. Larsen, O.R. (2001). "Warm Asphalt Mix with Foam-WAM Foam." *IRF 2001 Partie B: Thèmes Techniques*, S.00469. Kolo Veidekke, Norway.
108. Lee, S. J., Amirkhanian, S. N., Park, N. W., and Kim, K. W. (2009). "Characterization of Warm Mix Asphalt Binders Containing Artificially Long-Term Aged Binders." *Construction and Building Materials*, Vol. 23(6), pp. 2371-2379.
109. Li, Q., Xiao, D. X., Wang, K. C., Hall, K. D., and Qiu, Y. (2011). "Mechanistic-Empirical Pavement Design Guide (MEPDG): a Bird's-Eye View." *Journal of Modern Transportation*, Vol. 19(2), pp. 114-133.
110. Li, X., Marasteanu, M., Williams, R. C., and Clyne, T. R. (2008). "Effect of RAP Proportion and Type and Binder Grade on the Properties of Asphalt Mixtures." *Transportation Research Record: Journal of the Transportation Research Board*, Washington, D.C., Vol. 2051, pp. 90-97.
111. Lu, Q., and Harvey, J. (2006). "Evaluation of Hamburg wheel-tracking Device Test with Laboratory and Field Performance Data." *Transportation Research Record: Journal of the Transportation Research Board*, Vol. 1970, pp. 25-44.
112. Lu, X. D., and Saleh, M. (2016). "Evaluation of Warm Mix Asphalt Performance Incorporating High RAP Content." *Canadian Journal of Civil Engineering*, Vol. 43(4), pp. 343-350.

113. Maccarrone, S., Holleran, G., Leonard, D. J., and Hey, S. (1994). "Pavement Recycling Using Foamed Asphalt." *Proc., 17th ARRB Conf. Australian Road Research Board, Gold Coast, Vol. 17(3)*, pp. 349–365.
114. Malladi, H. (2015). "Investigation of Warm Mix Asphalt Concrete Mixtures with Recycled Asphalt Pavement Material." *PhD Thesis*, North Carolina State University, Raleigh, USA.
115. Mallick, R., Kandhal, P., Cooley, L. A., and Watson, D. (2000). "Design Construction and Performance of New-Generation Open-Graded Friction Courses." *Asphalt Paving Technology, Vol. 69*, pp. 391-423.
116. Mallick, R. B., Pelland, R., and Hugo, F. (2005). "Use of Accelerated Loading Equipment for Determination of Long Term Moisture Susceptibility of Hot Mix Asphalt." *International Journal of Pavement Engineering, Vol. 6(2)*, pp. 125-136.
117. Martin, A. E. (2014). "Evaluation of the Moisture Susceptibility of WMA Technologies." *Transportation Research Record: Journal of the Transportation Research Board, Vol. 763*, pp. 2-3.
118. McDaniel, R. S., and Shah, A. (2003). "Use of Reclaimed Asphalt Pavement (RAP) under Superpave Specifications." *Asphalt Paving Technology, Vol. 72*, pp. 226-252.
119. McDaniel, R. S., Soleymani, H., Anderson, R. M., Turner, P., and Peterson, R. (2000). "Recommended Use of Reclaimed Asphalt Pavement in the Superpave Mix Design Method." *NCHRP Web document*, 30.  
[https://onlinepubs.trb.org/Onlinepubs/nchrp/nchrp\\_w30-a.pdf](https://onlinepubs.trb.org/Onlinepubs/nchrp/nchrp_w30-a.pdf)  
(Accessed Date: 12.30.2018)
120. Moghadas, N. F., Azarhoosh, A., Hamed, G. H., and Roshani, H. (2014). "Rutting Performance Prediction of Warm Mix Asphalt Containing Reclaimed Asphalt Pavements." *Road Materials and Pavement Design, Vol. 15(1)*, pp. 207-219.
121. Mo, L., Hurrman, M., Wu, S., and Molenaar, A.A.A. (2009). "Raveling Investigation of Porous Asphalt Concrete Based on Fatigue Characteristics of Bitumen-Stone Adhesion and Mortar." *Materials and Design, Vol. 30*, pp. 170–179.
122. Mo, L., Li, X., Fang, X., Hurrman, M., and Wu, S. (2012). "Laboratory Investigation of Compaction Characteristics and Performance of Warm Mix Asphalt Containing Chemical Additives." *Construction and Building Materials, Vol. 37*, pp. 239-247.

123. Moreno, F. and Rubio, M.C. (2013). "Effect of Aggregate Nature on the Fatigue-Cracking Behavior of Asphalt Mixes." *Materials and Design*, Vol. 47, pp. 61-67.
124. Miller, T., Ksaibati, K., and Farrar, M. (1995). "Using Georgia Loaded-Wheel Tester to Predict Rutting." *Transportation Research Record: Journal of the Transportation Research Board*, Vol. 1473, pp. 17-24.
125. Mull, M. A., Stuart, K., and Yehia, A. (2002). "Fracture Resistance Characterization of Chemically Modified Crumb Rubber Asphalt Pavement." *Journal of materials science*, Vol. 37(3), pp. 557-566.
126. Muthen, K. M. (1998). "Foamed Asphalt Mixes-Mix Design Procedure." *CSIR Transportek Project TRA79*: South Africa.
127. NAPA (2015). "Simple Durability Tests on Mixes from the FHWA ALF Experiment." *National Asphalt Pavement Association*.  
[https://www.asphaltpavement.org/PDFs/Engineering\\_ETGs/Mix\\_201604/07%20West%20Mix%20Cracking%20Test%20Studies%20Mix%20ETG%20SLC.pdf](https://www.asphaltpavement.org/PDFs/Engineering_ETGs/Mix_201604/07%20West%20Mix%20Cracking%20Test%20Studies%20Mix%20ETG%20SLC.pdf)  
 (Accessed Date: 12.30.2018)
128. NCAT (2017). "Twins at Birth Differed as They Aged, by Don Watson." *National Center for Asphalt Technology*.  
<http://eng.auburn.edu/research/centers/ncat/newsroom/2016-fall/watson-twins.html>  
 (Accessed Date: 12.30.2018)
129. NCHRP Report-673 (2012). "Special Mixture Design Considerations and Methods for Warm Mix Asphalt: A Supplement to NCHRP Report 673: A Manual for Design of Hot Mix Asphalt with Commentary." *Advanced Asphalt Technologies, LLC*, Report prepared for Transportation Research Board of the National Academics, DC.
130. NCHRP Report-714 (2013). "QC/QA Testing differences between Hot Mix Asphalt (HMA) and Warm Mix Asphalt (WMA)." *Final Report ~ FHWA-OK-13-02*, Report prepared for Oklahoma Department of Transportation, OK.
131. Oklahoma Department of Transportation (ODOT) (2011). "Special Provision for Hamburg Rut Testing of Hot Mix Asphalt." *708-23(a) 09*, Oklahoma Department of Transportation.  
[http://www.okladot.state.ok.us/c\\_manuals/specprov2009/oe\\_sp\\_2009-708-23.pdf](http://www.okladot.state.ok.us/c_manuals/specprov2009/oe_sp_2009-708-23.pdf)  
 (Accessed Date: 12.30.2018)

132. Oklahoma Department of Transportation (ODOT) (2012). “Special Provision for Warm Mix Asphalt Material Requirements.” *SP No. 708-22 9 (a)*, Oklahoma Department of Transportation.  
[http://www.okladot.state.ok.us/c\\_manuals/specprov2009/oe\\_sp\\_2009-411-13.pdf](http://www.okladot.state.ok.us/c_manuals/specprov2009/oe_sp_2009-411-13.pdf)  
(Accessed Date: 8.30.2018)
133. Oklahoma Department of Transportation (ODOT) (2013a). “Oklahoma Department of Transportation Special Provision for Reclaimed Asphalt Pavement and Shingles.” *SP No. 708-21*, Oklahoma Department of Transportation,  
[http://www.odot.org/c\\_manuals/specprov2009/oe\\_sp\\_2009-708-21.pdf](http://www.odot.org/c_manuals/specprov2009/oe_sp_2009-708-21.pdf).  
(Accessed Date: 8.30.2018)
134. Oklahoma Department of Transportation (ODOT) (2013b). “Oklahoma Department of Transportation Special Provision for Warm Mix Asphalt Material Requirements.” *SP No. 708-22 (a)*, Oklahoma Department of Transportation,  
[http://www.odot.org/c\\_manuals/specprov2009/oe\\_sp\\_2009-708-22.pdf](http://www.odot.org/c_manuals/specprov2009/oe_sp_2009-708-22.pdf)  
(Accessed Date: 1.1.2019)
135. Ozer, H., Al-Qadi, I.L., Lambros, J., El-Khatib, A., Singhvi, P., and Doll, B. (2016). “Development of The Fracture-Based Flexibility Index for Asphalt Concrete Cracking Potential Using Modified Semi-Circle Bending Test Parameters.” *Construction and Building Materials, Vol. 115*, pp. 390–401.
136. Pandey, S. (2016). “Performance Characterization of Recycled Asphalt Pavements with Warm Mix Asphalt Technologies.” *MS Thesis*, University of Nevada, Reno, USA.
137. Parker, F. (1989). “A Field Study of Stripping Potential of Asphalt Concrete Mixtures.” *Final Report*, The State of Alabama Highway Department, Montgomery, AL.
138. Pirmohammad, S., and Ayatollahi, M. R. (2014). “Fracture Resistance of Asphalt Concrete Under Different Loading Modes and Temperature Conditions.” *Construction and building materials, Vol. 53*, pp. 235-242.
139. Prowell, B.D., Hurley, G.C. and Crews, E. (2007). “Field Performance of Warm-Mix Asphalt at National Center for Asphalt Technology Test Track.” *Transportation Research Record: Journal of the Transportation Research Board, Vol. 1998*, pp. 96–102.

140. Punith, V. S., Xiao, F., Putman, B., and Amirkhanian, S. N. (2012). "Effects of Long-term Aging on Moisture Sensitivity of Foamed WMA Mixtures Containing Moist Aggregates." *Materials and structures*, Vol. 45(1-2), pp. 251-264.
141. Rahman, M. A., Arshadi, A., Ghabchi, R., Ali, S. A., and Zaman, M. (2018). "Evaluation of Rutting and Cracking Resistance of Foamed Warm Mix Asphalt Containing RAP." *In Civil Infrastructures Confronting Severe Weathers and Climate Changes Conference*, Springer, Cham, pp. 129-138.
142. Rahman, M.A., Zaman, M., Ghabchi, R., Ali, S.A., Arshadi, A., and Barman, M. (2019). "Laboratory Characterization of Rutting and Moisture-Induced Damage Potential of Foamed Warm Mix Asphalt (WMA) Containing RAP." *Submitted to 99th Annual Meeting of Transportation Research Board*. Conference Paper.
143. Rani, S. (2018). "Characterization of Rutting in Asphalt Pavements Using Laboratory Testing." *PhD Thesis*, University of Oklahoma, Norman, OK, USA.
144. Rani, S., Ghabchi, R., Ali, S. A., and Zaman, M. (2019). "Laboratory Characterization of Asphalt Binders Containing a Chemical-Based Warm Mix Asphalt Additive." *Journal of Testing and Evaluation*, Vol. 48(2), 17 pages.
145. Roy, N., Veeraragavan, A., and Murali Krishnan, J. (2015). "Interpretation of Flow Number Test Data for Asphalt Mixtures." *In Proceedings of the Institution of Civil Engineers-Transport*, June, 2015, Vol. 168, No. 3, pp. 191-199
146. Rubio, M.C., Martínez, G., Baena, L. and Moreno, F. (2012). "Warm mix asphalt: an overview." *Journal of Cleaner Production*, Vol. 24, pp. 76-84.
147. Saeidi, H., and Aghayan, I. (2016). "Investigating the Effects of Aging and Loading Rate on Low-Temperature Cracking Resistance of Core-Based Asphalt Samples Using Semi-Circular Bending Test." *Construction and Building Materials*, Vol. 126, pp. 682-690.
148. Sargand, S., Nazzal, M. D., Al-Rawashdeh, A., and Powers, D. (2011). "Field Evaluation of Warm-Mix Asphalt Technologies." *Journal of Materials in Civil Engineering*, Vol. 24(11), pp. 1343-1349.
149. Sebaaly, P. E., Hajj, E. Y., and Piratheepan, M. (2015). "Evaluation of Selected Warm Mix Asphalt Technologies." *Road Materials and Pavement Design*, Vol. 16(sup1), pp. 475-486.

150. Sebaaly, P. E., Hand, A. J., McNamara, W. M., Weitzel, D., and Epps, J. A. (2004). "Field and Laboratory Performance of Superpave Mixtures in Nevada." *Transportation research record: Journal of the Transportation Research Board*, Vol. 1891(1), pp. 76-84.
151. Sel, I., Yildirim, Y., and Ozhan, H. B. (2014). "Effect of Test Temperature on Hamburg Wheel-Tracking Device Testing." *Journal of Materials in Civil Engineering, ASCE*, Vol. 26(8), pp. 04-37.
152. Sengoz, B. and Oylumluoglu, J. (2013). "Utilization of Recycled Asphalt Concrete with Different Warm Mix Asphalt Additives Prepared with Different Penetration Grades Bitumen." *Construction and Building Materials*, Vol. 45, pp. 173–183.
153. Shah, A., McDaniel, R., Huber, G., and Gallivan, V. (2007). "Investigation of Properties of Plant-Produced Reclaimed Asphalt Pavement Mixtures." *Transportation Research Record: Journal of the Transportation Research Board*, Vol. 1998, pp. 103-111.
154. Shaowen, D., and Shanshan, L. (2011). "The Raveling Characteristic of Porous Asphalt Mixture." *Third International Conference on Transportation Engineering, ASCE*, pp. 1880-1885.
155. Shu, X., Huang, B., Shrum, E.D., and Jia, X. (2012). "Laboratory Evaluation of Moisture Susceptibility of Foamed Warm Mix Asphalt Containing High Percentages of RAP." *Construction and Building Materials*, Vol. 35, pp. 125–130.
156. Shu, X., Huang, B., Xiang, S., and Vukosavljevic, D. (2008). "Laboratory Evaluation of Fatigue Characteristics of Recycled Asphalt Mixture." *Construction and Building Materials*, Vol. 22, pp. 1323–1330.
157. Silva, H.M.R.D., Oliveira, J.R.M., Peralta, J., and Zoorob, S.E. (2010). "Optimization of Warm Mix Asphalts Using Different Blends of Binders and Synthetic Paraffin Wax Contents." *Construction and Building Materials*, Vol. 24 (9), pp. 1621-1631.
158. Singh, D. (2011). "A Laboratory Investigation and Modeling of Dynamic Modulus of Asphalt Mixes for Pavement Applications." *PhD Thesis*, University of Oklahoma, Norman, Oklahoma, USA.
159. Solaimanian, M., Harvey, J., Tahmoressi, M., and Tandon, V. (2003). "Test Methods to Predict Moisture Sensitivity of Hot-Mix Asphalt Pavements." *Transportation Research*

- Board Report: Moisture Sensitivity of Asphalt Pavements*, Topic 3. TRB National Seminar, San Diego, pp. 77–113.
160. Tarefder, R. A., and Ahmad, M. (2014). “Evaluating the Relationship between Permeability and Moisture Damage of Asphalt Concrete Pavements.” *Journal of Materials in Civil Engineering*, Vol. 27(5), pp. 04014172 (1-10).
  161. Tarefder, R. A., Weldegiorgis, M. T., and Ahmad, M. (2014). “Assessment of the Effect of Pore Pressure Cycles on Moisture Sensitivity of Hot Mix Asphalt Using MIST Conditioning and Dynamic Modulus.” *Journal of Testing and Evaluation*, Vol. 42(6), pp. 1530-1540.
  162. Tarrer, A. R., and Wagh, V. (1991). “The Effect of the Physical and Chemical Characteristics of the Aggregate on Bonding.” *SHRP Report*, National Research Council, Washington, DC.
  163. Tashman, L., and Elangovan, M. A. (2008). “Dynamic Modulus Test Laboratory Investigation and Future Implementation in the State of Washington.” Research Report WA-RD 704.1, *Washington State Transportation Center (TRAC)*, University of Washington, Seattle, WA.
  164. Tsai, B.W., Coleri, E., Harvey, J.T. and Monismith, C.L. (2016). “Evaluation of AASHTO T 324 Hamburg-Wheel Track Device test.” *Construction and Building Materials*, Vol. 114, pp. 248–260.
  165. Tran, N.H., and Hall, K.D. (2006). “An Examination of Strain Levels Used in the Dynamic Modulus Testing.” *Journal of Association of Asphalt Paving Technologists*, Vol. 75, pp. 321-343.
  166. Valdes-Vidal, G., Calabi-Floody, A., and Sanchez-Alonso, E. (2018). “Performance Evaluation of Warm Mix Asphalt involving Natural Zeolite and Reclaimed Asphalt Pavement (RAP) for Sustainable Pavement Construction.” *Construction and Building Materials*, Vol. 174, pp. 576-585.
  167. Van De Ven, M. F. C., Jenkins, K. J., Voskuilen, J. L. M., and Van Den Beemt, R. (2007). “Development of (Half-) Warm Foamed Bitumen Mixes: State of the Art.” *International Journal of Pavement Engineering*, Vol. 8(2), pp. 163-175.
  168. Walubita, L., Zhang, J., Das, G., Hu, X., Mushota, C., Alvarez, A., and Scullion, T. (2012). “Hot-mix Asphalt Permanent Deformation Evaluated by Hamburg Wheel

- Tracking, Dynamic Modulus, and Repeated Load Tests.” *Transportation Research Record: Journal of the Transportation Research Board*, Vol. 2296, pp. 46-56.
169. Williams, B. A., Copeland, A., and Ross, T. C. (2018). “Asphalt Pavement Industry Survey on Recycled Materials and Warm-Mix Asphalt Usage: 2017.” *8th Annual Survey (IS 138)*. National Asphalt Pavement Association, Lanham, Maryland.  
doi:10.13140/RG.2.2.30240.69129
  170. Wasiuddin, N., Selvamohan, S., Zaman, M., and Guegan, M. (2007). “Comparative Laboratory Study of Sasobit And Aspha-Min Additives in Warm-Mix Asphalt.” *Transportation Research Record: Journal of the Transportation Research Board*, Vol. 1998, pp. 82-88.
  171. Watson, D.E., Moore, K.A., Williams, K., and Cooley, L.A. Jr. (2003). “Refinement of New-Generation Open-Graded Friction Course Mix Design.” In *Transportation Research Record: Journal of the Transportation Research Board*, Vol. 1832, pp. 78-85.
  172. Weldegiorgis, M. T., and Tarefder, R. A. (2014). “Towards a Mechanistic Understanding of Moisture Damage in Asphalt Concrete.” *Journal of Materials in Civil Engineering*, Vol. 27(3), 04014128, pp. 1-11.
  173. Witczak, M. W., Kaloush, K., and Pellinen, T. El-Basyouny, and Von Quintus, H. (2002). “Simple Performance Test for Superpave Mix Design.” *National Cooperative Highway Research Program (NCHRP) Rep*, 465.
  174. Witczak, M. W. (2005). “Simple Performance Tests: Summary of Recommended Methods and Database.” *Research Report NCHRP 547, Transportation Research Board*, Washington, D.C.
  175. Wielinski, J., Hand, A., and Rausch, D. M. (2009). “Laboratory and Field Evaluations of Foamed Warm-Mix Asphalt Projects.” *Transportation Research Record: Journal of the Transportation Research Board*, Vol. 2126(1), pp. 125-131.
  176. Wu, Z., Mohammad, L. N., Wang, L. B., and Mull, M. A. (2005). “Fracture Resistance Characterization of Superpave Mixtures Using the Semi-Circular Bending Test.” *Journal of ASTM International*, Vol. 2(3), pp. 1-15.
  177. Washington State Department of Transportation (WSDOT) (2012). “Warm Mix Asphalt Technologies.” *Tech Note, Engineering and Regional Operations Construction Division*, Washington State Department of Transportation.



<https://www.wsdot.wa.gov/NR/rdonlyres/285203F7-7738-440D-8182-F3B785742382/0/WarmMixAsphaltTechnologies.pdf>

(Accessed Date: 1.1.2019)

178. Xiao, F., Hou, X., Amirkhanian, S., and Kim, K. W. (2016). “Superpave Evaluation of Higher RAP Contents Using WMA Technologies.” *Construction and Building Materials, Vol. 112*, pp. 1080-1087.
179. Xiao, F., Punith, V. S., and Putman, B. J. (2012). “Effect of Compaction Temperature on Rutting and Moisture Resistance of Foamed Warm-Mix-Asphalt Mixtures.” *Journal of materials in civil engineering, Vol. 25(9)*, pp. 1344-1352.
180. Xu, S., Xiao, F., Amirkhanian, S., and Singh, D. (2017). “Moisture Characteristics of Mixtures with Warm Mix Asphalt Technologies—a Review.” *Construction and Building Materials, Vol. 142*, pp. 148-161.
181. Yildirim, Y., and Kennedy, T. W. (2002). “Hamburg Wheel Tracking Device Results on Plant and Field Cores Produced Mixtures.” No. *FHWA/TX-04/0-4185-2*, Center for Transportation Research, Bureau of Engineering Research, University of Texas at Austin.
182. Yu, X., Liu, S., and Dong, F. (2016). “Comparative Assessment of Rheological Property Characteristics for Unfoamed and Foamed Asphalt Binder.” *Construction and Building Materials, Vol. 122*, pp. 354-361.
183. Zaumanis, M. (2010). “Warm mix asphalt Investigation.” *PhD Thesis*, Riga Technical University, Kgs. Lyngby, Denmark.
184. Zaman, M., Ghabchi, R. and Hossain, Z. (2019). “Enhancing Sustainability of Transportation in the 21st Century.” *Chapter 5 in US Infrastructure: Challenges and Directions for the 21st Century, Routledge-Taylor and Francis*, 25 pages (in press).
185. Zhao, S., Huang, B., Shu, X., Jia, X., and Woods, M. (2012). “Laboratory Performance Evaluation of Warm-Mix Asphalt containing High Percentages of Reclaimed Asphalt Pavement.” *Transportation Research Record: Journal of the Transportation Research Board, Vol. 2294(1)*, pp. 98-105.
186. Zhao, S., Huang, B., Xiang, S. and Woods, M. (2013). “Comparative Evaluation of Warm Mix Asphalt Containing High Percentages of Reclaimed Asphalt Pavement.” *Construction and Building Materials, Vol. 44*, pp. 92–100.

## Appendix A: Abbreviation

AASHTO	American Association of State Highway and Transportation Officials
AMPT	Asphalt Mixture Performance Tester
ASTM	American Society for Testing and Materials
APA	Asphalt Pavement Analyzer
AV	Air Voids
COV	Coefficient of Variation
DM	Dynamic Modulus
DOT	Department of Transportation
ESAL	Equivalent Single Axle Load
FN	Flow Number
HMA	Hot Mix Asphalt
HWT	Hamburg Wheel Tracking
ITS	Indirect Tensile Strength
JMF	Job Mix Formula
LWT	Loaded Wheel Testers
M-EPDG	Mechanistic-Empirical Pavement Design Guide
ML	Mass Losses
MMFE	Micro Mechanical Finite Element
NCAT	National Center for Asphalt Technology
NMAS	Nominal Maximum Aggregate Size
ODOT	Oklahoma Department of Transportation
PG	Performance Grade
RLPD	Repeated Load Permanent Deformation
RTFO	Rolling Thin Film Oven
SGC	Superpave <sup>®</sup> Gyratory Compactor
SIP	Stripping Initiation point
TRLPD	Triaxial Repeated Load Permanent Deformation
TSR	Tensile Strength Ratio
VFA	Voids Filled with Asphalt
VMA	Voids in the Mineral Aggregate WSDOT
WMA	Warm Mix Asphalt